CRMP1 Protein Complexes Modulate PolyQ-Mediated Htt Aggregation and Toxicity in Neurons

DISSERTATION

zur Erlangung des akademischen Grades
doctor rerum naturalium
(Dr.rer.nat.)
im Fach Biologie
eingereicht an der
Mathematisch-Naturwissenschaftlichen Fakultät I
Humboldt-Universität zu Berlin

von
Herr Dipl.-Ing. Yacine Bounab

Präsident der Humboldt-Universität zu Berlin:
Prof.Dr. Christoph Markschies
Dekan der Mathematisch-Naturwissenschaftlichen Fakultät I:
Prof.Dr. Lutz-Helmut-Schön
Gutachter:
1. Prof.Dr. Erich Wanker
2. Prof.Dr. Andreas Herrmann

Eingereicht am: 29.Juli 2009
Tag der mündlichen Prüfung: 21. Januar 2010

Abstract

Huntington's disease (HD) is an inherited neurodegenerative disorder characterized by the accumulation of N-terminal polyglutamine (polyQ)-containing huntingtin (Htt) fragments in affected neurons. The mutant Htt (mHtt) protein is ubiquitously expressed but causes specific dysfunction and death of striatal medium-sized spiny neurons (MSNs) (Albin, 1995; Herden, 1995; Sharp, 1995; Trottier, 1995). Several lines of evidence indicate that mHtt misfolding and aggregation is associated with cytotoxicity in HD models and patients (Sanchez, 2003). It is assumed that striatum specific proteins interacting with Htt might play an important role in HD pathogenesis (Ross, 1995; Harjes and Wanker, 2003). Thus, the identification and characterization of striatum-specific Htt interaction partners modulating mHtt-mediated aggregation and toxicity is critical for understanding HD pathogenesis.
Previous protein-protein interaction (PPI) studies demonstrated that many Htt-interacting proteins colocalize with insoluble Htt inclusions in HD brains and modulate the mHtt phenotype (Goehler 2004; Kaltenbach 2007). A striatum-specific, dysregulated PPI network has been created recently by integrating PPI networks with information from gene expression profiling data (Chaurasia, unpublished data). One of the identified dysregulated proteins potentially involved in HD pathogenesis was the neuron-specific Collapsin Response Mediator Protein 1 (CRMP1).
The focus of my thesis was to investigate the role of the CRMP1 protein in HD pathogenesis using *in vitro* and *in vivo* model systems.
Cell-free aggregation experiments with purified recombinant proteins demonstrated that CRMP1 reduces the self-assembly of fibrillar, SDS-insoluble mHtt protein aggregates in a filter retardation assay. This was confirmed by atomic force microscopy (AFM), indicating a direct role of CRMP1 on the mHtt aggregation process. Coimmunoprecipitation studies indicated that CRMP1 and Htt associate in mammalian cells under physiological conditions. In addition, CRMP1 localizes to abnormal neuronal inclusions and efficiently modulates polyQ-mediated Htt aggregation and toxicity in cell and *Drosophila* models of HD. This suggests that dysfunction of the protein is crucial for disease pathogenesis. Finally, I observed that CRMP1 localizes to neuronal inclusions and is selectively cleaved by calpains in R6/2 mouse brains, indicating that its distribution and function are altered in pathogenesis.
In conclusion, this study presents new findings on the function of CRMP1 and its role in the pathogenesis of HD. The protein interacts with Htt and modulates its aggregation and neuronal toxicity, in this way influencing the molecular course of the disease.

Keywords

Neurodegenerative disorders, Huntington's disease (HD), Mutant Huntingtin (mHtt), Polyglutamine, Aggregation, Cytotoxicity, Protein-Protein Interaction Networks, CRMP1 (Collapsin Response Mediator Protein 1)

Zusammenfassung

Chorea Huntington (HD) ist eine erbliche neurodegenerative Erkrankung, die durch Ablagerungen von N-terminalen Polyglutamin-reichen Huntingtin (Htt) -Fragmenten in den betroffenen Neuronen charakterisiert ist. Das mutierte Htt (mHtt) Protein wird ubiquitär exprimiert. Es verursacht jedoch das zellspezifische Absterben von „medium-sized spiny neurons“ (MSN) im Striatum von HD Patienten (Albin, 1995; Herden, 1995; Sharp, 1995; Trottier, 1995). Ergebnisse mehrerer Studien deuten darauf hin, dass Fehlfaltung und Aggregation von mHtt mit der Zytotoxizität in HD-Modellen und -Patienten assoziiert sind (Sanchez, 2003). Es wird angenommen, dass Striatum-spezifische Proteine, die mit Htt interagieren, eine wichtige Rolle in der Pathogenese von HD spielen (Ross, 1995; Harjes and Wanker, 2003). Die Identifizierung und Charakterisierung von Striatum-spezifischen Htt-Interaktionspartnern, die Aggregation und Toxizität von mHtt modulieren, ist somit entscheidend für ein besseres Verständnis der Krankheitsentstehung.
Protein-Protein-Interaktionsstudien haben gezeigt, dass einige der Htt-Interaktionspartner mit unlöslichen Htt-Ablagerungen in den Gehirnen von HD-Patienten kolokalisieren und die Bildung von Protein-Aggregaten beeinflussen (Goehler 2004; Kaltenbach 2007). Kürzlich wurde durch die Integration von Genexpressions- und Interaktionsdaten ein Striatum-spezifisches Protein-Interaktionsnetzwerk erstellt (Chaurasia, unveröffentlichte Daten). Eines der identifizierten Proteine ist CRMP1 (Collapsin Response Mediator Protein 1), das in Neuronen spezifisch exprimiert wird und möglicherweise eine wichtige Rolle bei der Pathogenese von HD spielt.
Der Hauptziel dieser Arbeit bestand darin, die Rolle von CRMP1 in der Pathogenese von HD mittels *in vitro* und *in vivo* Modelsystemen zu untersuchen.
Aggregations-Experimente mit aufgereinigten, rekombinanten Proteinen im Filter-Retardationsassay zeigten, dass CRMP1 die Anordnung von Htt zu fibrillären, SDS-unlöslichen Aggregaten verringert. Durch Rasterkraftmikroskopie wurde der direkte Effekt von CRMP1 auf den Aggregationsprozess vin Htt bestätigt. Ko-Immuno-präzipitationsstudien zeigten, dass CRMP1 und Htt in Säugerzellen unter physiologischen Bedingungen miteinander interagieren. CRMP1 konnte in anormalen neuronalen Ablagerungen gefunden werden. Außerdem wurde nachgewiesen, dass CRMP1 die Polyglutamin-abhängige Aggregation und Toxizität von Htt in Zell- und *Drosophila*-Modellen von HD moduliert. Schließlich konnte CRMP1 in neuronalen Ablagerungen in R6/2 Mäusegehirnen und dessen selektive Spaltung durch Calpaine gezeigt werden. Diese Ergebnisse deuten darauf hin, dass Lokalisation und Funktion von CRMP1 in der Krankheitsentstehung verändert sind.
In dieser Arbeit konnten wesentliche neue Erkenntnisse zur Funktion von CRMP1 und seiner Rolle in der Pathogenese von Chorea Huntington gewonnen werden. Das Protein interagiert mit Htt und moduliert dessen Aggregation und neuronale Toxizität, wodurch der molekulare Entstehungsweg der Krankheit beeinflusst wird.

Schlagwörter

Neurodegenerative Erkrankung, Chorea Huntington (HD), Mutierte Huntingtin (mHtt), Polyglutamin, Aggregation, Zytotoxizität, Protein-Protein-Interaktions-netzwerk, CRMP1 (Collapsin Response Mediator Protein 1)

Contents

List of Figures

List of Tables

Chapter 1
Introduction

1 Introduction

The brain is the most complex and fascinating organ in the human body; it consists of a vast network of more than 100 billion neurons that communicate with each other via around 100 trillion synapses. The human brain controls movements and motor activities combined with perceptual, cognitive and affective processes. Vulnerability of neuronal circuits of the human brain is illustrated by plethora of severe neurodegenerative disorders such as Alzheimer's and Parkinson's diseases (AD and PD) or polyglutamine (PolyQ) disorders like Huntington's disease (HD) and several forms of spinocerebellar ataxia (SCAs). Although these neurodegenerative diseases have distinct clinical manifestations, mainly due to the neuronal loss of specific brain areas, they have features in common, including the intra- or extracellular accumulation of misfolded proteins, mitochondrial dysfunction, alteration of cytoskeletal components, impairment of stress response and inflammation (McMurray, 2000). Most of those processes are influenced by aging, a unifying risk factor for all neurodegenerative disorders (Li Gan and Lennart Mucke, 2006). Significant efforts and progress have been made in order to decipher the molecular mechanisms underlying neurodegenerative disorders and to find effective therapies. However, there is currently no treatment for preventing or delaying the course of neurodegenerative diseases.

Although monogenic diseases (e.g. HD) are caused by mutations of single genes, the degree of phenotypic changes they display might vary due to the influence of additional genetic modifiers and environmental factors to which the individual is exposed (Djousse, 2004; Wexler, 2004). Indeed, it is well accepted that large numbers of genes coding-proteins act in a similar manner to predispose an individual to disease (Liu, 2006). Furthermore, with the scientific developments of the postgenomic era it has become apparent that most of the genes and their products interact in complex networks to convey cellular functions (Barabasi and Oltvai, 2004). Recently, considerable efforts have been carried out in the emerging field of systems biology in order to understand the complexity of biomolecular systems and networks that underlie normal or disease states. In this respect, system-based analyses of complex biological networks have been applied successfully to investigate many human disorders, allowing novel insights into the

molecular mechanisms of diseases (Loscalzo, 2007).

Network analyses utilizing protein-protein interaction (PPI) data have been used for neurodegenerative disorders, including HD (Goehler, 2004) and SCAs (Lim, 2006) to identify potential disease modifiers. An interaction network for HD led to the identification of GIT1, a G-protein-coupled receptor kinase interactor 1 that functions as a new enhancer of Htt aggregation. A PPI network for inherited human ataxias demonstrated that many ataxia-causing proteins share interacting partners, a subset of which have been found to modulate neurodegeneration in animal models. Calvano et al. 2005 constructed an endotoxin inflammatory response network of human blood leukocytes by integrating PPI networks with information from gene expression profiling studies. This analysis revealed a global dysregulation of potential functional modules in mitochondrial bioenergetics, protein synthesis and protein degradation in human blood leukocytes during acute systemic inflammation (Calvano, 2005). Pujana and collegues conducted a study identifying new target genes potentially associated with higher risk of breast cancer (Pujana, 2007). Starting with four known breast-cancer associated genes: BRCA1, BRCA2, ATM and CHEK2, they combined gene expression profiling with functional genomic and proteomic data from various species to create a breast cancer-related molecular network. This information was subsequently used to identify a novel gene, the hyaluronan-mediated motility receptor (HMMR) that is associated with a higher risk for breast cancer (Pujana, 2007). These illustrative examples demonstrate that network modeling is a powerful strategy to identify novel genes associated with diseases.

Recently, Gautam Chaurasia and Dr. Matthias Futschik (Institute for Theoretical Biology Berlin, ITB and MDC-Berlin) have developed a generic bioinfomatic strategy by integrating PPI networks with information from gene expression profiling data derived from clinical case-control studies to create tissue-specific dysregulated interaction network of HD. One of the identified network components was the neuron-specific Collapsin Response Mediator Protein 1 (CRMP1), which is pathologically downregulated during HD pathogenesis.

During my Ph.D. studies, using several complementary methods, I investigated the role of the CRMP1 protein in HD pathogenesis.

1.1 Huntington's disease

HD is a devastating neurodegenerative disorder named after George Summer Huntington who first described the disorder in 1872. He published his original paper under the title `On Chorea´ in the Medical and Surgical Reporter (Huntington, 1872). In this work, George Huntington described the clinical features of HD such as movement disability, personality changes and cognitive decline (Martin and Gusella, 1986). The disease follows an autosomal-dominant pattern of inheritance affecting around 3-7 in 100.000 persons worldwide (Cowan, 2006). The HD prevalence is highest in North America and Europe, with 5 and 10 cases per 100.000 individuals, and lowest in Africa and Asia (Hayden, 1981; Conneally, 1984; Vonsattel and DiFiglia, 1998). In Germany about 8000 people are affected by HD. An extremely high incidence of HD was found within a large group of interrelated families living in a fishing village along the border of lake Maracaibo in Venezuela (Okun, 2004).

Genetic linkage analysis using polymorphic DNA markers in these families led to the localization of the HD locus to the short arm of chromosome 4 (Gusella, 1983). Ten years later, in 1993, the gene responsible for HD was isolated and cloned by the Huntington Disease Collaborative Group (HDCG). It contains 67 exons spanning over 210 kb and encodes for a large protein termed huntingtin (Htt) with a molecular weight of ~ 350 kDa (HDCG, 1993). The *IT15* gene (Interesting Transcripts 15) contains a polymorphic CAG trinucleotide repeat within the first exon. In healthy individuals, the CAG triplet repeats range from 11 to 34 whereas people with HD have more than 35 repeats (HDCG, 1993). Generally, the *IT15* gene in healthy individuals contains 17 to 20 CAG repeats. Repeats between 27 and 35 are rare and are not associated with the disease, but they are meiotically unstable in parental transmission and can be expanded to the disease ranges (Myers, 2004). There is a strong inverse correlation between the age of disease onset and the number of CAG repeats (HDCG, 1993). Longer CAG repeats lead to an earlier age of onset and more severe symptoms (HDCG, 1993). Indeed, most adult-onset cases have 40-55 CAG repeats, and disease symptoms appear at the age of 35-50 years (Vonsattel and DiFiglia, 1998). A repeat length of more than 70 CAGs lead to a juvenile form of HD with an age of onset between 20-30 years

(Vonsattel and DiFiglia, 1998). However, it has been demonstrated that individuals with identical CAG repeat lengths show a wide variation in the age of disease onset, suggesting that the pathogenesis is influenced by additional genetic and environmental factors (Djousse, 2004; Wexler, 2004).

To date, ten neurodegenerative disorders caused by the expansion of CAG trinucleotide repeats within the coding region of the associated genes have been described. CAG encodes glutamine, and thus mutated proteins have an abnormally expanded polyglutamine (polyQ) tract. In each case, the elongated polyQ leads to the formation of large intranuclear and/or cytoplasmic aggregates and the degeneration of specific brain regions (Table 1.1) (Zoghbi and Orr, 2000; Orr and Zoghbi, 2007; Jieya Shao, 2007).

Table 1-1: Polyglutamine disorders, proteins and related pathology.

Disease	Mutated protein	Localization	Brain region most affected
HD	Huntingtin	Nuc, Cyt	Striatum and cerebral cortex
SBMA	Androgen receptor	Nuc, Cyt	Anterior horn, bulbar neurons and dorsal root ganglia
DRPLA	Atrophin 1	Nuc	Cerebellum, cerebral cortex and basal ganglia
SCA1	Ataxin 1	Nuc	Cerebellar Purkinje cells brain stem
SCA2	Ataxin 2	Nuc	Cerebellar Purkinje cells brain stem
SCA3	Ataxin 3	Nuc	Cerebellar dentate neurons, basal ganglia and brain stem
SCA7	Ataxin 7	Nuc	Cerebellum, brain stem
SCA17	TBP	Nuc	Cerebellar Purkinje cells, inferior olive
SCA6	Calcium channel subunit α1a	Cyt	Cerebellar Purkinje cells, dentate nucleus and inferior olive
SCA8	Unknown	Nuc	Cerebellar Purkinje cells, granule cells and inferior olive

HD, Huntington disease; SBMA, Spinal and bulbar muscular atrophy; DRPLA, Dentaterubral and pallidoluysian atrophy; SCAs, Spinocerebellar ataxias; TBP, TATA box binding protein; Nuc, nucleus; Cyt, Cytoplasm (Zoghbi and Orr, 2000; Orr and Zoghbi, 2007; Jieya Shao, 2007)

1.2 Neuropathological classification of HD

The neuropathological feature of HD is a progressive and selective loss of specific brain regions and astrogliosis (Vonsattel, 1985; Ross, 1995). In the early stages of the disease, neurodegeneration is highly selective for a subset of striatal neurons. The GABAergic medium-sized spiny neurons (MSNs) are the most severely affected (Graveland, 1985), resulting in atrophy of the caudate nuclei and the putamen, which are substructures of the basal ganglia known as the striatum (Albin, 1989). The basal ganglia consist of a collection of subcortical nuclei, including the caudate nuclei, the putamen, the globus pallidus, the subthalamic nucleus, and the substania nigra. These regions are responsible for motor behavior (Albin, 1989) (Figure 1.1 A).

Post-mortem brains of advanced HD patients are characterized by the dilatation of the lateral ventricles due to the neuronal death in the basal ganglia (Figure 1.1 B) (Vonsattel, 1985).

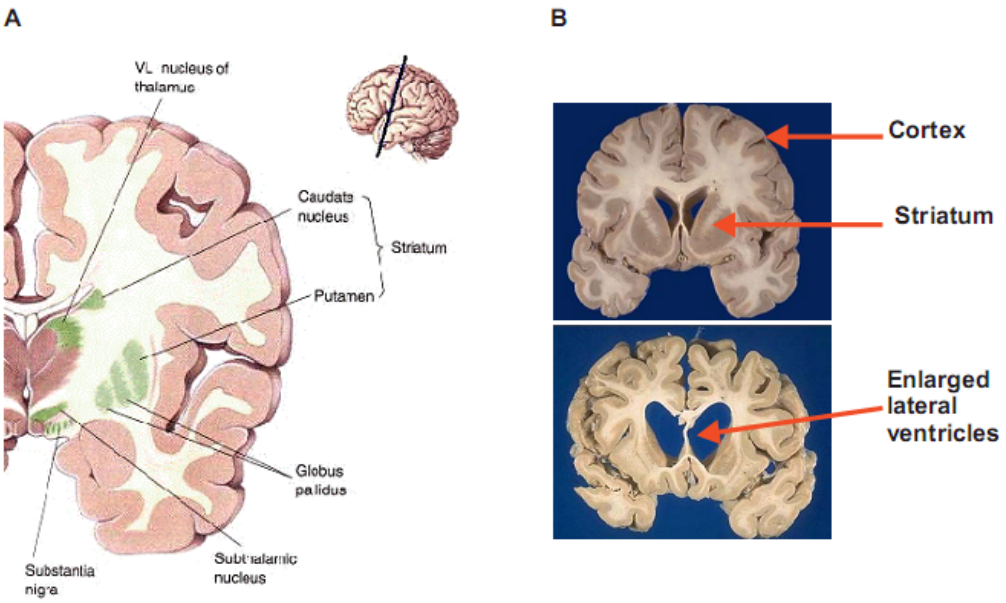

Figure 1-1: Characteristics of HD brain pathology.

(A) Schematic representation of a coronal section of human brain. It shows the position of the basal ganglia and the different sub-nuclei in green (Bear, 1996).

(B) The pathological picture of HD patient brains. Top: normal control brain; bottom: brain section from an HD patient. The enlargement of the lateral ventricles is due to neuronal death in the basal ganglia (Vonsattel, 1985).

The neurodegeneration in the cortex is less severe, the large pyramidal neurons in layer III, V, and VI, which project directly to the striatum are mostly affected (Hedreen, 1991; Sotrel, 1991). This part of the brain is responsible for mental, sensation and movement functions (Cowan and Raymond, 2006).

In later stages of the disease, brain atrophy becomes visible, with subsequent total weight loss of ~10-20 %. The atrophy occurs in many different brain regions, including globus pallidus, thalamus, subthalamic region, pons, medulla, amygdale, hippocampus, spinal cord, superior olive, claustrum and cerebellum (Vonsattel, 1985; Vonsattel and DiFiglia, 1998).

The astrogliosis, which consists of an abnormal increase in the number of astrocytes, is observed only in the striatum of HD brains (Myers, 1991; Vonsattel and DiFiglia, 1998).

Based on different pathological aspects of HD such as striatum atrophy, neuronal loss and astrogliosis, a system for grading the severity of HD pathology was established by macroscopic and microscopic criteria (Vonsattel, 1985). The neuropathological grades closely correlate with the clinical severity and are ranked from grade 0 (no detectable neuropathological changes) to grade 4 (severe striatal atrophy and 95% of neuronal loss) (Table 1.2) (Vonsattel, 1985).

Table 1-2: Characteristics of the neuropathological grades of HD.

	Caudate nucleus			Putamen		
Grades	Atrophy	Neuronal loss	Astrogliosis	Atrophy	Neuronal loss	Astrogliosis
0	-	-	-	-	-	-
1	-	+	+	-	-	+
2	+	++	++	+	++	++
3	++	+++	+++	++	+++	+++
4	++++	++++	++++	+++	++++	++++

-, no abnormality; +, mild; ++, moderate; +++, severe; ++++, very severe (Vonsattel, 1985).

Accumulation of conformationally defective protein aggregates in the brain and specific neuronal loss is a common key feature of many neurodegenerative disorders such as AD, PD, HD, SCAs, ALS (Amyotrophic lateral sclerosis), and TSEs (Transmissible encephalopathies) (Soto, 2003). In HD, the mutant Htt (mHtt) forms intranuclear and cytoplasmic aggregates. These aggregates are mainly found in the striatum and cortex and their appearance partially correlates with the

symptoms (Davies, 1997; DiFiglia, 1997). However, there is an intense debate whether mHtt aggregates directly lead to neurodegeneration or are protective. Both toxic as well as protective roles of mHtt aggregates have been described (Figure 1.2).

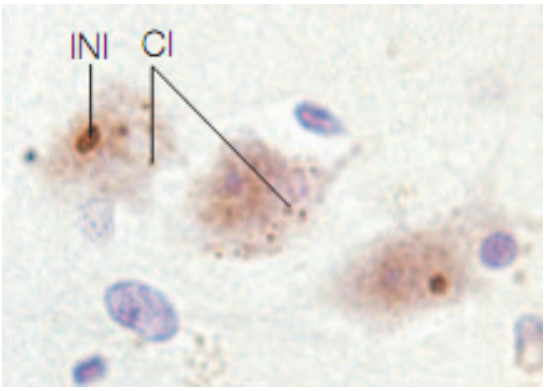

Figure 1-2: Intranuclear inclusions (INI) and cytoplasmic inclusions (CI) in the motor cortex of a Huntington's disease patient recognized with 1C2 antibody (Ross and Poirier, 2005).

The clinical manifestation of HD involves progressive movement disturbance, cognitive dysfunction and psychiatric symptoms (Martin and Gusella, 1986). The initial clinical symptoms are different for each person. The first signs are mild and increase gradually during the progression of the disease (Harper, 1992; Paulsen, 2001). In general, psychiatric symptoms such as learning, planning and attention, often occur before the onset of the clinical symptoms (Harper, 1992; Rosenberg, 1995; Paulsen, 2001). Minor motor abnormalities including involuntary movement of face, finger, feet or thorax manifest the first onset.

As the disease progresses, the motor symptoms become more pronounced. Chorea and dystonia gradually appear and in the later stage of the disease, the patients become severely rigid and akinetic. People with advanced HD lose weight and may become unable to walk and to talk. Personality changes such as irritability, temper outbursts, loss of motivation, apathy and even aggression are also noted (Harper, 1992; Rosenberg 1995; Paulsen, 2001).

HD patients die approximately 15 to 20 years after the onset of the first symptoms by causes associated with the disease such as pneumonia, poor nutrition, infections and heart failure (Beighton and Hayden, 1981).

1.3 Huntingtin

Htt is a multi-domain protein with a polymorphic glutamine/proline (Q/P)-rich domain at the N terminus (HDCG, 1993). The polyQ stretch begins at the 18th amino acid position of Htt and is followed by two proline-rich domains of 11 and 10 amino acids, which are required for many protein-protein interactions (Li SH, 2004). The first 17 amino acids at the N-terminus of Htt act as nuclear localization signal (NLS) (Cornett, 2005), while a conserved nuclear export signal (NES) has been found within the C-terminus of the protein (Xia, 2003). Thus may explain why Htt can shuttle between the nucleus and the cytoplasm (Xia, 2003; Cornett, 2005) (Figure 1.3 A).

Another characteristic feature of Htt is the presence of several HEAT repeats (named after the proteins: Huntingtin, Elongation factor 3, protein phosphatase 2A and TOR1), which are arranged in three main clusters (Andrade and Bork, 1995). A HEAT repeat is a ~38 amino acid sequence which forms a hairpin of two anti-parallel alpha helices (Andrade and Bork, 1995) (Figure 1.3 B and C). The HEAT domains are thought to be involved in protein-protein interactions and are found predominantly in proteins that play roles in intracellular transport processes, chromosomal segregation and condensation, mitotic spindle maintenance and tubulin assemblies (Andrade and Bork, 1995; Neuwald, 2000; Perry, 2003).

Htt undergoes several post-translational modifications that appear to play a role in the development of HD pathology. Several lysines, K6, K9 and K15 compete for SUMOylation and ubiquitination (Kalchman, 1996; Dohmen, 2004; Steffan, 2004) Htt is also palmitoylated at position Cys214 by HIP14 (Huntingtin Interacting Protein 14), a palmitoyltranferase, that regulates the function of Htt and potentially its toxicity (Yanai, 2006). Htt is phosphorylated at several serine residues (Ser) including Ser421, Ser434, Ser536, Ser1181, Ser1201, Ser 2653 and Ser2657 (Figure 3.1 A), and these phosphorylations modulate potential Htt functions (Humbert, 2002; Luo, 2005; Schilling, 2006). For example, phosphorylation at Ser421 by Akt1 is neuroprotective against mHtt mediated toxicity in cells (Humbert, 2002).

Several consensus cleavage sites of different intracellular proteases, including caspases-1-3-6-7 and-8, calpains and aspartic endopeptidase have been identified

in Htt (Kim, 2001; Gafni, 2004; Lunkes, 2002; Hermel 2004). Proteolytic cleavage of Htt produces a variety of toxic poly(Q)-containing fragments, which play an important role in the progression of HD. It has been demonstrated that preventing Htt proteolysis by inhibition of calpain or caspase activity, or by modifying the consensus cleavage site in Htt protects against neuronal dysfunction and degeneration (Gafni, 2004; Graham, 2006).

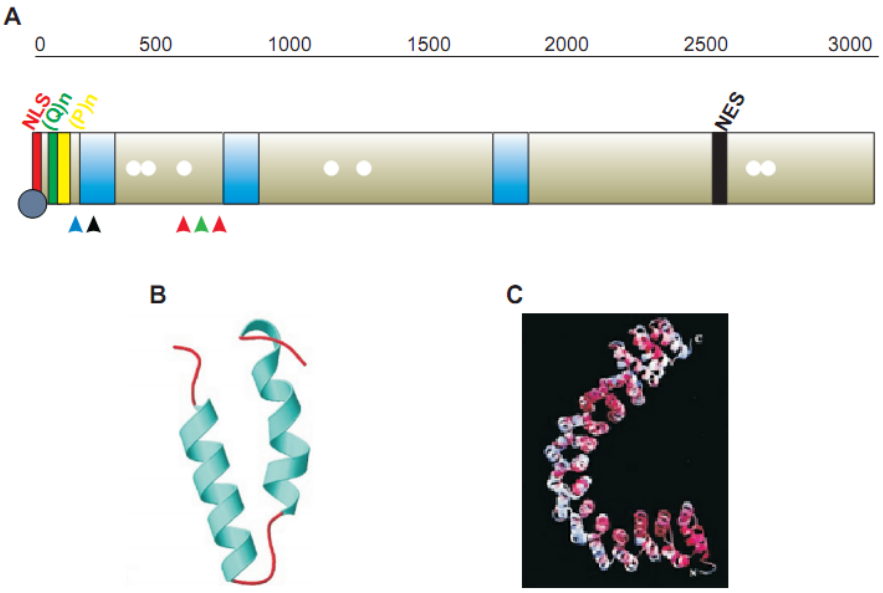

Figure 1-3: Structure of Huntingtin.

(A) Schematic representation of Htt protein. Red bar: NLS; green bar (Q)n: polyglutamine tract; yellow bar (P)n: polyproline sequence; blue bars: HEAT domains; black bar: NES; red arrowheads: caspase cleavage sites; green arrowhead: calpain cleavage site; blue arrowhead: aspartic endopeptidase cleavage site; black arrowhead: palmitoylation site; gray circle: sumoylation and ubiquitination sites; white circles: phosphorylation sites. (B) Model of a HEAT repeat. A HEAT repeat is a single helix-turn-helix motif. The helices (in cyan) vary in length, as do the intervening coil regions (red) (Li, 2006). (C) The crystal structure of the PR65/A subunit of protein phosphatase 2A show that HEAT repeats forms hydrophobic α helices, which assemble into an elongated superhelix containing a groove for protein-protein interactions. The structure of Htt HEAT-repeat clusters might be similar to this subunit (Groves, 1999).

The normal cellular functions of Htt are not well understood. This is mainly due to the large size of the protein (3144 amino acids; ~350 kDa) and the lack of obvious homology to other known proteins (HDCG, 1993). Htt is widely expressed in brain and peripheral tissues (Sharp, 1995; Trottier, 1995). Within the brain, Htt is expressed predominantly in neurons (Ross, 1995). It is found in cell bodies,

dendrites (DiFiglia, 1995), and is associated with large number of organelles, including the Golgi apparatus, mitochondria and the endoplasmic reticulum (ER) (DiFiglia, 1995; Kegel, 2005; Rockabrand, 2007).

Gene inactivation in living organisms is a powerful approach to study gene functions. Using this strategy a role of Htt in embryonic development has been proposed as knock-out of the HD gene in mice caused early embryonic lethality (Nasir, 1995; Zeitlin, 1995). In addition, inactivation of the HD gene in mouse brain and testes caused degeneration of these two organs, suggesting a functional role of Htt in cell survival pathways (Dragatsis, 2000). More recent studies from the Richard's lab have shown that Huntingtin-deficient zebrafishes exhibit a variety of early developmental defects such as small head and eyes, thin yolk extension and brain necrosis (Lumsden, 2007). Furthermore, several lines of genetic and biochemical experimental evidence indicate that wild-type Htt acts as an anti-apoptotic protein. Indeed, overexpression of wild-type Htt protects cells against a variety of apoptotic insults, including those caused by the overexpression of mHtt protein (Ho, 2001; Rigamonti, 2001). Increased apoptosis was also observed in knock-out mice lacking Htt protein (Zeitlin, 1995). One explanation of the anti-apoptotic activity of Htt is that it inhibits the activation of several apoptotic proteins including caspase-3-8 and-9 (Gervais, 2002; Rigamonti, 2001; Zhang, 2006). The anti-apoptotic activity of wild-type Htt may also occur by stimulating the expression of survival genes such as brain-derived neurotrophic factor (BDNF), which has been described as an important factor for the survival of striatal neurons (Zuccato, 2001). In accordance with these observations, wild-type Htt has been proposed to be a therapeutic factor for HD (Leavitt, 2001).

Another powerful strategy for elucidating the function of uncharacterized proteins is the identification of interacting partners. For this purpose, several interacting partners of Htt have been identified allowing novel insights into the biological function of the protein. For example, Htt interactions with HAP1 (Li, 1995), HIP1 (Wanker, 1997), PACSIN1 (Modregger; 2002) and SH3GL3 (Sittler, 1998) were identified. These proteins are involved in intracellular trafficking; strongly suggesting that Htt also plays a role in this process. Htt interacts with several transcription factors and transcriptional activators, including CREB (Bao, 1996),

Sp1 (Dunah, 2002), TBP (Huang, 1998), TP53 (Steffan, 2000) and TCERG1 (Holbert, 2001) as well as proteins involved in pre-mRNA splicing (Faber, 1998). These observations suggest a role of Htt in gene regulation and mRNA processing. In addition, a large number of cytoplasmic signaling proteins, e.g. GRAP (Burke, 1996), RASA1 (Burke, 1996), GRB2 (Liu, 1997) and MAP3K10 (Liu, 2000), form complexes with Htt, implying that Htt might influence different signaling pathways in neurons.

The large number of Htt interacting partners and its apparent role in several subcellular processes led to the hypothesis that Htt may serve as a scaffold protein, arranging protein complexes by modulating the binding of accessory factors (Harjes and Wanker, 2003).

1.4 Polyglutamine-mediated huntingtin aggregation and toxicity

The aggregation properties of polyQ peptides were described for the first time by Krull and colleagues. They demonstrated that polyQ tracts form large aggregates and become insoluble *in vitro* (Krull, 1965). In 1994, Max Pertuz proposed that polyQ stretches might self-associate and form cross ß-sheet structures (polar zippers) by hydrogen bonding involving the amide group of the glutamine residues (Perutz, 1994). This prediction suggested that extension of glutamine repeats might cause the affected proteins to aggregate and gradually precipitate in neurons (Perutz, 1994). In 1996, the first transgenic mouse of HD was generated by the laboratory of G. Bates. The mice, named R6/2, express a short N-terminal fragment of Htt (exon1) with an expanded polyQ tract (~150Q) and develop progressive behavioral symptoms and neuropathology observed in HD (Mangiarini, 1996). Immunohistochemical analyses of the R6/2 mouse brains revealed the presence of Htt aggregates in neuronal inclusions (Davies, 1997). Following these discoveries, Htt aggregates were subsequently detected in the post-mortem HD patients' brains (DiFiglia, 1997). Furthermore, Scherzinger et al. demonstrated that exon 1 of Htt with an expanded glutamine tract spontaneously forms amyloid fibrils *in vitro*, and that this process depends on the length of the polyQ repeats (Scherzinger, 1997). Consistent with this, the pathogenic length of

the polyQ stretch triggers misfolding of Htt and the formation of insoluble protein aggregates *in vitro* and *in vivo*.

Since then, there has been a considerable debate whether mHtt aggregates are neurotoxic or play a protective role in the pathogenesis of HD. In both HD transgenic mice and humans the neuronal intranuclear inclusions were observed before the onset of HD symptoms, suggesting a direct role of mHtt aggregates in neuronal dysfunction and toxicity (Davies, 1997; DiFiglia, 1997). Several lines of evidence demonstrate that overexpression of mHtt promotes aggregate formation and is sufficient to induce neuronal cell death in cellular and HD animal models (Li and Li, 1998). In addition, inhibition of mHtt misfolding and aggregation in cell and animal models of HD significantly reduces polyQ-mediated Htt cytotoxicity (Sanchez, 2003).

PolyQ-mediated Htt cytotoxicity is thought to result from interference of mHtt with various important cellular functions. In HD, the aggregates were found to be ubiquitinated and also abnormally contained many proteasome-associated proteins. This supports the hypothesis that sequestration of UPS (Ubiquitin-Proteasome-Systems) components and a subsequent failure of the degradative system leads to neurodegeneration (Jana, 2001; Ciechanover and Brundin, 2003). In addition, chaperone proteins are also sequestered into insoluble mHtt inclusion bodies (Hay, 2004). This sequestration reduces the amount of active soluble chaperones in cells, which in turn enhances abnormal protein folding (Hay, 2004). The restoration of active chaperone levels suppresses protein aggregation and toxicity mediated by mHtt. Indeed, overexpression of Hsp70, Hsp40, Hsp104, TRiC and CHIP is protective against proteotoxicity and cell death in HD cell and/or mouse model systems (Muchowski, 2000; Miller, 2005; Tam, 2007). Another potential mechanism by which mHtt aggregates might exert their toxicity is the sequestration of different transcription factors leading to the perturbation of several vital functions (Dunah, 2002; Landles and Bates 2004; Zhai, 2005).

However, certain studies argue against a primary role of mHtt aggregates in neurodegeneration. Neuropathological studies of post-mortem brain with different grades of HD showed a poor correlation between mHtt aggregates and the severity of clinical symptoms (Gutekunst, 1999). In addition, it was also observed

that many of the nuclear aggregates in striatum are present in neurons that resist neurodegeneration (Kuemmerle, 1998). These observations support a protective role of mHtt aggregates in HD (Kuemmerle, 1998; Gutekunst, 1999).
The R6/2 mouse model displays prominent intranuclear inclusions, but shows only little evidence for neuronal cell death (Davies, 1997). It was also observed that aggregate formation over time correlates with the neuronal survival in cell model systems (Arrasate, 2004). Therefore, the roles of polyQ aggregates in neurotoxicity/neuroprotection remain to be further investigated.

1.5 A protein interaction network for Huntington's disease

High throughput technologies have been used to identify Htt interaction partners in a systematic manner. Utilizing an automated yeast two hybrid system the research team of Prof. Wanker has created a highly connected PPI network for HD that contains 186 mostly novel interactions between 86 different proteins (Figure 1.4) (Goehler, 2004). Htt interacting proteins were broadly grouped into different functional categories such as transcription, protein trafficking, cellular signaling and metabolism, supporting the hypothesis that Htt functions in these processes (Goehler, 2004). Among the interactors, 19 proteins were identified to bind directly to Htt. Only four of these direct partners have been previously identified; huntingtin-interacting protein 1 (HIP1) (Wanker, 1997), the transcription-elongation factor CA150 (Holbert, 2001), the spliceosome protein HYPA (Faber, 1998), and the SH3-domain-containing Grb2-like protein SH3GL3 (Sittler, 1998).
The Htt interaction network allowed the identification of GIT1, a G-protein-coupled receptor kinase interactor 1, as a new enhancer of mHtt aggregation (Goehler, 2004), a process which is linked to disease progression and development of symptoms (Sanchez, 2003).

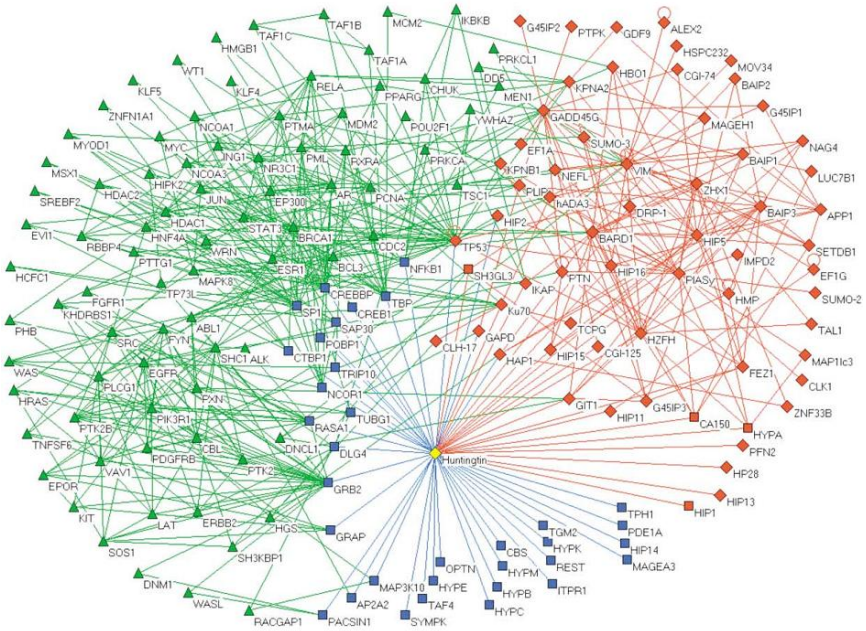

Figure 1-4: A protein interaction network for HD.

(Red diamonds) Y2H interactors of Htt newly identified; (Blue squares) previously published interactors; (Green triangles) interactors culled from human interaction databases; (Red squares) Htt interactions that were both newly identified and previously reported (Goehler, 2004).

More recently, Kaltenbach and colleagues combined high-throughput Y2H screening and affinity pull-downs followed by mass spectrometry to identify novel Htt interacting partners (Kaltenbach, 2007). This effort led to the identification of 234 Htt interacting partners. Based on the cellular properties, the Htt interacting proteins were grouped into several functional categories including proteins involved in cytoskeletal organization and biogenesis, signal transduction, synaptic transmission, proteolysis and regulation of transcription or translation.

Genetic screens for modifiers of mHtt-mediated neurodegeneration in a *Drosophila* eye model of HD revealed that 80% (48 of 60 proteins tested) of the proteins identified by interaction screening are suppressors or enhancers of the mHtt phenotype. This study demonstrated that potential modulators of HD pathogenesis are enriched in Htt interaction networks (Kaltenbach, 2007). Therefore, identification of cellular proteins that bind to Htt and modulate its pathological effects may facilitate the development of novel therapeutic strategies (Li and Li, 2007).

1.6 Generation dysregulated network of HD

The mHtt protein is ubiquitously expressed in central nervous system and peripheral tissues (Sharp, 1995; Trottier, 1995), but neuronal cell death is mostly observed in the striatum (Albin, 1995; Herdeen, 1995). One reason for this selective neuronal vulnerability might be the presence or absence of brain region-specific Htt-interacting proteins (Ross, 1995; Harjes and Wanker, 2003). Therefore, identification of tissue-specific Htt-interacting partners might help to understand the molecular mechanism of HD pathogenesis.

Recently, by integrating microarray gene expression and human PPI data, Chaurasia et al have developed a generic bioinformatic strategy to create a caudate nucleus-specific interaction network of HD. First, based on available literature information an Htt master PPI network was generated, which connects 506 proteins via 1319 interactions (Chaurasia, unpublished data). A large number of 62 direct Htt interactions were found, indicating that Htt is a hub in this human PPI network. In a second step, Chaurasia et al combined the PPI master network of Htt with gene expression profiles of genes differently expressed in the caudate nucleus compared to non-caudate tissues. The resulting map, termed caudate nucleus specific Htt protein network, connected 38 proteins via 44 interactions (Chaurasia, unpublished data).

Hodges et al reported gene expression profiles of 44 human HD brains and 36 unaffected controls (Hodges, 2006). They observed that the highest magnitude of differential gene expression changes occur in caudate nucleus of HD brains, suggesting that alterations in expression levels of Htt-interacting partners in the caudate nucleus might be crucial for the development of HD pathology (Hodges, 2006; Bhattacharyya, 2008).

Therefore, Chaurasia et al, combined the caudate nucleus-specific PPI network with the microarray gene expression data provided by Hodges et al, to generate a caudate nucleus specific dysregulated network of HD. This network contains 7 upregulated and 7 downregulated interacting partners directly or indirectly linked to Htt (Figure 1.5).

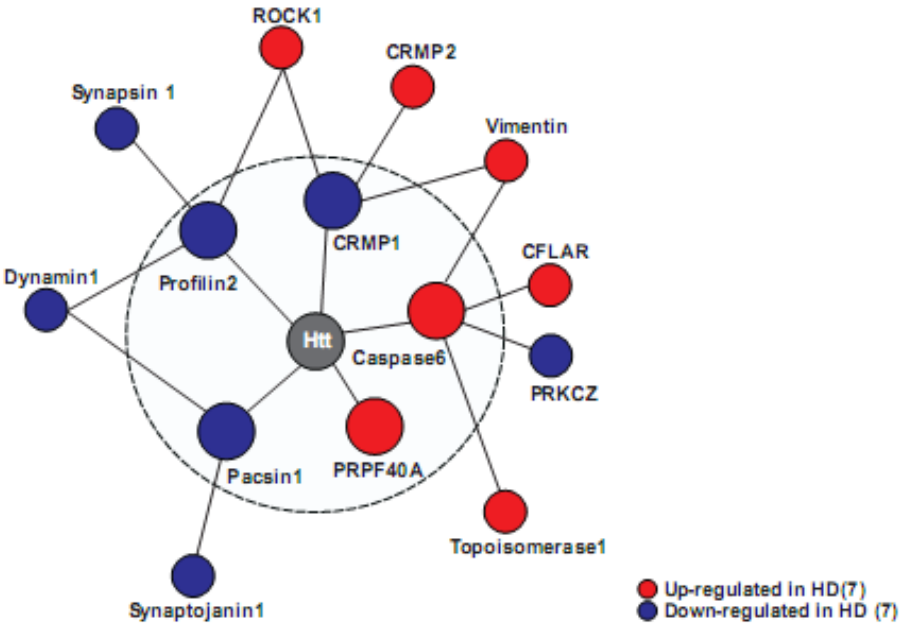

Figure 1-5: A caudate nucleus specific dysregulated network of HD.

The network comprises 15 proteins that are linked via 17 PPIs. The direct interaction partners of Htt are represented by large nodes; indirect partners are indicated by small nodes. The up-regulated proteins are colored in red; down-regulated proteins in blue. The dotted circle indicates the direct partners of Htt (Chaurasia et al, unpublished data).

The HD dysregulated network contains three proteins (Dynamin1, Pacsin1 and Profilin2) whose *Drosophila* orthologues influenced the neurodegenerative eye phenotype in a fly model of HD (Figure 1.6) (Kaltenbach, 2007; Burnett, 2008). Moreover, several other proteins including Caspase-6 (Graham, 2006), ROCK1 (Shao, 2008), and PRPF40A (Faber, 1998) have been already implicated in HD (Figure 1.6).

The network is also enriched with proteins related to apoptosis (Caspase 6, CFLAR, PRCKZ, PRPF40A, and ROCK1) and protein influencing the tubulin and actin cytoskeleton organization (CRMP1, CRMP2, Dynamin1, Pacsin1, Profilin2, and ROCK1) (Figure 1.6), processes known to be important for HD pathogenesis and other neurodegenerative disease (DiProspero, 2004; Graham, 2006; Zabel, 2009). This integrative network approach identified potential dysregulated proteins in the immediate molecular neighborhood of Htt, which might contribute to the HD pathogenesis.

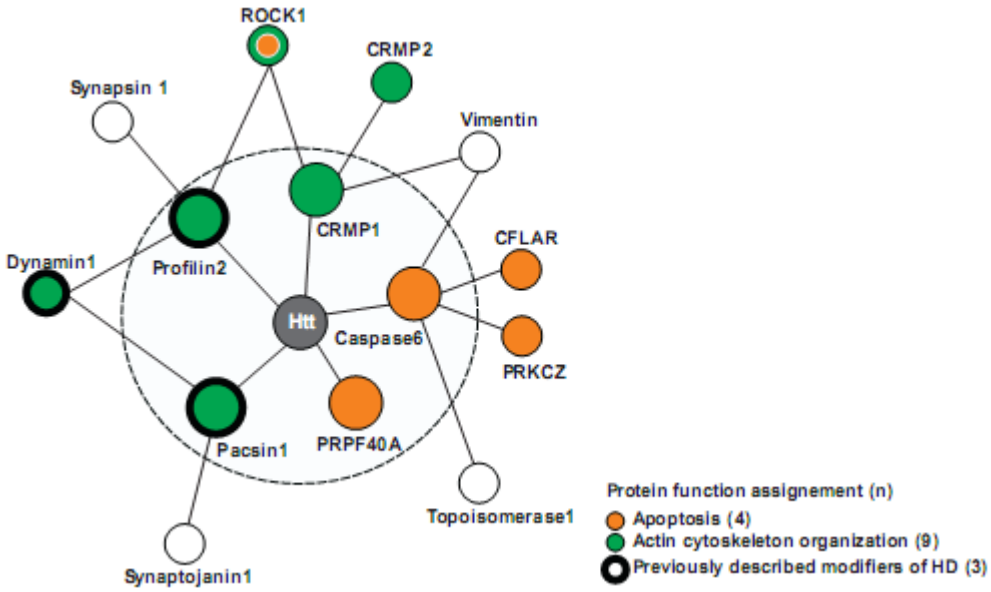

Figure 1-6: Functional annotation of the caudate nucleus dysregulated HD network.

The direct interaction partners of Htt are represented by large nodes; indirect partners are indicated by small nodes. The Htt-interacting partners potentially involved in apoptosis are colored in orange. Proteins involved in actin cytoskeleton organization are colored in green. Proteins whose *Drosophila* orthologues acted as modifiers are indicated as thick circles. Protein function assignment is based on the literature and Gene Onthology (GO) (Chaurasia et al, unpublished data).

Gene expression profiles from HD brains with small pathological alterations (grade 0 and 1) were compared with gene expression profiles obtained from patients with severe neuropathological changes (grade 2-4). It was observed that gene expression of CRMP1, encoding the neuron-specific Collapsin Response Mediator Protein 1 (CRMP1), undergoes the most significant dysregulation in the caudate nucleus of HD brains ($P \leq 0.0007$), suggesting a potential role of the CRMP1 protein in HD pathogenesis (Table 1.3) (Chaurasia et al, unpublished data).

Table 1-3: HD dysregulated network proteins.

Protein	full name	Expression	P-value
CRMP1	collapsin response mediator protein 1	down-regulation	**0.00007**
PRKCZ	protein kinase C, zeta	down-regulation	**0.00014**
CFLAR	CASP8 and FADD-like apoptosis regulator	up-regulation	**0.00014**
PACSIN1	protein kinase C and casein kinase substrate in neurons 1	down-regulation	**0.00014**
PRPF40A	PRP40 pre-mRNA processing factor 40 homolog A (S. cerevisiae)	up-regulation	**0.00069**
DNM1	dynamin 1	down-regulation	**0.00078**
SYN1	synapsin I	down-regulation	**0.00089**
ROCK1	Rho-associated, coiled-coil containing protein kinase 1	up-regulation	**0.00113**
SYNJ1	synaptojanin 1	down-regulation	0.05202
VIM	vimentin	up-regulation	0.05202
CRMP2	collapsin response mediator protein 2	up-regulation	0.06865
TOP1	topoisomerase (DNA) I	up-regulation	0.27113
PFN2	profilin 2	down-regulation	0.35600
CASP6	caspase 6, apoptosis-related cysteine peptidase	up-regulation	0.54886

The interaction partners of Htt found in the HD network listed according to the statistical significance of gene expression changes in the human caudate nucleus of HD brain patients (p-value). The table shows that the genes encoding for these interacting partners are down-regulated or up-regulated in the caudate nucleus of HD brains. (Chaurasia et al, unpublished data).

1.7 The CRMP protein family

The Collapsin Response Mediator Proteins (CRMPs) are a family of five homologous cytosolic phosphoproteins (CRMP1 to CRMP5), which are highly expressed throughout brain development (Minturn, 1995; Byk, 1996; Wang and Strittmatter, 1996). CRMP1-5 share ~50-75 % protein sequence identity (Byk, 1996; Hamajima, 1996; Wang and Strittmatter, 1996; Fukada, 2000) and are highly conserved throughout evolution (about 95% sequence conservation between mice and humans) (Byk, 1996). CRMPs are homologous to the worm unc-33 protein (30%) (Li, 1992; Minturn, 1995), and to the human dihydropyrimidinase (~60%) (Hamajima, 1996) or the bacterial enzyme D-hydantoinase (~40%) (Goshima, 1995). However, no enzymatic activity (dihydropyrimidinase or hydantoinase) has been detected for CRMPs. Interestingly, all CRMP proteins interact with each other and form homo- or heterotetramers (Wang and Strittmatter, 1997). This (homo)-hetero-oligomerization in multiple combinations builds diverse functional CRMP protein complexes with different physiological functions (Wang and Strittmatter, 1997). Several studies support a role of CRMPs in axonal outgrowth neurite differentiation (Quach, 2004), apoptosis (Shirvan, 1999) and neurodegenerative

disorders such as AD (Yoshida, 1998; Uchida, 2005) and PD (Stauber, 2008).

1.7.1 CRMPs influence neuronal survival

The sequence similarity of CRMPs with the nematode protein encoded by unc-33; a gene when mutated causes abnormalities in axonal arborization and uncoordinated worm movement (Hedgecock, 1985), has led several authors to suggest a role for CRMPs in axonal guidance and outgrowth (Li, 1992; Goshima, 1995). The expression patterns of CRMP family members are spatiotemporally regulated. They reach a peak during the first postnatal week, when maturation of neurons and synaptic development is active, and then they are downregulated when the axon growth processes are complete (Byk, 1996; Minturn, 1996; Wang and Strittmatter, 1996). In the adulthood, CRMPs are highly expressed in areas of the brain with a high degree of synaptic remodeling and plasticity such as the hippocampus, the olfactory system and the cerebellum, suggesting a role of CRMPs in neurogenesis (Charrier, 2003; Veyrac, 2005). A direct role of CRMPs in neuronal survival is also supported by observations that overexpression of CRMP2 induces axon formation in cultured hippocampal neurons (Inagaki, 2001) and accelerates nerve regeneration at injured motor neurons (Suzuki, 2003). Furthermore, blocking the function of endogenous CRMP1 in dorsal root ganglion neurons prevented neurotrophins-induced neurite outgrowth and extension (Quach, 2004). Neurotrophins are signaling molecules which play a role in the regulation of neurite extension and axonal arborization. Taken together, these observations suggest that CRMP proteins are key molecules that regulate neuritogenesis.

1.7.2 Calpains target CRMPs and induces neuronal cell death

Abnormal activation of glutamate receptor leads to excessive influx of calcium (Ca^{2+}) into neurons (Wang, 2000). The accumulation of toxic levels of intracellular Ca^{2+} activates cysteine proteases from both the caspase and calpain families (Wang, 2000). Calpains are a highly conserved family of Ca^{2+}-activated intracellular proteases, which are involved in the cleavage of a wide variety of proteins including cytoskeletal elements such as spectrin (Siman, 1996) or

signaling molecules such as CDK-5 (Smith, 2006).

A large number of neurological disorders, including AD (Saito, 1993; Tsuji, 1998), PD (Mouatt-Prigent, 1996), HD (Hodgson, 1999; Gafni and Ellerby, 2002), ALS (Ueyama, 1998), cerebral ischemia and spinal cord injury (Banik, 1997) have been associated with abnormal activation of calpains. Furthermore, it has been demonstrated that inhibition of calpains is neuroprotective (Bartus, 1994; 1995). Therefore, identification and characterization of calpain substrates will shed light on molecular mechanisms of neuronal cell death (Gafni and Ellerby, 2002).

Previous studies have implicated CRMPs in neuronal cell death processes. Evidence was that CRMP3 is cleaved by calpains during cerebral ischemia and glutamate excitotoxicity (Hou, 2006). Calpain cleavage of full-length CRMP3 protein (65 kDa) resulted in the production of an N-terminally truncated fragment of 55 kDa. The calpain-cleaved CRMP3 fragment translocated into the nucleus and induced neuronal cell death (Hou, 2006). In addition, it has been shown that all five CRMP proteins are cleaved by calpain in response to cerebral ischemia and glutamate toxicity (Kowara, 2005; Bretin, 2006; Jiang, 2007). Jiang and collegues showed that CRMP proteins colocalize with TUNEL-positive neurons and are translocated into nucleus in ischemic brains (Jiang, 2007). This suggests an important role of CRMPs in ischemia-induced neuronal toxicity. In conclusion, an alteration of the biological function of CRMP proteins may be a critical step in the process that leads to neuronal cell death.

1.7.3 CRMPs and diseases

Under pathological conditions, CRMPs have been proposed to play a role in neuronal alterations occurring in lysosomal disease (Cheillan, 2008), neuronal death and neurodegenerative disorders (Charrier, 2003). In particular, CRMP2 was found to be associated with neurofibrillary tangles in patients with AD (Uchida, 2000; Good, 2004). Interestingly, hyperphoshorylation of CRMP2 delineates early events in AD (Cole, 2007). Recently it was suggested that the proteins CRMP1 and CRMP2 might be use as biomarkers in PD (Stauber, 2008). Mice lacking CRMP1 display an alteration of both dendrites and dendritic spin morphology in hippocampal neurons leading to a reduction of LTP (Long Term Potentiation) and

impairment of spatial memory performance (Su, 2007). These observations suggest a role of CRMP1 in spatial learning and neuronal plasticity. Alteration of CRMP1 functions therefore may contribute to cognitive deficits (Su, 2007). Another member of the family, CRMP4, was implicated in the pathogenesis of bovine spongiform encephalopathy (Auvergnon, 2009). Therefore, further understanding of the function of CRMP proteins will be important for elucidating numerous aspects of nervous system development and pathology.

1.8 Aim of the thesis

Several lines of evidence indicate that many Htt-interacting proteins colocalize with insoluble Htt inclusions in HD brains and modulate the mHtt phenotype (Goehler, 2004; Kaltenbach, 2007).

A striatum-specific, dysregulated PPI network has been created recently by integrating PPI networks with information from gene expression profiling data (Chaurasia, unpublished data). One of the identified dysregulated protein was the neuron-specific Collapsin Response Mediator Protein 1 (CRMP1). The main focus of my study was to investigate the role of CRMP1 protein on mHtt aggregation and toxicity using diverse model systems of HD. This will increase our understanding of HD pathogenesis.

Chapter 2
Results

2 Result

2.1 Generation of polyclonal CRMP1 antibodies

In order to study the role of CRMP1 in HD pathogenesis, rabbit polyclonal antisera were raised against the peptides derived from the primary human CRMP1 sequences: **504-YEVPATPKYATPAPS-518** and **513-ATPAPSAKSSPSKHQ-527** (Figure 2.1). CRMP1-504 (for peptide 504-518) and CRMP1-513 (for peptide 513-527) antibodies were produced and affinity purified by Eurogentec SA, Belgium.

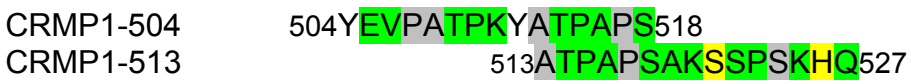

Figure 2-1: Peptide sequences used for antibody production.

The peptides 504-518 and 513-527 derived from the primary human CRMP1 protein were used for antibody production.

The specificity, signal strength and crossreactivity of affinity purified anti-CRMP1-504 and anti-CRMP1-513 antibodies were investigated using dot-blot assays and Western blotting.

Recombinant His-CRMP1 and His-CRMP2 proteins were produced in *E. coli* and purified under native conditions by affinity purification. Different amounts of both proteins were spotted onto a nitrocellulose membrane and the bound proteins were detected with affinity purified CRMP1-504 (1µg/ml), CRMP1-513 (1µg/ml), anti-CRMP2 (Abcam), or monoclonal anti-His antibodies.

I found that the affinity purified CRMP1-504 antibody recognized 5-10 ng purified His-CRMP1 protein in dot blot assays, while the His-CRMP2 protein was not detectable even much higher concentration (~1 µg). This indicates the high specificity of the CRMP1-504 antibody. In comparison, the polyclonal CRMP1-513 antibody recognized the His-CRMP1 protein very weakly. However, similarly to CRMP1-504 antibody, the CRMP1-513 antibody did not crossreact with His-CRMP2 protein. A commercial anti-CRMP2 antibody was used in the experiment to recognize the purified His-CRMP2 protein (Figure 2.2 A).

I also tested whether CRMP1 antibodies recognize the endogenous protein in mouse brain extracts. Protein lysates were prepared from mouse brain cortex of 12 weeks age, resolved in SDS-PAGE and blotted onto nitrocellulose membranes

(Schleicher and Schuell). Then, the membranes were immunodetected with anti-CRMP1 antibodies. The CRMP1-504 and CRMP1-513 antibodies recognized two bands running at ~ 65 kDa and 75 kDa, corresponding to the putative sizes of the CRMP1 protein (572 amino acids) and its N-terminal splice variant CRMP1A (686 amino acids), respectively (Quinn, 2003; Bretin, 2005) (Figure 2.2 B). These bands were not detectable with the preimmune sera, or antibodies that were preabsorbed with the corresponding peptides (Figure 2.2 B). In comparison to the CRMP1-513 antibody, the immunoreactivity of the CRMP1-504 antibody was much stronger when mouse brain extract were analyzed by Western blotting (Figure 2.2 B panel a, and c). Taken together, these results indicate that the purified polyclonal CRMP1 antibodies specifically recognize the endogenous CRMP1 proteins.

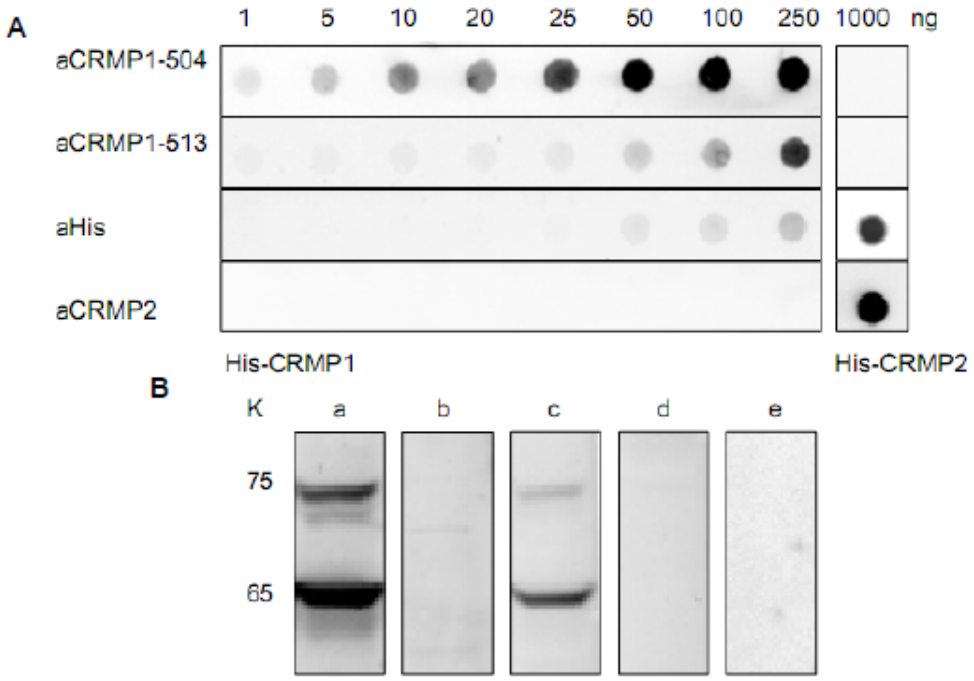

Figure 2-2: Characterization of polyclonal anti-CRMP1 antibodies.

(A) Dot-blot assay with anti-CRMP1 and anti-CRMP2 antibodies. Different amounts of His-CRMP1 and His-CRMP2 proteins were spotted onto nitrocellulose membranes. Then the membranes were detected with CRMP1-504, CRMP1-513, CRMP2 or His antibodies. (B) Immunoblot of mouse total brain extract using CRMP1 antibodies. Lane a, detection with affinity purified CRMP1-504 antibody; lane b, CRMP1-504 preabsorbed with 5 M excess of the corresponding peptide (aa 504-518); lane c, detection with affinity purified CRMP1-513 antibody; lane d, CRMP1-513 preabsorbed with 5 M excess of the corresponding peptide (aa 513-527); lane e, preimmune serum. K, kDa.

Next, due to the high sequence homology between CRMP family members, the specificity of anti-CRMP1-504 and anti-CRMP1-513 antibodies was further investigated by Western blotting using overexpressed hemagglutin (HA)-tagged versions of human CRMP proteins (HA-CRMP1, HA-CRMP2, HA-CRMP3, HA-CRMP4, and HA-CRMP5). COS1 cells were transfected with plasmids encoding the HA-CRMP proteins and 40 hours post-transfection, total extracts were prepared and analyzed by SDS-PAGE and Western blotting using CRMP isoform-specific and anti-HA antibodies. The antibodies anti-CRMP1-504 and anti-CRMP1-518 specifically recognized HA-CRMP1 and did not cross-react with any of the other CRMP isoforms. Anti-CRMP2 (Abcam), anti-CRMP4 (BD Pharmingen), and anti-CRMP5 (BD Transduction Laboratories) antibodies detected their expected target proteins only (Figure 2.3). These studies indicate that the purified CRMP1 antibodies specifically detect the overexpressed HA-CRMP1 protein in mammalian cells.

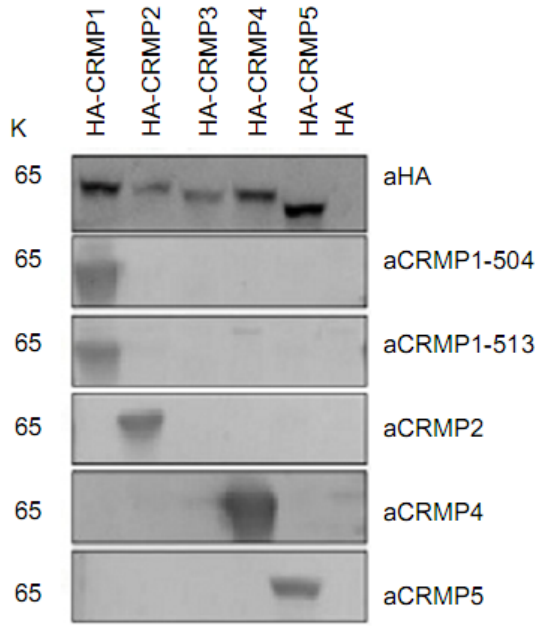

Figure 2-3: Characterization of the specificity of CRMP1antibodies in mammalian cells.

Polyclonal anti-rabbit CRMP1-504 and anti-rabbit CRMP1-513 antibodies were tested against a panel of overexpressed HA-CRMP1, HA-CRMP2, HA-CRMP3, HA-CRMP4, and HA-CRMP5 proteins. HA-CRMP protein expression was detected with HA-specific and CRMP isoform-specific antibodies. K, kDa.

Next, I examined the distribution of CRMP1 protein in primary cultures of mouse cortical neurons by immunocytochemistry. Immuonofluorescence staining with the anti-CRMP1-504 antibody revealed that CRMP1 protein is localized along neurites and homogenously distributed in the cell body. This is in agreement with previous studies describing a similar distribution pattern of CRMP1 in cultures of cortical neurons (Bretin, 2005).

No staining was observed when the antibody was preabsorbed against the peptide spanning amino acids 504-518 (Pre-CRMP1-504), indicating that the CRMP1-504 antibody specifically recognizes the endogenous CRMP1 protein in primary cortical neurons.

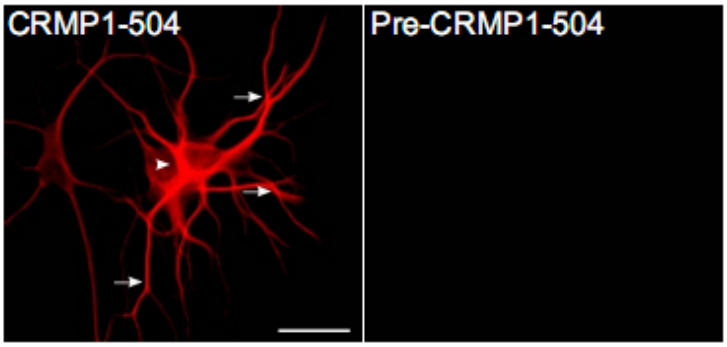

Figure 2-4: Localization of CRMP1 in cortical neurons.

Cortical neurons stained with affinity purified CRMP1-504 antibody or with Pre-CRMP1-504 antibody. Arrows show CRMP1 distribution along neurites and arrowheads show enrichment of CRMP1 in the cell body. Scale bar, 20 µm.

2.2 CRMP1 forms a complex with Htt

To investigate whether CRMP1 forms a complex with Htt, COS1 cells were cotransfected with plasmids encoding the first 510 amino acids of Htt with 17 glutamines (HD510Q17) and an N-terminally hemagglutin (HA)-tagged HA-CRMP1 protein. 40 hours post-transfection, total cell extracts were prepared and immunoprecipitated with polyclonal anti-Htt HD1 antibody. The immunocomplexes were analyzed by SDS-PAGE and Western blotting using either the monoclonal anti-Htt antibody 4C8 or the monoclonal anti-HA antibody. HD510Q17 and HA-CRMP1 proteins were detected in the immunoprecipitates, suggesting that these

proteins form a complex in mammalian cells (Figure 2.5A). In control experiments, neither the non-immune serum nor the empty beads precipitated the HA-CRMP1 protein.

In addition, the CRMP1-Htt interaction was analyzed using a tandem affinity purification assay (Stelzl, 2005; Horn, 2006). COS1 cells were transiently cotransfected with constructs encoding HA-CRMP1 and a protein A (PA)-tagged Htt protein (TAP-HD510Q17). After 48 hours post-transfection, cell extracts containing the TAP-HD510Q17 and HA-CRMP1 proteins were prepared and incubated with IgG-coated beads (Rigaut, 1999). The interaction of HA-CRMP1 with TAP-HD510Q17 was detected by SDS-PAGE and immunoblots using anti-HA or anti-CRMP1-504 antibodies. Figure 2.5 B shows that HA-CRMP1 was pulled down from COS1 cell extracts with TAP-HD510Q17, confirming the results of the coimmunoprecipitation experiments.

Next, the CRMP1-Htt interaction was analyzed *in vivo* (Figure 2.5 C). Protein extracts prepared from mouse brain were immunoprecipitated with the polyclonal anti-Htt antibody HD1 and the precipitate was analyzed for the presence of endogenous CRMP1 using SDS-PAGE and immunoblotting with anti-CRMP1-504 antibody. Full-length CRMP1 was immunoprecipitated with the anti-Htt HD1 antibody, indicating that the protein of CRMP1 and Htt form a complex under physiological conditions. In control experiments, no detectable CRMP1 was precipitated with non-specific IgG, non-immune serum or an anti-synaptobrevin antibody.

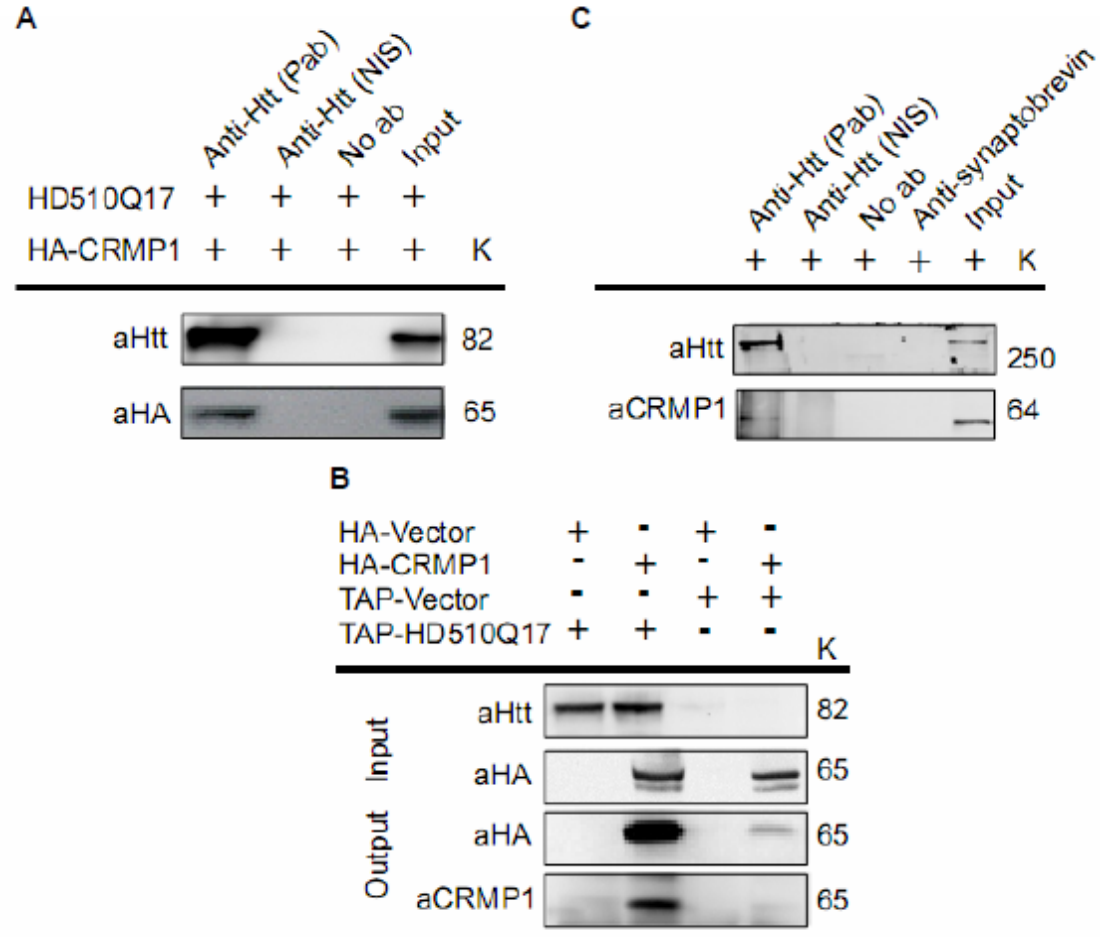

Figure 2-5: CRMP1 forms a complex with Htt.

(A) Immunoprecipitations (IPs) from COS1 cells expressing HA-CRMP1 and HD510Q17. IPs were performed with a polyclonal anti-Htt antibody (HD1). As a control non-immune serum (NIS), or empty beads without antibody addition were used. The immunoprecipitated material was analyzed by Western blotting using monoclonal anti-Htt (4C8) and anti-HA antibodies. (B) Tandem affinity purification experiment with COS1 cells extracts containing TAP-HD510Q17 and HA-CRMP1 proteins. The interaction between the HA-CRMP1 and TAP-HD510Q17 proteins was detected with anti-CRMP1 or anti-HA antibodies. (C) IPs from wild-type mouse brain extracts with polyclonal anti-Htt (HD1) and anti-synaptrobrevin antibodies. Control experiments were carried out with beads containing anti-Htt non-immune serum (NIS) or beads without antibody. Immunodetection was performed with polyclonal anti-CRMP1-504 antibody. K, kDa.

2.3 CRMP1 localizes with inclusion bodies containing mutant huntingtin

Accumulation of insoluble, aggregated polyQ-containing Htt protein in brains of patients and polyQ disease models represents one of the pathological hallmarks of the HD (Davies, 1997; DiFiglia, 1996). To this day a number of different proteins

have been found to localize to the neuronal inclusions, including members of the heat shock/chaperone family, components of the ubiquitin/proteasome machinery, proteins involved in intracellular trafficking and transcription factors (Holbert, 2001; Jana, 2001; Ciechanover and Brundin, 2003; Goehler, 2004).

Since CRMP1 forms a complex with Htt, I have investigated whether the protein associates with mHtt aggregates in a ponasterone (PonA) inducible cultured rat pheochromocytoma (PC12) cells model of HD (Apostol, 2002, 2006), in a transgenic HD *Drosophila* model (Kaltenbach, 2007), and in R6/2 HD transgenic mice (Mangiarini, 1996).

The PC12 cells stably express the first 17 amino acids of Htt with 103 glutamines fused at the C-terminus to the enhanced green fluorescent protein (EGFP-HttQ103). In this cell model accumulation of insoluble mHtt aggregates is observed and cellular dysfunction (e.g. caspase-3 activation) was detected (Apostol, 2002, 2006).

The cells were induced for 48 hours with 5 µM PonA and immunolabeled with anti-CRMP1-504 antibody. Analysis by immunofluorescence microscopy demonstrated that endogenous CRMP1 protein, indeed, is associated with mHtt aggregates in PC12 cells (Figure 2.6).

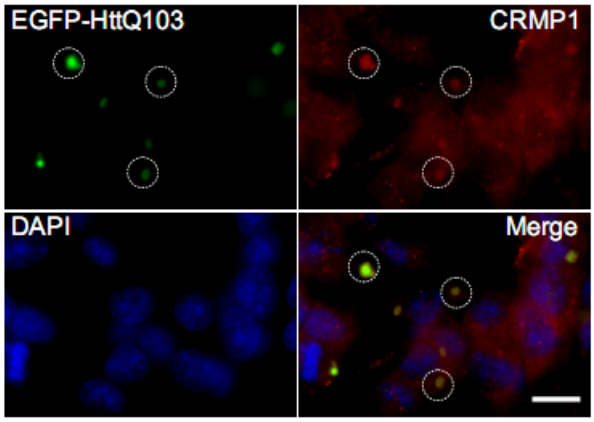

Figure 2-6: CRMP1 localizes with mHtt aggregates in a PC12 cell model of HD.

CRMP1 and EGFP-HttQ103 co-localization was detected by immunofluorescence microscopy using anti-CRMP1-504 antibody and EGFP fluorescence. DAPI stain was used to visualize the nuclei. Colocalization was demonstrated by merging EGFP-HttQ103 and CRMP1 images (merge images). The dotted circles indicate mHtt aggregates. Scale bar: 10 µM.

Next, I have investigated whether CRMP1 localizes to the mHtt inclusions in *vivo* using a transgenic *Drosophila* HD model (Kaltenbach, 2007) and R6/2 transgenic mice (Mangiarini, 1996).

The *Drosophila* model expresses an N-terminal fragment of human Htt with 336 amino acids and 128 glutamines (N-336Q128). Overexpression of the mHtt fragment, by the glass multimer reporter, (GMR)-GAL4 driver in cells of the retina leads to the formation of large perinuclear inclusions containing mHtt aggregates and a progressive eye photoreceptor degeneration phenotype (Marsh, 2003; Kaltenbach, 2007).

Eye imaginal discs of third instar larvae overexpressing mHtt and Myc-CRMP1 were immunostained with monoclonal anti-Htt 1-82 (Millipore) and anti-Myc antibodies 71D10 (Cell Signaling Technology). Confocal immunofluorescence microscopy analysis revealed that the Myc-CRMP1 protein co-localized with insoluble mHtt aggregates in photoreceptor neuron precursor imaginal discs, supporting the results obtained with the PC12 cell model of HD (Figure 2.7 A).

The R6/2 transgenic mouse model of HD expresses exon 1 of the human HD gene with ~150 CAG repeats (Mangiarini, 1996). The R6/2 mice display several symptoms which resemble the pathogenesis of HD in human. The mice exhibit an early onset of motor symptoms (5-6 weeks), severe body and brain weight loss, clasping, tremor, convulsions and a premature death at 13-15 weeks (Mangiarini, 1996, Davies, 1997; Carter, 1999). In addition, neuropathological analysis revealed the presence of mHtt aggregates in neuronal inclusion already at 4-5 weeks of age (Li, 1999; Morton, 2000).

Striatal slices of R6/2 (12 weeks old) HD transgenic mice were immunostained with antibodies recognizing CRMP1 (anti-CRMP1-504) and Htt (EM48) and analyzed with confocal immunofluorescence microscopy. I found that CRMP1 immunoreactivity was enriched in large nuclear inclusions containing mHtt aggregates (Figure 2.7 B), suggesting that CRMP1 is recruited to mHtt aggregates in HD transgenic mice.

Collectively, I found that CRMP1 co-localizes with mHtt aggregates in PC12 cells, *Drosophila* HD cell and neurons of HD transgenic mice.

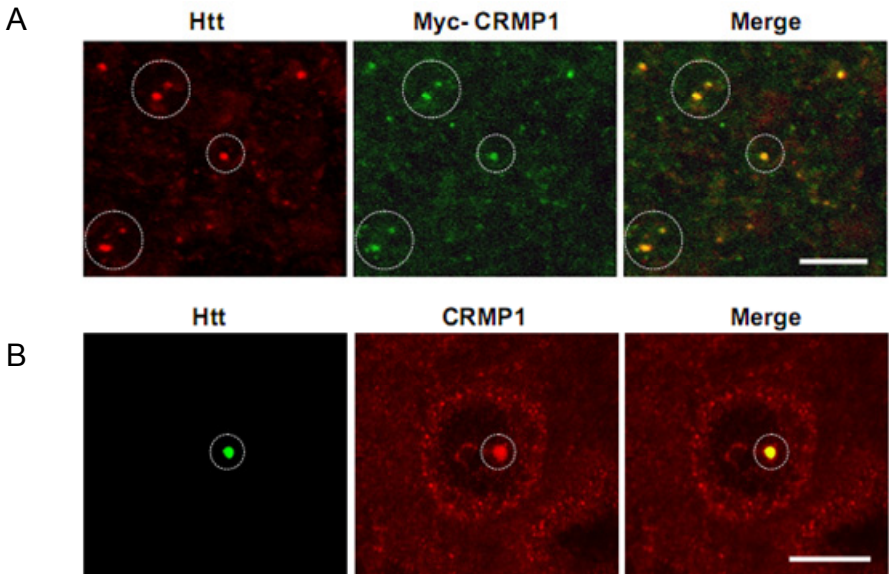

Figure 2-7: CRMP1 is localized to mHtt aggregates in *Drosophila* and R6/2 transgenic animal models of HD.

(A) Double immunostaining of Htt (Htt: 1-82 mouse antibody; in red) and Myc-CRMP1 (Myc 71D10 rabbit antibody; in green) in imaginal discs of third instar larvae. The degree of colocalization was illustrated by merging Htt and Myc-CRMP1 images (merge image). (B) Double immunostaining of Htt (Htt: EM48 mouse antibody; in green) and CRMP1 (CRMP1-504 rabbit antibody; in red) in the striatum of R6/2 brains at 12 weeks. The degree of colocalization was illustrated by merging Htt and CRMP1 images (merge image). The dotted circles indicate mHtt aggregates. Scale bar: 10 μM.

2.4 CRMP1 prevents aggregation and rescues mutant huntingtin toxicity

I investigated whether up and down-regulation of CRMP1 levels influences mHtt aggregation and toxicity in the PC12 cell model of HD (Apostol, 2002). Previous studies have demonstrated that PonA induction of EGFP-HttQ103 in this model leads to the formation of EGFP-Htt aggregates and a marked elevation of caspase-3 activity in comparison to non-induced cells (Apostol, 2006). The increase in caspase-3 activity indicates cellular dysfunction and toxicity (Budihardjo, 1999).

I employed the short-interfering RNA (siRNA) technology to knock-down the endogenous CRMP1 protein. The PC12 cells were transfected with CRMP1-specific siRNA or with non-coding siRNA as a control and 48 hours post-

transfection the cells were induced with 5 µM PonA. 40 hours post-induction cell protein extracts were prepared and analyzed by Western blotting and native filter retardation assay. Western blot analysis with CRMP1-504 antibody revealed that the CRMP1 siRNA treatment significantly reduced endogenous CRMP1 levels by ~80%, whereas the levels of CRMP2, ß-actin or soluble EGFP-HttQ103 remained stable. This indicates a specific reduction of CRMP1 protein by siRNA treatment (Figure 2.8 A).

Next, the protein lysates were filtered through a cellulose acetate membrane (Schleicher and Schuell, 0.2 µM pore size) and EGFP-HttQ103 aggregates retained on the filter membrane were detected using EGFP fluorescence under blue light in an image reader. As shown in Figure 2.8 A and B knock-down of CRMP1 in PC12 HD cells significantly ($P < 0.01$) increased the amount of EGFP-HttQ103 aggregates.

Subsequently, in follow-up experiments, I evaluated whether overexpression of HA-CRMP1 influences the amount of EGFP-HttQ103 aggregates. The PC12 cells were transfected with a construct encoding a HA-tagged CRMP1 protein and 12 hours post-transfection the cells were induced with 5 µM PonA. 40 hours post-induction cell protein extracts were prepared and analyzed by Western blotting and native filter retardation assay (Figure 2.8 C). Overexpression of HA-CRMP1 in PC12 cells was confirmed by Western blotting using an anti-HA monoclonal antibody. Similarly as in knock-down experiments, the expression of HA-CRMP1 did not influence the expression of the EGFP-HttQ103 protein. EGFP-HttQ103 aggregates were detected using the native filter retardation assay by measuring EGFP fluorescence. Figures 2.8 C and D show that overexpression of HA-CRMP1 strongly reduced the formation EGFP-HttQ103 aggregates ($P < 0.001$).

Taken together, these results strongly indicate that CRMP1 levels in cells influences the process of mHtt aggregate formation.

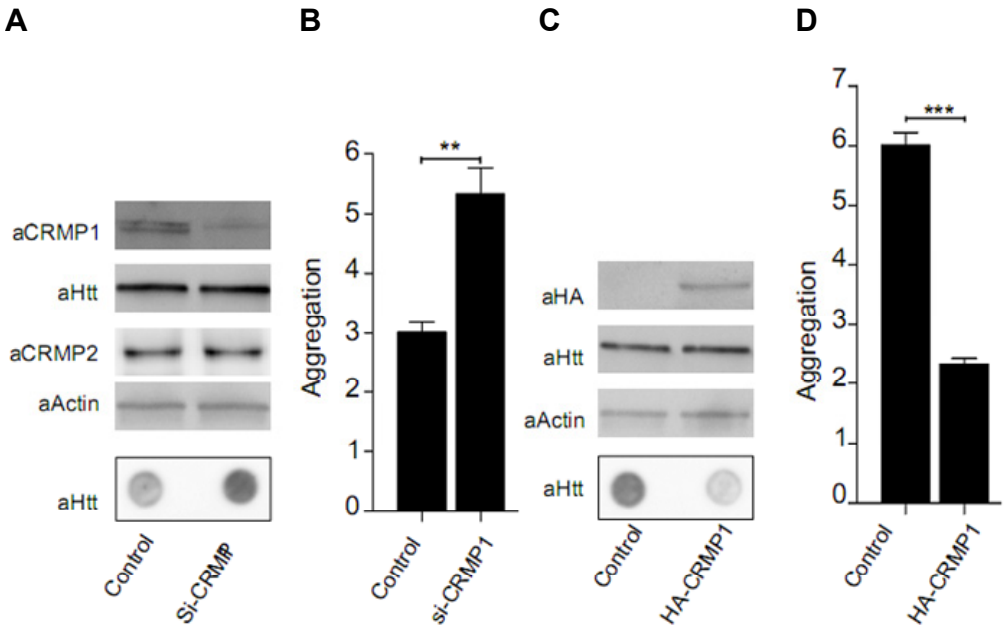

Figure 2-8: CRMP1 levels influence EGFP-HttQ103 aggregation in a PC12 HD model.

(A) Silencing of endogenous CRMP1 increases the formation insoluble EGFP-HttQ103 aggregates, while (C) overexpression of HA-CRMP1 decreases the aggregation. (B), (D) Quantification of the results shown in A and C, respectively. EGFP- HttQ103 aggregates retained on the filter membrane were detected by EGFP fluorescence under blue light using an image reader. The bars depict the mean and SD of three independent experiments. Significance levels were determined using unpaired student's t-test. ***Significance, P<0.001, **significance, P<0.01.

Given the key role of mHtt aggregates in triggering toxicity and cell death (Sanchez, 2003) I speculated that the ability of CRMP1 to suppress mHtt aggregation might also translate into its ability to inhibit mHtt-mediated toxicity.

To test this possibility, I investigated whether altering the levels of CRMP1 influences apoptosis caused by overexpression of mHtt in the PC12 HD model.

It has been shown previously that induction of EGFP-HttQ103 expression in PC12 cells causes cellular dysfunction and caspase-3 activation (Apostol, 2006). Therefore, I have evaluated caspase-3/7 activation as an indicator of apoptotic stress mediated by overexpression of mHtt in PC12 cells.

The activity of caspase-3/7 can be quantified using the Apo-ONE caspase-3/7 assay (Promega). PC12 cells treated with CRMP1 specific siRNA or transfected with a plasmid encoding the HA-CRMP1 protein were incubated with a bifunctional cell lysis/activity buffer containing the pro-fluorescent substrate Z-DEVE-R110. The

substrate can be cleaved by active caspase-3/7 revealing a fluorescent group, what can be quantified by measuring the absorbance at 499 nm. The increase in fluorescence signal correlates with elevated caspase-3/7 activity.

I found that reduction of endogenous CRMP1 levels resulted in a significant increase ($P<0.01$) of caspase-3/7 activity (Figure 2.9 A), while overexpression of HA-CRMP1 reduced caspase-3/7 activity (~ 58%± 7.92, $P< 0.01$) (Figure 2.9 B). This indicates that altering CRMP1 levels influences mHtt-mediated cellular toxicity in PC12 cells.

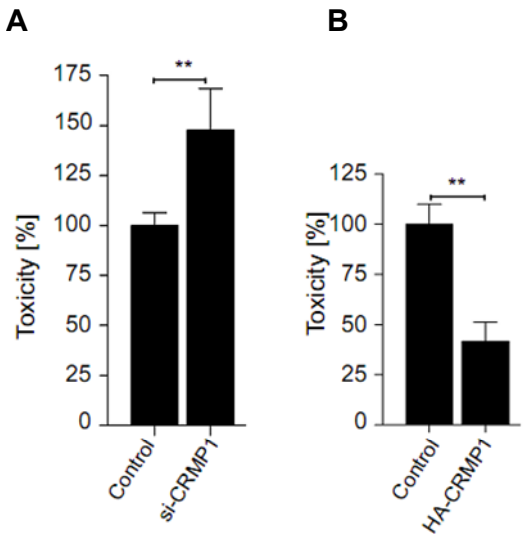

Figure 2-9: CRMP1 influences mHtt-mediated toxicity in a PC12 HD model.

(A) Silencing of CRMP1 increases EGFP-HttQ103 toxicity, while (B) overexpression of HA-CRMP1 decreases the toxicity. The bars depict the mean and SD of three independent experiments. Significance levels were determined using unpaired student's t-test, **significance, $P<0.01$.

Next, I investigated whether overexpression of human Myc-tagged CRMP1 protein influences mHtt-induced aggregation and neurodegeneration in a *Drosophila* model of HD (Marsh, 2003; Kaltenbach, 2007).

Eye imaginal discs of third instar larvae co-expressing a human Htt fragment (Htt336Q128) with or without a human Myc-tagged CRMP1 protein were immunolabeled with anti-Htt 1-82 antibody. Immunofluorescence microscopy analysis revealed that the formation of typical neuronal inclusion bodies with aggregated mHtt protein was dramatically reduced after co-expression of Myc-

CRMP1. In comparison, no such effect was observed with the control protein GFP (Figure 2.10 A and B).

The overexpression of the transgenes was analyzed by SDS-PAGE and Western blotting. Protein extracts prepared from eye imaginal discs of third instar larvae containing the proteins Htt336Q128/Myc-CRMP1 or Htt336Q128/GFP were investigated. The target proteins were recognized with anti-Htt HD1, anti-CRMP1-504, anti-Myc and anti-GFP antibodies as expected. These experiments also revealed that overexpression of the proteins Myc-CRMP1 or GFP did not influence the expression of the Htt336Q128 protein (Figure 2.10 C).

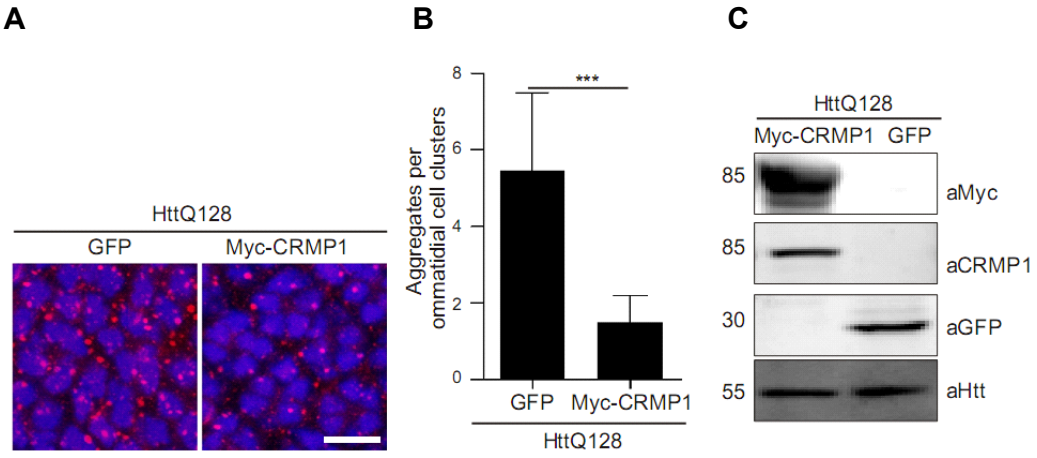

Figure 2-10: Overexpression of Myc-CRMP1 reduces mHtt aggregation in a *Drosophila* HD model.

(A) Htt aggregate formation in eye imaginal discs was analyzed by immunofluorescence microscopy using the anti-Htt 1-82 antibody. (B) Quantification of the results shown in A. (C) Western blot analysis of transgene expression in the eye imaginal discs in third instar larvae. The bars depict the mean and SD. Significance levels were determined using unpaired student's t-test, ***significance, P<0.001. K, kDa.

Previous studies have demonstrated that expression of Htt proteins with expanded polyQ tracts cause a progressive photoreceptor degeneration in *Drosophila* eyes (Marsh, 2003; Kaltenbach, 2007). The degenerative phenotype is evident by retinal histology changes and can be monitored by light microscopy (Kaltenbach, 2007). I have found that over-expression of Myc-CRMP1 can partially rescue the Htt336Q128-medited neurodegenerative eye phenotype *in vivo*. Such an effect

was not observed when the control protein GFP was co-expressed together with mHtt (Figure 2.11). Therefore, my results strongly indicate that CRMP1 is able to ameliorate the mHtt-induced retinal degeneration phenotype.

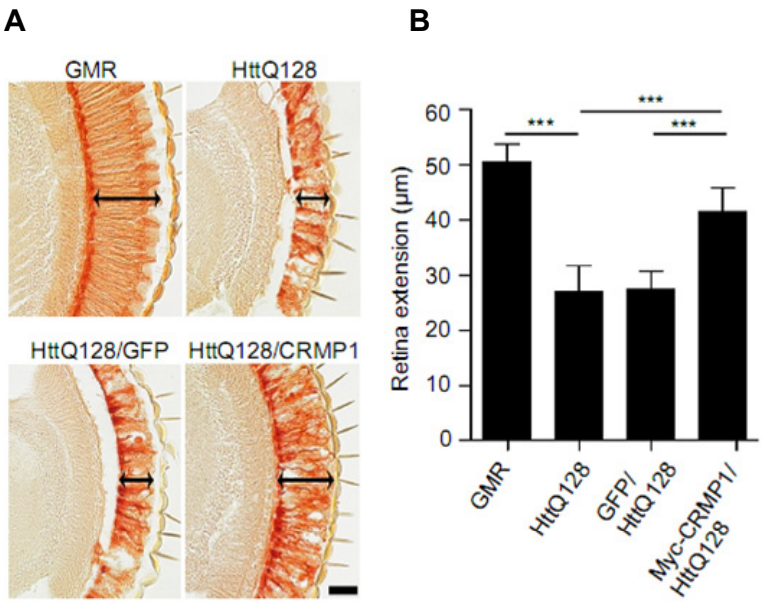

Figure 2-11: Overexpression of Myc-CRMP1 reduces mHtt toxicity in a Drosophila HD model.

(A) Light microscopy analysis of paraffin sections of 2-day-old flies expressing HttQ128 alone or together with Myc-CRMP1 or GFP. (B) Quantification of the results shown in A. The bars depict the mean and SD. Significance levels were determined using unpaired student's t-test, ***significance, P<0.001

2.5 CRMP1 modulates Htt polyQ aggregation *in vitro*

2.5.1 Production of recombinant proteins

Since CRMP1 forms a complex with Htt and modulates polyQ aggregation *in vivo*, I decided to examine whether CRMP1 can directly influence the self-assembly of insoluble Htt protein aggregates *in vitro*. To perform such experiments the proteins GST-FLAG-HttQ23 (G-HttQ23), GST-FLAG-HttQ51 (G-HttQ51), GST-CRMP1 (G-CRMP1), GST, His-CRMP1, and His-GAPDH were expressed in *E. coli* and purified under native condition by affinity purification (Scherzinger, 1997). SDS-PAGE analysis and Coomassie blue staining of purified proteins revealed that the

proteins G-HttQ23 and G-HttQ51 migrated in SDS-gels at positions higher than their calculated molecular weights, which were 40 and 55 kDa respectively (Figure 2.12). This shift in migration has been described before for proteins containing a polyQ tract (Scherzinger, 1997). The proteins GST, G-CRMP1, His-CRMP1, and His-GAPDH migrated at their expected molecular weights, which were 26, 90, 65 and 36 kDa respectively (Figure 2.12).

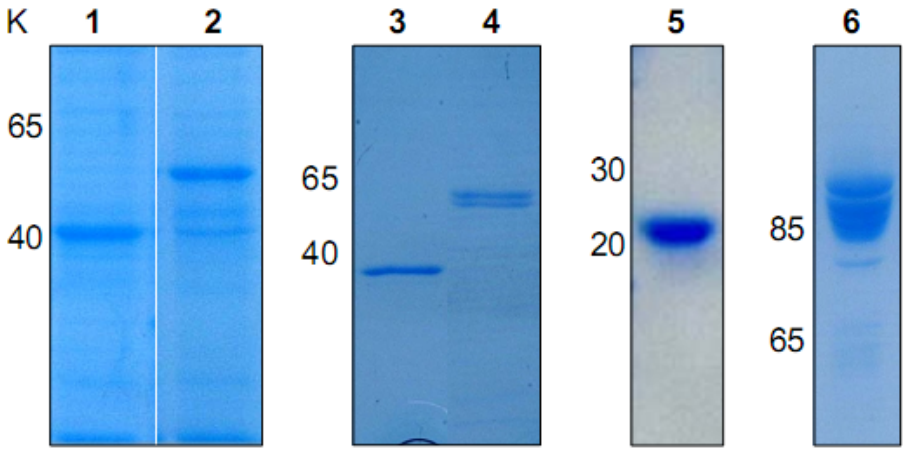

Figure 2-12: Analysis of purified recombinant proteins by SDS-PAGE and Coomassie staining.

25 µg of purified protein samples were separated on a 12.5% gel and stained with Coomassie blue R-250. Lane 1, GST-FLAG-HttQ23; lane 2, GST-FLAG-HttQ51; lane 3, His_7-GAPDH; lane 4, His_7-CRMP1; lane 5, GST; and lane 6, GST-CRMP1. K, kDa.

2.6 Aggregation of GST-Htt exon1 proteins

The epitope-tagged G-Htt exon1 proteins with polyQ sequences in the normal (Q23) and pathogenic (Q51) range possess a unique cleavage site for Prescission Protease® (PP). This site is located between the GST and FLAG –Htt exon 1 protein (Figure 2.13). The GST-tag, which can be removed from the fusion protein by PP cleavage, increases the solubility of the Htt proteins, while the polyQ sequence stimulates the formation of insoluble Htt aggregates (Scherzinger, 1997).

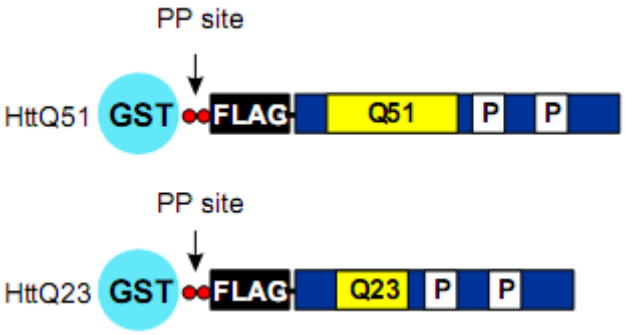

Figure 2-13: Schematic representation of the structure of GST-Htt fusion proteins.

Q and P represent polyglutamine and polyproline sequences, respectively. The arrows indicate the Prescission protease (PP) cleavage site.

The G-Htt fusion proteins (with polyQ tracts of 23Q or 51Q) were incubated at concentration of 2 µM with PP for 3 hours at 8°C to remove the GST-tag. After cleavage, the samples were incubated for 16 hours at 30 °C to trigger the formation of SDS-resistant aggregates. Subsequently, the samples were denatured by boiling with 4% SDS and 100 mM DTT and formation of Htt insoluble aggregates was monitored using a filter retardation assay and immunodetection with an anti-Htt antibody CAG53b. FLAG-HttQ51 (HttQ51) protein formed SDS-insoluble high molecular weight aggregates, whereas FLAG-HttQ23 (HttQ23) protein remained soluble and did not form aggregates (Scherzinger, 1997; Busch, 2003) (Figure 2.14 A).

To explore the morphology of the aggregates formed *in vitro*, aliquots of the aggregation assays were analyzed by atomic force microscopy (AFM). As shown in Figure 2.14 B, the HttQ51 protein showed a distinct fibrillar morphology typical for amyloid, whereas no fibrils were observed with cleaved GST-FLAG-HttQ23 protein (Busch, 2003).

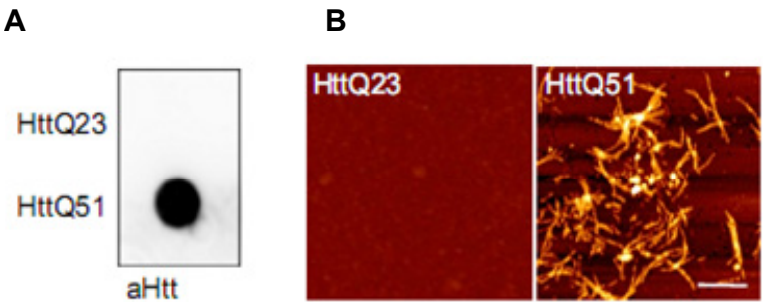

Figure 2-14: *In vitro* aggregation assay of GST-Htt fusion proteins.

(A) The polyQ length dependence of Htt exon1 protein aggregation. Htt aggregation was initiated by proteolytic cleavage of the G-Htt fusion proteins with PP. Protein simples were filter-trapped, and aggregates were detected with the anti-Htt CAG53b antibody. (C) AFM analysis of cleaved HttQ23 and HttQ51 proteins. Scale bar= 500 nm.

Next, I investigated the formation of HttQ51 and HttQ23 aggregates using time course experiments. After removal of the GST tag from G-Htt fusion proteins, the samples were incubated at 30°C to stimulate aggregation. At different time points, aliquots were taken and analyzed by filter retardation assay and immunodetection with CAG53b antibody (Busch, 2003). Formation of heat-stable, SDS-resistant HttQ51 aggregates was observed after a lag phase of 2-3 hours. Saturation of aggregation was observed after an incubation period of ~10 hours. As expected, no SDS-stable aggregates were observed after cleavage of G-HttQ23 fusion protein (Busch, 2003) (Figure 2.15 A and B).

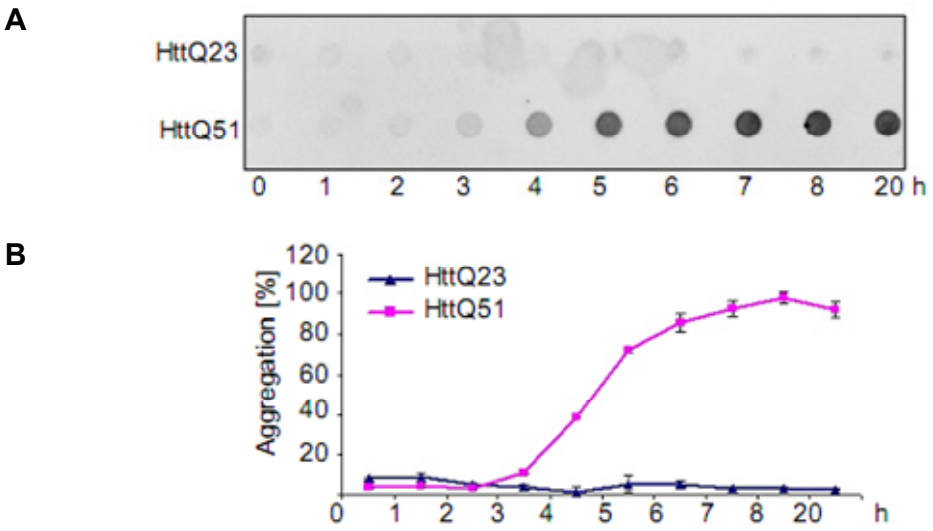

Figure 2-15: Kinetic studies of HttQ23 and HttQ51 aggregation reactions.

(A) 2 µM G-HttQ23 or G-HttQ51 were incubated with PP for 3 h at 8°C and then incubated at 30°C. Samples were taken at various time points, denatured, and analyzed by filter trap assay. The aggregates were detected with anti-Htt CAG53b antibody. (B) Quantification of the results shown in A.

2.7 CRMP1 inhibits the formation of HttQ51 aggregates *in vitro*

In order to investigate whether CRMP1 influences mutant HttQ51 protein aggregation *in vitro*, 2 µM of G-HttQ51 fusion protein was incubated with an equimolar concentration of GST or G-CRMP1 and PP. After cleavage of fusion protein at 8°C for 3 hours, the samples were transferred to 30 °C to start aggregation. SDS-insoluble HttQ51 protein aggregates were monitored over time by filter retardation assay using the anti-Htt CAG53b antibody. A third sample containing G-HttQ51 protein alone and PP (buffer) was also processed in the same way.

I found that G-CRMP1 efficiently suppressed the formation of HttQ51 aggregates *in vitro*. In contrast, such an effect was not observed when an equal amount of GST protein was added to the aggregation reactions (Figure 2.16 A and B).

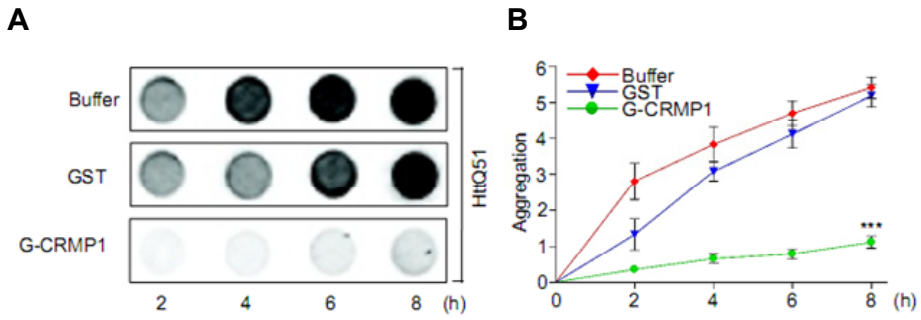

Figure 2-16: CRMP1 inhibits HttQ51 aggregation *in vitro.*

(A) G-HttQ51 was preincubated in the absence (buffer) or presence of GST or G-CRMP1 and PP for 3 hours at 8 °C, followed by incubation at 30°C to trigger HttQ51 aggregation. At various time points samples were taken, denatured, and analyzed by filter trap assay. The retained aggregates were detected with anti-Htt CAG53b antibody. (B) Quantification of the results shown in A. The bars depict the mean and SD of four independent experiments. Significance levels were determined using unpaired student's t-test. ***Significance, P<0.001.

Next, I explored whether CRMP1 influences the morphology of HttQ51 aggregates using AFM (Figure 2.17). Cleaved GST-FLAG-HttQ51 protein showed a typical fibrillar morphology (length = 300 ± 100 nm, height = 6 ± 1 nm). In contrast, in the presence of G-CRMP1, the amount of fibrils was significantly reduced and large (15 ± 5 nm) as well as small (3 ± 1 nm) amorphous protein aggregates were observed. This indicates that G-CRMP1 blocks the fibrillogenesis of HttQ51 *in vitro*. Addition of GST protein to the incubation mixture did not have a significant effect on the morphology of HttQ51 aggregates. As it is known that CRMP1 forms tetramers (Wang, 1997) I also have analyzed the morphology of G-CRMP1 protein alone by AMF. No fibrillar or amorphous protein aggregates were observed under these conditions. Thus, my data strongly indicate that CRMP1 influences the morphology of HttQ51 aggregates *in vitro.*

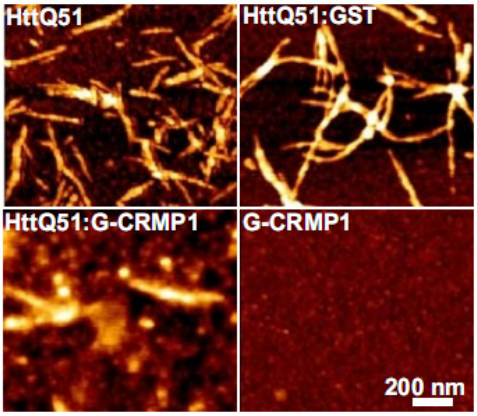

Figure 2-17: AFM analysis of HttQ51 fibrils grown in the absence or presence of G-CRMP1.

2 µM of G-HttQ51 was preincubated in the absence (buffer) or presence of GST or G-CRMP1 proteins as well as PP for 3 hours at 8°C, followed by incubation at 30°C for 6 hours to trigger aggregates formation. The samples were denatured and visualized by AFM.

In subsequent experiments, I have assessed whether the effect of G-CRMP1 on HttQ51 aggregation is concentration dependent. 2 µM of G-HttQ51 protein was incubated with different concentrations of G-CRMP1 or GST protein (0.25, 0.5, 1 or 2 µM) and PP. After cleavage (3 hours at 8°C), the samples were incubated at 30°C for 12 hours and aliquots were analyzed by filter retardation assay. I observed that G-CRMP1 suppresses HttQ51 aggregation in dose-dependent manner. Furthermore, G-CRMP1 was able to suppress the formation of SDS-insoluble aggregates by 50% even at sub-stochiometric concentration (0.25 µM). In contrast, such an effect was not observed when the control protein GST was incubated with HttQ51. Therefore, my results strongly indicate that G-CRMP1 suppresses HttQ51 aggregation *in vitro* (Figure 2.18 A and B).

In order to evaluate whether addition of GST or G-CRMP1 influences PP activity, aliquots from the cleavage reaction were analyzed by SDS-PAGE and Western blotting using anti-Htt HD1 antibody. As shown in Figure 2.18 C, protein addition did not interfere with PP cleavage, indicating a specific effect of G-CRMP1 on HttQ51 aggregation.

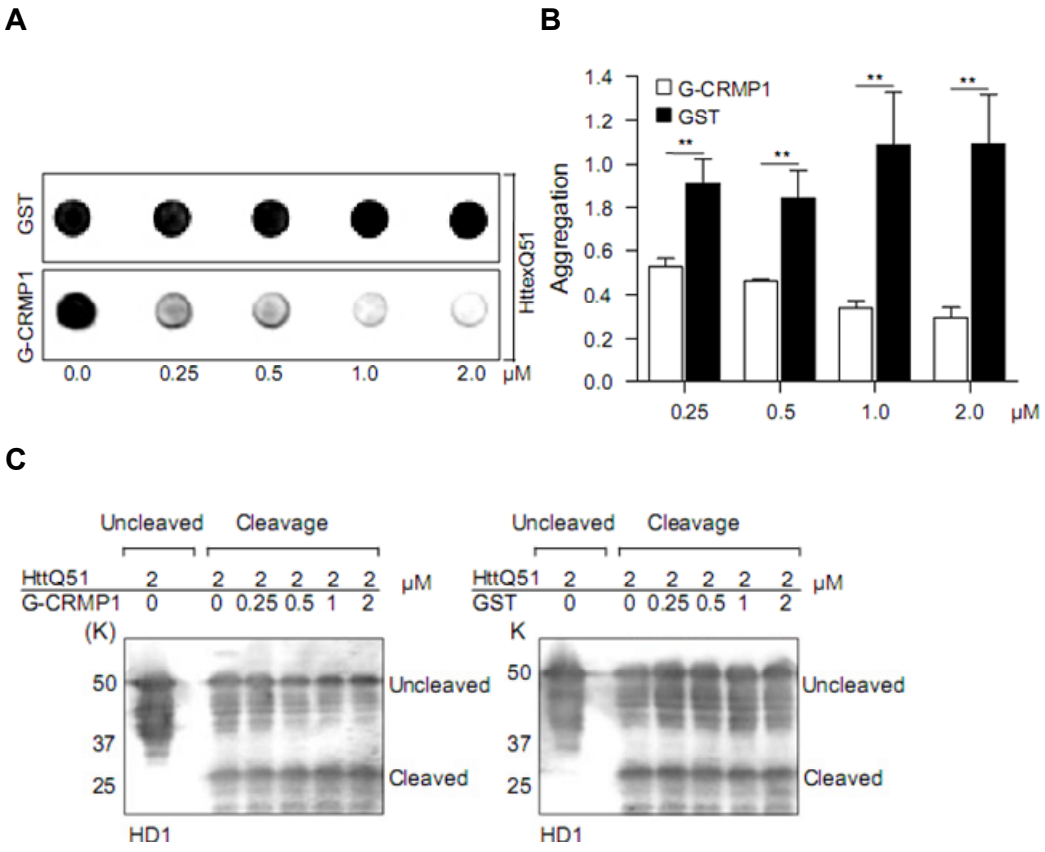

Figure 2-18: Effect of different G-CRMP1 protein concentrations on HttQ51 aggregate formation.

(A) 2 μM GST-FLAG-HttQ51protein was incubated with different concentrations (0.25-2μM) of GST-CRMP1 or GST protein as well as PP for 3 hours at 8°C. The aggregation reactions were stopped after incubation for 12 hours at 30°C by heating in 4% SDS/100 mM DTT. The retained aggregates were detected with anti-Htt CAG53b antibody. (B) Quantification of the results shown in A. The bars depict the mean and SD of four independent experiments. Significance levels were determined using unpaired student's t-test. ***Significance, P<0.001, **significance, P<0.01. (C) Protein addition does not inhibit PP-mediated cleavage of GST-Flag-HttQ51. The anti-Htt HD1 antibody detected the uncleaved G-HttQ51 protein running at ~55 kDa and the cleaved HttQ51 protein migrating at ~30 kDa in SDS-gels. K, kDa.

The inhibitory effect of CRMP1 on HttQ51 aggregation was further analyzed using natively purified His-tagged CRMP1 protein. 0.5 or 1 μM His-CRMP1 or His-GAPDH were added to reactions containing 2 μM GST-FLAG-HttQ51 and PP. Following removal of the GST tag from the fusion protein, samples were transferred to 30°C for 12 hours to trigger HttQ51 aggregation. Subsequently the reactions were denatured by boiling with 4% SDS/100 mM DTT and filtered

through cellulose acetate membrane. The retained aggregates were detected with anti-Htt CAG53b antibody. I found that, similarly to G-CRMP1 protein, His-CRMP1 suppressed the formation of HttQ51 aggregates in a concentration dependent manner (Figure 2.19 A and B). In contrast, His-GAPDH, another Htt-interacting protein, known to be sequestered to mHtt aggregates and potentially involved in mHtt translocation to the nucleus (Bae, 2006; Wu, 2007) did not have any effect on HttQ51 aggregation. Together, these results indicate that CRMP1 binds to mHtt protein and reduces the formation of SDS-stable Htt aggregates in a concentration-dependent manner.

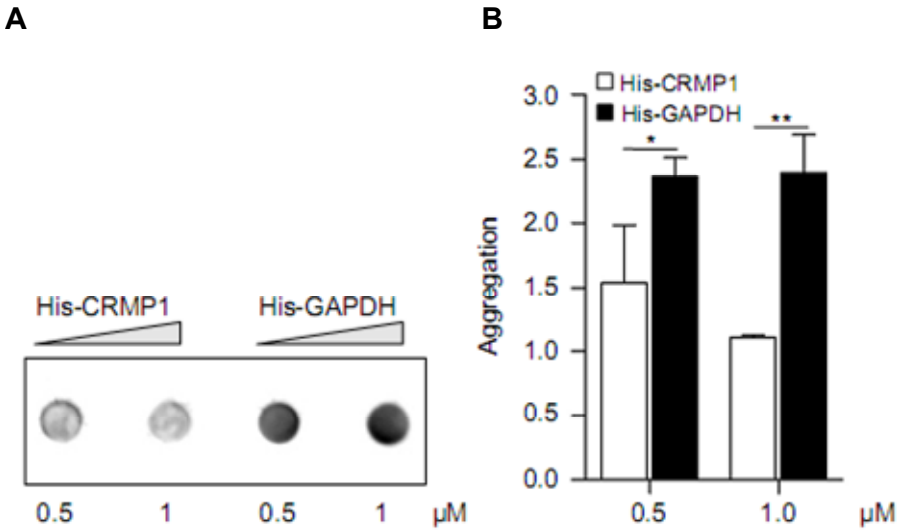

Figure 2-19: His-CRMP1 reduces the formation of HttQ51 aggregates *in vitro.*

2 µM G-HttQ51 was incubated with different concentrations (0.5-1µM) of His-CRMP1 or His-GAPDH as well as PP for 3 hours at 8°C. The aggregation reactions were stopped after incubation for 12 hours at 30°C by heating in 4% SDS/100 mM DTT. The retained aggregates were detected with an anti-Htt CAG53b antibody. Statistical analysis was performed using unpaired student's t-test: mean +/- SD, n= 3 experiments. ** Significance, P<0.01, *Significance, P<0.1.

2.8 Analysis of CRMP1 levels in mouse brain

I have investigated the expression levels and the integrity of CRMP1 protein in the striatum of R6/2 transgenic mice and aged-matched controls by Western blotting using CRMP1 specific antibodies.

First, the whole brain of a wild type adult mouse was dissected and rapidly placed in an artificial cerebrospinal fluid buffer (aCSF) bubbled with 95% O_2 and 5% CO_2. Subsequently, the brains were sliced using a vibratome and 300 µM thick pieces were collected in aCSF buffer. The striatum and cerebral cortex tissues were isolated under light microscopy and rapidly frozen in liquid nitrogen. The purity of the extracts prepared from striatum were analyzed by SDS-PAGE and immunoblotting for the presence of the dopamine and cyclic AMP regulated phosphoprotein of 32 kDa, DARPP-32 (Walaas, 1983). DARPP-32 is mainly expressed in medium-size spiny neurons and is the most commonly used striatum marker (more than 95 % of striatal neurons are medium spiny neurons) (Ouimet and Greengard, 1990; Ouimet, 1998).

Figure 2.20 B shows that in comparison to cerebral cortex, the DARPP-32 protein is highly enriched in the striatum samples, indicating the quality of the brain region preparations.

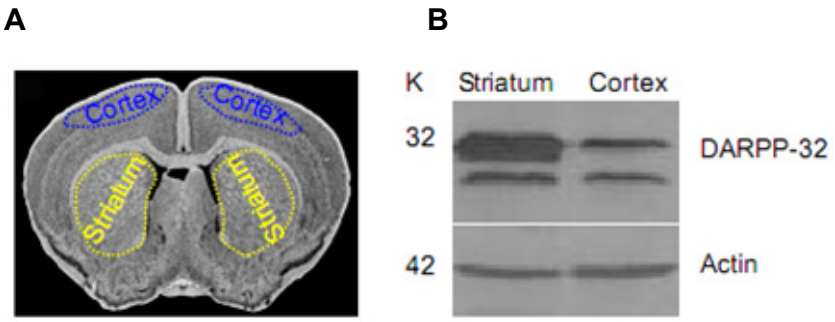

Figure 2-20: Immunoblot analysis of striatal and cortical mouse brain preparations.

(A) A schematic representation of a coronal section of mouse brain, showing the position of the striatum and cortex. (B) Western blot analysis of lysates from striatum and cortex showing DARPP-32 enrichment in the striatal preparations in comparison to the cortical lysates. Actin served as an internal loading control for the Western blotting experiments. K, kDa.

In a similar way, protein lysates prepared from the striatum of 12 weeks old R6/2 transgenic mice and aged matched controls were analyzed by Western blotting using the CRMP1-504 antibody. The anti-CRMP1-504 antibody detect the predicted 65-kDa protein and its 75-kDa isoform corresponding to its N-terminal splice variant (CRMP1A) (Bretin, 2005) in striatum lysates of wild type brain.

These proteins, however, were diminished in R6/2 transgenic HD mice. Interestingly, in the transgenic HD R6/2 mice, prominent CRMP1 fragments migrating at about 55 kDa (CRMP1B-trunc) was observed, indicating that the protein gets abnormally cleaved in the striatum of R6/2 mice (Figure 2.21 A).

In order to determine when CRMP1 cleavage occurred in R6/2 mice, striatal brain extracts from 4, 8 and 12 weeks old R6/2 and wild-type control mice were analyzed by Western blotting using CRMP1-504 antibody. The cleavage of CRMP1 was only detected with older HD mouse brain (12 weeks), indicating that it is a relatively late event in HD pathogenesis (Figure 2.21 B).

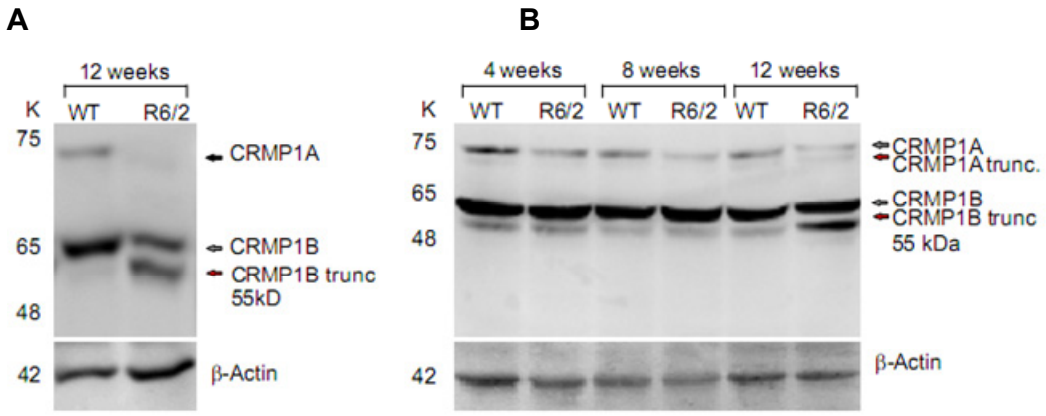

Figure 2-21: CRMP1 is cleaved in R6/2 HD mouse brains.

(A) Western blot analysis of striatal brain lysates from wild-type (WT) and R6/2 mice at 12 weeks of age. A marked reduction of full-length CRMP1 protein was observed along with the appearance of a truncated form (CRMP1B trunc), running at ~55 kDa. (B) CRMP1 is cleaved in R6/2 mice at later stages of pathogenesis (12 weeks). Actin served as an internal loading control for the Western blot experiments. K, kDa.

I have also investigated the expression levels and the integrity of the CRMP1 protein in the striatum of 4 months old N-171-82Q HD transgenic mice (Schilling, 1999) and aged-matched non-transgenic littermates by immunoblotting using the CRMP1-504 antibody.

The N-171-82Q transgenic mouse model of HD expresses an N-terminal fragment of Htt (171 amino acid residues) with 82 glutamines (Schilling, 1999). These mice develop behavioral and pathological symptoms that recapitulate the features of HD

such as loss of coordination, tremor, hypokinesis, and presence of both nuclear and neuritic aggregates in the brain. The N-171-82Q mice have a lifespan of 5-6 months (Schilling, 1999). As shown in figure 2.22, the CRMP1 proteins (CRMP1A and 1B) were cleaved in the striatum of N-171-82 transgenic mice, confirming my previous observations in R6/2 transgenic mice.

These observations indicate that CRMP1 proteins are prone to proteolytic cleavage during HD pathogenesis.

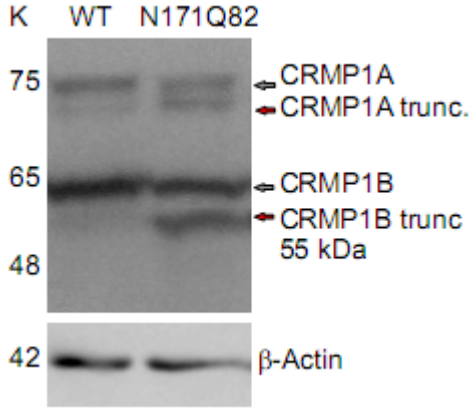

Figure 2-22: CRMP1 is cleaved in N-171Q-82 HD mouse brains.

Western blots analysis of striatal brain lysates from wild-type (WT) and N-171Q82 mice at 4 months of age. Immunodetection was performed using CRMP1-504 antibody. Actin served as an internal loading control for the Western blot experiments. K, kDa.

2.9 CRMP1 is cleaved by calpain under pathological conditions

Aberrant activation of calpains has been associated with several neurological disorders such as AD (Tsuji, 1998), PD (Mouatt-Prignet, 1996), HD (Gafni, 2002), and cerebral ischemia (Banik, 1997). Calpains are a family of Ca^{2+}-dependent intracellular cysteine proteases that cleave many important substrates such as spectrins (Siman, 1996), CDK5 (Smith, 2006), and CRMPs (Kowara 2005; Hou, 2006; Kowara, 2006; Touma, 2007; Zhang, 2007).

In order to examine whether CRMP1 cleavage is mediated by calpains in the HD brain, I applied exogenous calpain I or II and caspase-3 to the cytosolic fractions prepared from the striatum tissue of wild-type brain. Western blot analysis using specific CRMP1-504 antibody showed that calpains at a very low concentration

(Figure 2.23 A and B), but not caspase-3 (Figure 2.23 C), were able to cleave CRMP1 to a breakdown product of ~55 kDa. Similar sizes were also observed in lysates prepared from the striatum of R6/2 transgenic mice, indicating an association between calpain activation and CRMP1 cleavage during HD pathogenesis.

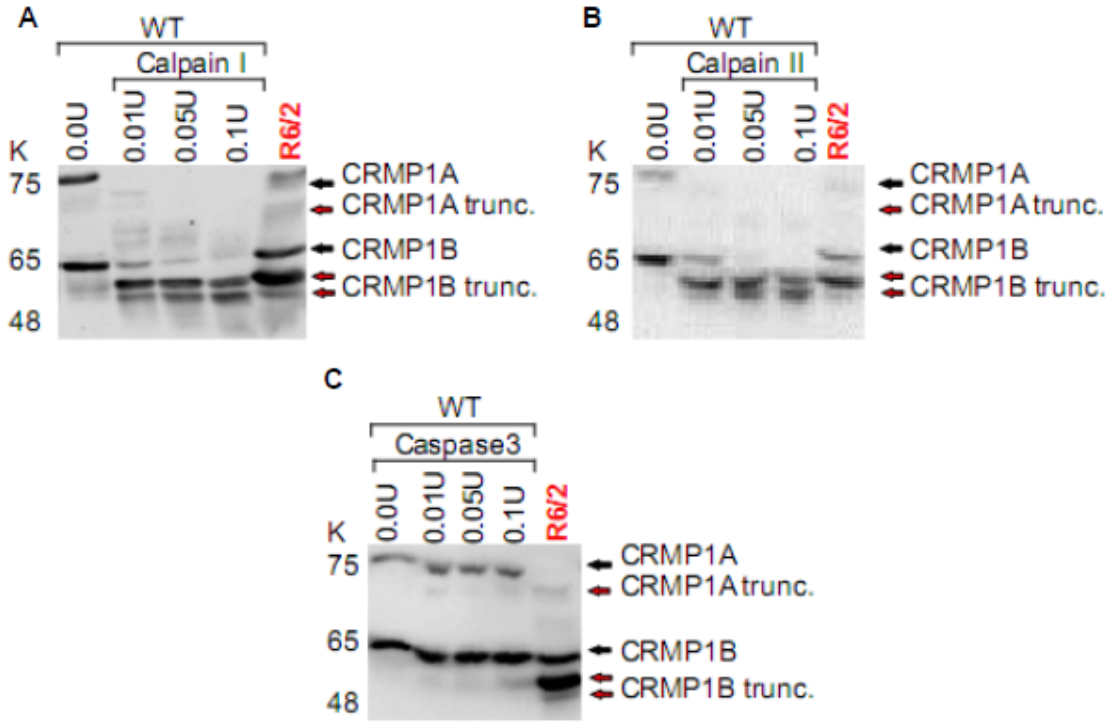

Figure 2-23: CRMP1 is cleaved by calpains in R6/2 transgenic mouse brains.

(A) Western blot analysis of CRMP1 cleavage after treatment with calpain I, (B) calpain II or (C) caspase-3 of wild-type mouse striatum lysates. Immunodetection was performed using the CRMP1-504 antibody. An untreated striatum lysate of wild type mice was used as a negative control (0.0U), while a striatum lysate of R6/2 transgenic mice was used as a positive control. K, kDa.

In order to demonstrate that endogenous calpain in the striatum can also cleave CRMP1, normal striatum lysates were pretreated either with or without calpain inhibitor calpeptin (10 μM) or caspase-3 inhibitor Z-VAD-FMK (20 μM). Then, calcium (5 mM) was added to the brain lysates to activate endogenous Ca^{2+}-dependent cysteine proteases such as calpains and caspases (Wang, 2000; Hou, 2006).

The samples were incubated at 4°C for 18 hours and equal amounts of protein extracts (20 µg) were analyzed by SDS-PAGE and Western blotting using the CRMP1-504 antibody. As shown in Figure 2.24, calcium treatment resulted in the appearance of breakdown product of similar molecular weight as was observed in the HD transgenic mice. The cleavage was blocked by the presence of the calpain specific inhibitor calpeptin, but not by caspase-3 inhibitor Z-VAD-FMK. Taken together, these results suggest that CRMP1 proteins are cleaved in the brain by calpains during HD pathogenesis.

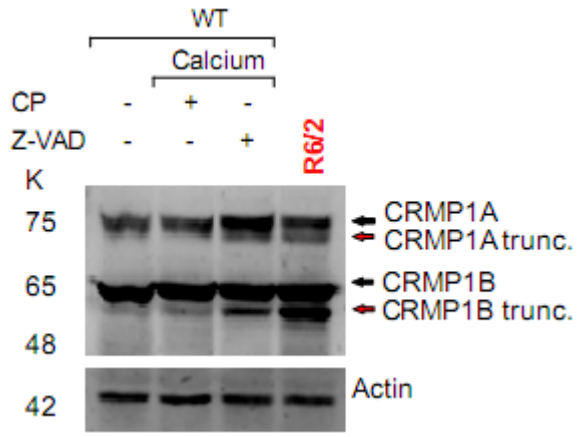

Figure 2-24: Endogenous calpains cleave CRMP1 proteins.

Western blot analysis of CRMP1 proteins after calcium treatment of wild-type mouse striatal lysate in the presence or absence of calpain inhibitors. CP, calpeptin; Z-VAD, caspase-3 inhibitor. Immunodetection was performed using CRMP1-504 antibody. K, kDa.

2.10 CRMP1 is cleaved by calpains at the N- and C-termini

Previous studies, have shown that CRMP3 can be cleaved by calpain at the N-terminus (Hou, 2006), while CRMP2 and CRMP4 are cleaved at the C-terminus (Deo 2004; Chung, 2005; Kowara, 2005; Bretin 2006; Jiang, 2007).

To investigate the calpain cleavage sites in the CRMP1 protein, constitutively active calpain I or II (0.25-5.0 units) were mixed with purified recombinant His-tagged-CRMP1 protein. After incubation at 4°C for 18 hours the digestion products were analyzed by SDS-PAGE and Western blotting using CRMP1 specific antibodies and an anti-His tag monoclonal antibody. The CRMP1-504 and CRMP1-513 antibodies are specific to the C-terminus of CRMP1, while the anti-

His antibody recognizes the histidine tag (His) at the N-terminus of the protein.

First, I observed that addition of both active calpain I and II cleaved the full-length 65kDa His-CRMP1 protein resulting in the appearance of a smaller band of ~55 kDa (Figure 2.25, Coomassie stain). This indicates that CRMP1 is directly targeted by the calpains. The antibody against the N-terminal His-tag recognized only the full-length CRMP1 protein (65 kDa), while the 55 kDa breakdown product of CRMP1 was undetectable, indicating that both calpains cleave His-CRMP1 at the N-terminus (Figure 2.25). The anti-CRMP1-504 antibody which recognizes amino acids 504-518 in the CRMP1 protein detected cleavage products running at ~55 kDa. No CRMP1 cleavage bands were detected with the anti-CRMP1-513 antibody (amino acids 513-527 of CRMP1). This result suggests that calpains cleave both at the N- and C-terminus of the CRMP1 protein, and the sequence for the C-terminal cleavage is located within the stretch of amino acids 513-527 of CRMP1 protein.

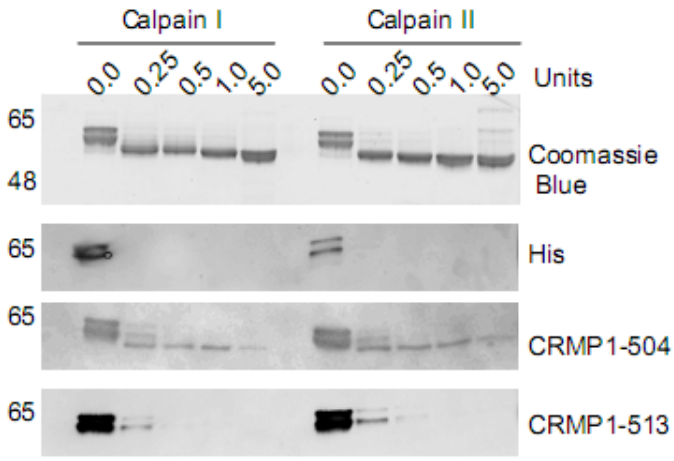

Figure 2-25: Calpains cleave CRMP1 both at the N- and C-terminus.

Active calpain I or II at the concentrations indicated were mixed with 2 µg of recombinant His-CRMP1. CRMP1 cleavage was monitored by Western blotting using the anti-His (recognizing the N-terminal His-tag) and anti-CRMP1 antibodies (recognizing sequences at the C-terminus of CRMP1). K, kDa

To determine the N-terminal cleavage sites in CRMP1 protein N-terminal sequencing by Edman degradation was used (Hou, 2006). Purified His- CRMP1 was digested with active calpain I or II. After digestion, the samples were

separated on 8% SDS–PAGE gel and blotted onto a polyvinylidene difluoride (PVDF) membrane (Amersham Biosciences). Ponceau S stained-CRMP1 bands were excised for N-terminal microsequencing. N-terminal microsequencing of cleaved recombinant His-CRMP1 protein revealed that calpain cleavage occurred between amino acids 3-4 and 7-8.

Chapter
Discussion

3 Discussion

Huntington's disease is an autosomal dominant late-onset monogenic neuro-degenerative disorder caused an expanded polyglutamine tract in the protein Htt (HDCG, 1993). The polyQ expansion (beyond ~35-40 glutamines) drives aberrant protein-protein interactions, folding and aggregation of the mHtt protein, leading to the deposition of insoluble protein aggregates in HD brain and in polyQ disease models. The mHtt protein is widely expressed in the central nervous system and peripheral tissues but causes specific neurodegeneration in the striatum (1995 Albin, 1995; Herdeen, 1995). It is thought that striatum specific Htt-interacting proteins might play an important role in HD pathogenesis (Ross, 1995; Harjes and Wanker, 2003). Therefore, identification of striatum-specific Htt-partners might help to decipher the molecular mechanism underlying HD pathogenesis.

Recently, with the development of systems biology, network-based analyses have been applied successfully for HD. (Goehler, 2004; Kaltenbach, 2007). It was demonstrated that many Htt-interacting partners colocalize with insoluble mHtt inclusions in HD brains and modulate the mHtt phenotype (Goehler, 2004; Kaltenbach, 2007)

PPI studies result in large, highly connected, however, static interaction maps. Analyses of network topologies and motifs generated useful information, however, this knowledge alone can not portray spatial-temporal aspects of protein complexes in a cellular environment (Barabasi, 2004). One of the possible ways to pinpoint biologically relevant local networks and to decipher vital functional modules is to integrate PPI maps with other types of information, such as gene expression, protein localization or genetic data (de Lichtenberg, 2005; Huh, 2003; Calvano, 2005; Pujana, 2007; Yeger-Lotem, 2009).

A striatum-specific, dysregulated PPI network has been created recently by integrating PPI networks with information from gene expression profiling data derived from clinical case-control studies (Chaurasia, unpublished data). One of the identified dysregulated protein was the neuron-specific Collapsin Response Mediator Protein 1 (CRMP1), suggesting a potential role of CRMP1 in HD pathogenesis.

3.1 CRMP1 protein

Collapsin Response Mediator Protein 1 (CRMP1) belongs to the CRMP phosphoprotein family, which contains five members of high sequence similarity in humans (Wang and Strittmatter, 1997). CRMP1 protein is highly expressed in the central nervous system during embryonic development and is down-regulated in the adult brain. It can interact with other members of the CRMP family and most probably has a function as a multimer (Wang and Strittmatter, 1997). CRMP1 is involved in different physiological functions such as neurite outgrowth, axonal guidance, adult brain plasticity (Charrier, 2003) and apoptosis (Shirvan, 1999). Moreover, it is thought to be important for the regulation of cytoskeleton organization (Quach, 2004). Alteration of the cytoskeleton dynamics has been reported to be associated with HD pathogenesis (McMurray, 2000; DiProspero, 2004).

CRMP1 has been described to be involved in the Semaphorin3A (Sem3A)-induced spine development in the brain (Yamashita, 2007). In addition, CRMP1 knock-out mice display aberrant projection of both dendrites and dendritic spines (Yamashita, 2007). Alterations in the dendritic spine morphology represent early neuropathological changes in HD brains (Guidetti, 2001). Therefore, elucidating the functions of CRMP1 and its signaling pathways could be an important step for understanding the development of HD.

3.2 CRMP1 forms a complex with Htt

Several studies have demonstrated that the direct interacting partners of Htt are potential modifiers of HD pathogenesis. In addition, the alteration in the expression levels of Htt binding partners might either enhance or slow down the assembly of amyloidogenic aggregates, leading to a modulation of mHtt-mediated neurotoxicity (Goehler, 2004; Kaltenbach, 2007)

We previously identified a C-terminal fragment of CRMP1 as an Htt-interacting partner using the Y2H system and GST-pulldown assays (Goehler, 2004). The interaction between full-length CRMP1 and Htt, however, was not studied in detail. Using coimmunoprecipitation experiments I was able to demonstrate that full-

length CRMP1 forms a complex with N-terminal Htt fragment protein in cell based assays (Figure 2.5 A and B). Furthermore, the full-length Htt and CRMP1 proteins were also found in immunoprecipitates from mouse brain lysates, indicating that these two proteins form a functional complex under physiological conditions (Figure 2.5 C).

The formation and accumulation of large insoluble inclusions containing mHtt aggregates is a prominent feature of HD (Davies, 1997; DiFiglia, 1997). Immunohistochemical analysis of R6/2 mouse brains demonstrated that CRMP1 protein colocalizes with large insoluble inclusions containing mHtt protein (Figure 2.7 B), suggesting that CRMP1 is associated with pathological mHtt molecules in neurons. Co-localization of CRMP1 protein with inclusion bodies containing aggregated mHtt protein was also observed in *Drosophila* HD cells (Figure 2.7 A) and PC12 cell model systems (Figure 2.6), supporting the results obtained with the HD R6/2 mouse model. However, it remains to be determined whether CRMP1 is also colocalized to nuclear inclusion in HD patient brains.

Previous studies have demonstrated that several other proteins that are regulators of cytoskeleton organization such as SH3GL3 (Sittler, 1998), profilin 2 (Kaltenbach, 2007; Burnett, 2008) and dynamin 1 (Kaltenbach, 2007) bind to Htt protein and modulate mHtt-mediated aggregation and toxicity. For example, profilin 2, which is enriched in neurons, modulates actin polymerization and acts as a modifier of mHtt phenotype. Profilin 2 reduces the formation of mHtt aggregates and ameliorates mHtt toxicity in cell culture and *Drosophila* model of HD (Kaltenbach, 2007; Burnett, 2008). SH3GL3 binds to the Htt protein and stimulates the assembly of SDS-resistant Htt aggregates, indicating that this protein is an enhancer of amyloidogenesis (Sittler, 1998). These observations suggested that the Htt-interacting partner CRMP1 may behave as a potential modifier of HD pathogenesis.

3.3 CRMP1 inhibits Htt aggregation and toxicity in HD models

Cellular proteins that influence Htt aggregation are potential modulators of HD pathogenesis (Goehler, 2004). Using complementary cellular assays and animal

models, I have demonstrated that CRMP1 is modulator of mHtt aggregation and toxicity.

I found that downregulation of CRMP1 increases both the formation of mHtt aggregates and cytotoxicity, while the overexpression of the protein significantly reduces both aggregation and toxicity in PC12 cells (Figure 2.8 and 2.9). This suggests that CRMP1 may be important for suppressing mHtt aggregation and toxicity in mammalian cells. A dysfunction or dysregulation of CRMP1 levels may considerably influence HD pathogenesis.

Similar results were obtained in a *Drosophila* HD model expressing the protein Htt336Q128 (Kaltenbach, 2007), supporting the protective effect of CRMP1. I found that over-expression of a human Myc-CRMP1 protein rescues the Htt336Q128-mediated neurodegenerative eye phenotype *in vivo* (Figure 2.11). In addition, a dramatic reduction of insoluble mHtt aggregates in fly eyes was observed (Figure 2.10). Such an effect was not observed when the control protein GFP was over-expressed with the mHtt (Figures 2.10 and 2.11). Thus, my results strongly indicate that CRMP1 binds to mHtt and modulates mHtt-mediated neurodegeneration and dysfunction.

3.4 CRMP1 inhibits Htt exon 1 aggregation *in vitro*

A well established cell-free aggregation assay was used to address the direct role of CRMP1 on polyQ-mediated Htt exon1 aggregation (Scherzinger, 1997). As reported previously, mHtt exon1 protein aggregates in a polyQ-length dependent manner *in vitro* and SDS-stable aggregates can be detected by filter retardation assay (Figure 2.14).

I found that CRMP1 was able to suppress the formation of HttQ51 aggregates *in vitro* (Figure 2.16). In contrast, GST protein or His-GAPDH, a well-known HD modifier (Bae, 2006; Wu, 2007), were unable to inhibit HttQ51 aggregation (Figures 2.16 and 2.19). This indicates a direct role of CRMP1 in the aggregation process of the mHtt fragments.

Subsequently, the effect of CRMP1 on mHtt aggregation was also investigated by AFM. In the absence of CRMP1, insoluble HttQ51 protein aggregates exhibited

typical fibrillar morphology (Figure 2.17). In contrast, in the aggregation reactions with CRMP1 the formation of fibrils was suppressed. Instead of fibrillar structures, however, relatively large (15 nm) as well as small (3 nm) amorphous mHtt aggregates were observed (Figure 2.17). No, such effect was observed, when GST alone was added to aggregation reactions or CRMP1 in the absence of mHttQ51 protein (Figure 2.17). These results indicate that CRMP1 might prevent fibrillogenesis and function as molecular chaperone.

The molecular chaperones play a pivotal role in different stress pathways and prevent the misfolding and toxicity of abnormal proteins. Indeed, in protein misfolding diseases such as HD, molecular chaperones (e.g. Hsp70, Hsp40, CHIP and TRiC) were found to be associated with insoluble protein aggregates, suppressing protein aggregation and preventing the cytotoxicity (Cummings, 1998; Muchowski, 2000; Tam, 2006).

Therefore, the finding that CRMP1 forms a complex with Htt and suppresses the aggregation and toxicity of mHtt in both *in vitro* and *in vivo* model systems, raises the possibility that CRMP1 inhibits aggregates formation in a similar way like chaperone proteins, by redirecting the aggregation pathway to protein complexes with non-amyloidogenic morphology.

Interestingly, a recent study demonstrated that the brain specific CRAG (Collapsin Response Mediator Protein (CRMP)-associated GTPase) modulates polyQ-mediated aggregation and toxicity through the ubiquitin-proteasome pathway in cultured cell models (Qin, 2006). Furthermore, lentivector-mediated expression of CRAG in Purkinje cells *in vivo* rescued the cells from signs of tremor in a mouse model of spinocerebellar ataxia (Torashima, 2008). The expression patterns of CRAG are similar to those of CRMP proteins. CRAG levels are very high in the developing brain and decrease thereafter in the adult brain (Qin, 2006). As CRMP proteins share 50-75% protein sequence identity and may exist as heterotetramers in neurons (Wang and Strittmatter, 1997). It seems possible that other CRMP proteins might act as modulators of the HD phenotype. Indeed, in a recent collaborative study with Prof. Josef Priller, Charité Berlin, I found that CRMP4, similar to CRMP1, suppresses mHtt aggregation and toxicity in a cell model system of HD (Nicoletti, Bounab et al. 2009, in preparation). Therefore, further

work will be necessary to evaluate whether also other CRMP proteins function as potential chaperones *in vitro.*

3.5 Calpain cleaves CRMP1 in the striatum of HD mouse models

Western blot analysis revealed an alteration of CRMP1 expression in the striatum of R6/2 mice as compared to the wild-type mice. In addition to a decrease in the amount of full-length CRMP1 protein (65 kDa), I also observed the appearance of CRMP1 breakdown products, running at ~ 55 kDa (Figure 2.21). Similar cleavage of CRMP1 protein was also observed in another HD mouse model (N171Q82) (Schilling, 1999) (Figure 2.22), suggesting that loss function of CRMP1 protein by proteolytic cleavage may contribute to HD pathogenesis.

Ca^{2+}-dependent proteases may be implicated in this cleavage. mHtt triggers a cascade of events that alter the Ca^{2+} homeostasis in neurons, leading to the activation of various neurotoxicity pathways (Gafni, 2002). N-Methyl-D-aspartate receptor (NMDAR) and metabotropic glutamate receptor (mGluR) are enriched in striatal medium spiny neurons and play a major role in the dysregulation of Ca^{2+} homeostasis during HD pathogenesis. mHtt sensitizes and activates NMDAR receptor in the brain, leading to excessive influx of Ca^{2+} into neurons (Chen, 1999; Sun, 2001; Zeron, 2001). mHtt sensitizes the endoplasmic reticulum type 1 inositol (1, 4, 5)-triphosphate receptor, leading to enhanced Ca^{2+} release from the endoplasmic reticulum following mGluR activation (Figure 3.1) (Tang, 2003). Accumulation of abnormal intracellular Ca^{2+} in neurons activates the Ca^{2+}-dependent cysteine proteases from both caspase and calpain families (Wang, 2000). The activated Ca^{2+}-dependent cysteine proteases play a major role in neuronal degeneration and induction of apoptosis (Harwood, 2005). Abnormal activation of calpains has been observed in striatal neurons of HD mice and postmortem HD brains of humans (Gafni and Ellergy, 2002; Gafni, 2004; Cowan, 2008). Furthermore, it is well known that proteins of the CRMP family are abnormally cleaved by calpains under different acute stress conditions, e.g. brain ischemia or excitotoxic oxidative stress (Kowara 2005; Hou, 2006; Jiang, 2007; Touma, 2007; Zhang, 2007). These observations support the hypothesis that

CRMP1 might be targeted by calpains during HD pathogenesis.

Application of exogenous calpains or addition of calcium to normal brain lysates generates fragments of CRMP1 that are similar in size to those observed in HD transgenic mouse models (Figures 2.21, 2.22). An effect that could be blocked by addition of calpain inhibitor (Figure 2.24). This data suggest that CRMP1 is cleaved by calpain during HD pathogenesis and loss of protein function may be important for the disease.

To identify the calpain cleavage sites in CRMP1 protein N-terminal sequencing and Western blotting were used. I have found that CRMP1 can be cleaved by calpains both at the very N-terminus as well as at the C-terminus part (Figure 2.25). The C-terminal cleavage site was mapped using the C-terminal anti-CRMP1-504 (aa 504-518) and anti-CRMP1-513 (aa 513-527) antibodies. As only the anti-CRMP1-504 (504-518) antibody detected the ~55 kDa proteolytic fragment, the C-terminal cleavage site, should be located between residues 513-527.

No CRMP1 breakdown product was observed with the N-terminal anti-His antibody, suggesting that the calpains also cleave at N-terminal part of the CRMP1 protein. N-terminal microsequencing of cleaved recombinant His-CRMP1 protein revealed that calpain cleavage occurred between amino acids 3-4 and 7-8 of the CRMP1 protein. Cleavage of CRMP1 protein will likely alter its cellular functions.

3.6 Proposed role of CRMP1 cleavage in HD

CRMP1 is involved in cytoskeletal organization that contributes to neuronal development such as neurite outgrowth (Quach, 2004), axonal guidance (Uchida, 2005) and spine morphogenesis (Yamashita, 2007). The CRMP protein family (CRMP1-5) share 50-75 % protein sequence identity and interact with each other to form tetramers (Wang and Strittmatter, 1997). The C-terminal tail region of all CRMPs has no detectable sequence homology to other proteins; it is characterized by a very high pI of 10.8 and a high content of serine residues (Stenmark, 2007). The C-terminal part of CRMP proteins is proteolytically unstable and structurally disordered (Deo, 2004). In addition, it has been predicted that

important functional sites reside in this domain. Therefore, calpain cleavage of CRMP1 may affect its biological function *in vivo* (Deo, 2004; Stenmark, 2007).

It has been suggested that proteolytic cleavage of CRMPs affects their binding to the tubulin and actin cytoskeleton (Jiang, 2007). For example, it was reported that the C-terminal truncated form of CRMP4 (~100 aa) loses its F-actin binding capability, suggesting an important role of this region in the regulation of actin cytoskeleton dynamics (Rosslenbroich, 2005). Fukata et al have shown that a region encompassing at least residues 323-381 at C-terminus of CRMP2 is required for neurite formation, axonal growth and branching via a regulation of microtubule assembly (Fukata, 2002). Furthermore, an interaction between CRMP2 and light chain of kinesin-1 is mediated by the C-terminal region of CRMP2 (residues 440-572). This interaction regulates transport of soluble tubulin to the distal part of the growing axon (Kimura, 2005). Truncation of 183 amino acids from the C-terminal region of the CRMP1 protein caused a significant decrease in neurite formation and extension of dorsal root ganglion neurons (Quach, 2004).

In addition, the C-terminal sequence of CRMPs is phosphorylated by several kinases such as GSK3ß (Cole, 2004; 2006), Rho kinase (Arimura, 2000) and Cdk5 (Cole, 2004; Yamashita, 2007). These phosphorylations may regulate the tetramerization and the biological functions of the CRMP proteins (Deo, 2004). It has been demonstrated that phosphorylation of CRMPs decreases their ability to bind to tubulin heterodimers, thereby deregulating the microtubule cytoskeleton dynamics (Fukata, 2002; Arimura, 2005; Uchida, 2005; Yoshimura, 2005). Phosphorylation of CRMP1 at Thr509 and Ser522 by Cdk5 kinase plays a pivotal role in spine development, dendritic branching and synaptic transmission (Yamashita, 2007). These functions are thought to regulate cytoskeleton organization.

Based on these studies, it seems that calpain cleavage of CRMP1 at the C-terminus disrupts the biological functions of the protein and influences the regulation of cytoskeleton organization.

An alteration of tubulin and actin cytoskeleton is a critical event, observed in HD patients and transgenic mouse models (DiProspero, 2004; Zabel, 2009).

Moreover, cytoskeletal dynamics play an important role in triggering mHtt aggregation and toxicity (Trushina, 2003; Iwata, 2005; Kaminosono, 2008).

These observations suggest that the calpain-mediated cleavage of CRMP1 protein might play an important role in the disturbance of the cytoskeleton dynamics observed in HD. Also, the alteration of CRMP1 expression levels might explain the abnormal spine morphology found in neurons of HD patients and animal models (Guidetti, 2001).

The physiological and pathological significance of this cleavage for cell survival and apoptosis is not yet clear. Recent studies demonstrated that CRMP3 is cleaved by calpain under ischemic and excitotoxic conditions, leading to the production of a breakdown product of ~54 kDa (Hou, 2006). The cleavage product of CRMP3 acts as a positive injury signal to induce neuronal death after cerebral ischemia and excitotoxic conditions (Hou, 2006). Furthermore, it has been reported that overexpression of CRMP2 lacking the C-terminal residues 413-572 caused apoptosis in mammalian cells (Tahimic, 2006).

In addition, I have found that abnormal CRMP1 cleavage occurs only at later stages during HD progression (Figure 2.21B), suggesting that the cleavage product of CRMP1 may contribute to the neuronal death during HD pathogenesis.

In contrast, it has been suggested that the calpain cleavage product of CRMP2 might play an important role in neuronal plasticity and survival (Bretin, 2006). Therefore, further studies are required to address the role of the truncated CRMP1 fragment in HD pathogenesis.

In summary, my studies provide evidence that CRMP1 modulates aggregation and toxicity of the polyQ Htt protein. Using a variety of complementary approaches I was able to demonstrate that the CRMP1 protein reduces mHtt aggregates and toxicity *in vitro* and *in vitro*. In addition, I clearly demonstrated that CRMP1 is specifically cleaved by calpains during HD pathogenesis. The calpain-mediated cleavage of CRMP1 protein might play a crucial role in HD progression.

Further understanding of the function of CRMP proteins may give us new insights into mechanism of neuronal damage and a better understanding of HD pathogenesis.

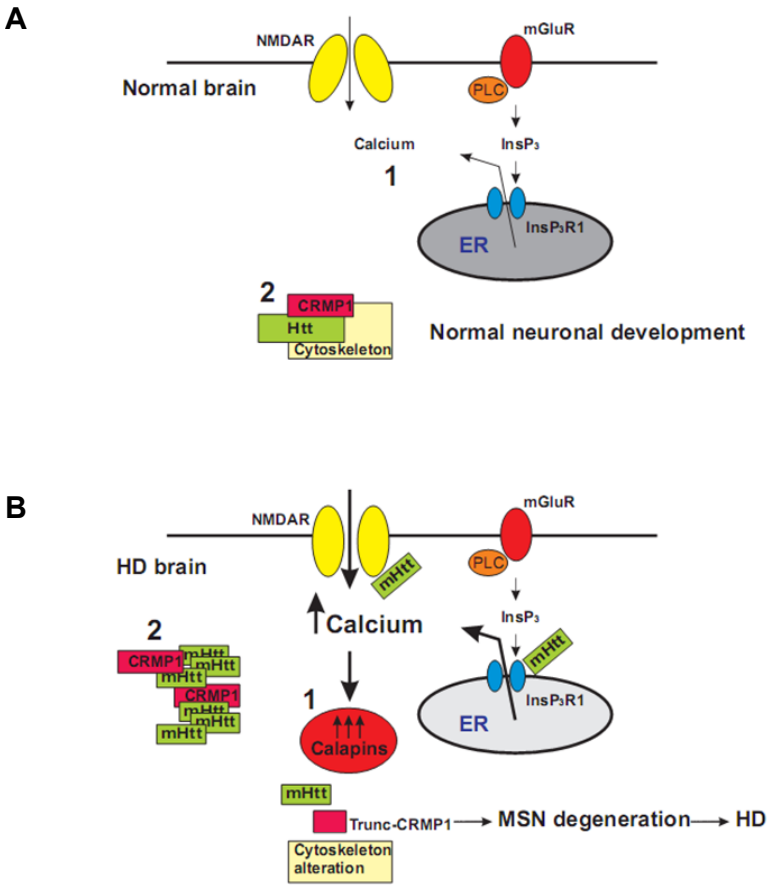

Figure 3-1: A model for a possible role of CRMP1 on HD pathogenesis.

(A) In normal brain, NMDAR activation triggers Ca^{2+} influx. Activation of mGluR stimulates phospholipase C (PLC) to generate inositol triphosphate ($InsP_3$) second messengers. The $InsP_3$ does not trigger robust Ca^{2+} release from the endoplasmic reticulum (ER) since endoplasmic reticulum type 1 inositol (1, 4, 5)-triphosphate receptor ($InsP_3R1$) sensitivity to $InsP_3$ is low (1). CRMP1-Htt forms a complex under physiological conditions. This complex might be involved in cytoskeletal organization that contributes to neuronal development (2). (B) In HD brain, mHtt sensitizes and activates NMDAR, leading to enhanced intracellular Ca^{2+} influx (Chen, 1999; Sun, 2001; Zeron, 2001). mHtt sensitizes $InsP_3R1$, leading to enhanced Ca^{2+} release from the ER following mGluR activation (Tang, 2003). Activated calpains, in response to abnormal intracellular Ca^{2+} levels, cleave CRMP1 protein (1). The calpains cleavage of CRMP1 (Trunc-CRMP1) may affect its ability to bind to the cytoskeleton and to mHtt. An alteration of physiological protein complexes containing Htt and CRMP1 in medium spiny neurons (MSN) may contribute to HD. Full-length CRMP1 binds to mHtt and might function as molecular chaperone that prevents misfolding and aggregation (2).

3.7 Future Directions

Future experiments should address mainly the role of the truncated CRMP1 fragments in cell model systems. The first step is to construct a plasmid vector encoding a truncated form of the CRMP1 protein (residues 8-518 aa). Second, this construct will be transfected into PC12 HD cell lines to determine whether it influences mHtt-mediated toxicity.

Phosphorylation of CRMP proteins at the C-terminus may also be important for neurodegeneration, since CRMP2 is hyper-phosphorylated at Thr509, Ser518, and Ser522 in neurofibrillary tangles of AD brains (Gu, 2000).

The proteins CRMP1-4 share a high level of sequence homology (~75%) and the residues Thr509, Ser518, and Ser522 are conserved in the human CRMP1 and CRMP4 proteins (Cole, 2006). It is thus planed to generate specific antibodies for these phosphorylation sites (Thr509, Ser518, and Ser522) in the CRMP proteins. These antibodies will be used to evaluate the phosphorylation levels of CRMP1, CRMP2 and CRMP4 proteins on HD pathogenesis.

In a recent collaborative study, we have found that the CRMP4 protein, similar to CRMP1, suppresses mHtt-mediated aggregation and toxicity in cell model systems (Nicoletti, Bounab et al. 2009, in preparation). Therefore, it will be also interesting to investigate the role of other CRMP proteins (CRMP2, 3 and 5) in HD pathogenesis.

The misfolding and amyloid fibril formation of conformationally defective disease proteins is a common pathological feature of many neurodegenerative disorders including AD, PD, HD as well as multiple sclerosis (Wang, 2002). Several lines of evidence indicated that these neurodegenerative disorders might share common pathophysiological processes. It will thus be important to investigate the role of different CRMP proteins in the pathophysiology of other neurological disorders.

Chapter 4

Materials

4 Materials

4.1 Laboratory equipment

AFM	NonoWizard II microscope
Centrifuges	Mikro 22R
Confocal microscope (Zeiss)	Leica DM 2500 confocal
Edman	Applied Biosystems
Electroporator	Bio-Rad
Electroporation cuvettes	Bio-Rad
Image reader LAS-100	Fujiflm
pH meter	Schott
Photometer Ultraspec 3000	Amersham
Gel electrophoresis equipment	BioRad
Quartz glass cuvettes	Hellmer
Semi dry Western blotting apparatus	Bio-Rad
Termocycler	Bio-Rad
Termomixer	Eppendorf
Water bath	Julabo

4.2 Kits

Apo-ONE homogenous caspase-3/7 assay	Promega
Expanded high fidelity polymerase	Roche
On-target Plus smart pool siRNA	Dharmacon
Plasmid mini und maxi preparation	Qiagen
PCR Kit	Roche
Lipofectamine 2000	Invitrogen
Lipofectamine Plus transfection reagent	Invitrogen

4.3 Antibodies

Antibodies	Species	Dilution	Supplier
Anti-Htt CAG53b	Rabbit	1:5000	Scherzinger, 1997
Anti-Htt HD1 (Htt exon 1)	Rabbit	1:5000	Scherzinger, 1997
Anti-Htt EM48	Mouse	1:1000	Chemicon
Anti-Htt 4C8	Mouse	1:2000	Chemicon
Anti-Htt 1-82	Mouse	1:1000	Millipore
Anti-HA	Mouse	1:5000	Roche Diagnostics
Anti-His	Rabbit	1:1000	Sigma
Anti-Myc 71D10	Mouse	1:1000	Cell Signaling Technology
Anti-GFP	Rabbit	1:5000	Sigma
Anti-GAPDH	Mouse	1:5000	Sigma
Anti-Actin	Rabbit	1:2000	Abcam
Anti-CRMP2	Mouse	1:2000	Abcam
Anti-CRMP4	Rabbit	1:2000	BD Pharmingen
Anti-CRMP5	Rabbit	1:1000	BD Transduction Laboratories
Anti-DRPL32	Mouse	1:2000	Chemicon
Anti-Synaptobrevin	Rabbit	1:3000	Synaptic systems GmbH
Alex 549	Rabbit	1:1000	Invitrogen
Alex 488	Mouse	1:500	Invitrogen

4.4 Enzymes

Benzonase purity grade II	Merck
Caspase-3	Millipore
Lysozyme	Sigma-Aldrich
Prescission protease	Amersham Biosciencess
Proteinase K	Sigma
Purified porcine erythrocytes calpain I	Calbiochem
Rat recombinant calpain II	Calbiochem

4.5 Chemicals and consumables

3 MM blotting paper	Whatman GmbH, Göttingen
Agarose	Invitrogen
Agar plates Bio Assay Dish	Nunc GmbH & Co. KG, Wiesbaden
Amicon™ Ultra-15 centrifugal filter units	Millipore
Ampicillin-trihydrate	Sigma-Aldrich
Benchmark pre-stained protein ladder	Invitrogen
Bromophenol blue	Merck Eurolab GmbH
Calpeptin	Calbiochem
Caspase-3 inhibitor Z-VAD-FMK	R&D Systems
Cell culture dishes	TRP
Cell scrapers (COSTAR)	Corning Inc
Cellulose acetate membrane 0.2 µm	Schleicher and Schuell
Complete protease inhibitor cocktail	Roche
Cryo 1C freezing container	Nalgene
Dialysis discs 0.025 µm pore size	Millipore
Dialysis tubes, 5.000kDa cut of	SpectraPor
Dithiothreitol (DTT)	Serva
Dimethylsulfoxide (DMSO)	Sigma-Aldrich
Eppendorf tubes	Eppendorf
Ethidium bromide solution 10mg/ml	Sigma-Aldrich
Filter paper GB005	Schleicher and Schuell
Fluoronunc 96 well plates	Nunc
Glutathione-agarose	Sigma-Aldrich
Glutathione, reduced	Sigma-Aldrich
Glucose	Merck
Glycerol	Merck Eurolab GmbH
G Sepharose CL-4B beads	Amersham
IgG-coated beads	Amersham
J1 and J2 primers	The Jackson laboratory
Microtiter plates for filter assays	Costar

Ni-NTA-Agarose	Qiagen
Protran BA 83 nitrocellulose membrane	Schleicher and Schuell
PD-10 desalting columns	Amersham Biosciences
Phenylmethylsulfonylfuoride (PMSF)	Sigma-Aldrich
Polyoxyethylensorbitan-Monolaureat Tween20	Sigma-Aldrich
Ponceau S-solution, 0.1%	Sigma-Aldrich
P-t-Octylphenyl-polyoxyethylen Triton X-100	Sigma-Aldrich
PVDF membrane	Amersham Biosciences
Sodium	Sigma-Aldrich
TEMED	Life Technologies
Thiamine	Sigma-Aldrich

4.6 Enzymes

Benzonase purity grade II	Merck
Caspase-3	Millipore
Lysozyme	Sigma-Aldrich
Prescission protease	Amersham Biosciencess
Proteinase K	Sigma
Purified porcine erythrocytes calpain I	Calbiochem
Rat recombinant calpain II	Calbiochem

4.7 Solutions and buffers

10X CAPS buffer pH 11	100 mM, pH 11
10x DNA sample buffer	0.42% bromophenol blue, 0.42% xylenecyanol, 25% ficoll type 400, stored at 4°C.
10X PBS	80 g NaCl, 2 g KCl, 11.4 g Na_2HPO_4, 1l water.
10X Prescission	500 mM Tris-HCl, 1,5 M NaCl, 10mM EDTA, 10 mM
Protease™ buffer	DTT (add immediately before use) pH7, -20°C.
25X Protease inhibitors	one tablet of Complete™ protease inhibitor dissolved in 2 ml water, stored at -20°C (Roche).

5X SDS loading buffer	250 mM Tris-HCl pH 6.8, 500 mM DTT, 10% SDS, 5 mg/ml bromophenol blue, 50% glycerol, store at 4°C.
5% skim milk	skim milk powder was dissolved in TBS.
10X TBS	100 mM Tris-HCl pH 7.4, 150 mM NaCl, pH 7.4.
aCSF buffer	134 mM NaCl, 2.5 mM KCl, 1.3 mM $MgCl_2$, 2 mM $CaCl_2$, 1.2 mM K_2HPO_4, 10 mM Glucose, 26 mM $NaHCO_3$.
Ampicillin (1000X)	100mg/ml stored at -20.
AttoPhos™ buffer	50mM Tris-HCl pH9.0, 500mM NaCl, 1mM $MgCl_2$.
AttoPhos™ reagent	10mM AttoPhos reagent dissolved in 100 mM Tris pH9.0.
Calpain buffer	63 mM imidazole, pH 7.3, 10 mMβ-mercaptoethanol and 5 mM CaCl2
Coomassie blue	0.2% Coomassie blue, 7.5% Acetic acid, 50% ethanol
Destaining solution	10% ethanol, 0.75% Acetic acid.
Dialysis buffer	50 mM NaCl, 10 mM Tris-HCl pH7.4, 0.1mM EDTA.
DNA digestion buffer	50 mM KCl, 10 mM Tris HCl, pH 8.3, 2.5 mM $MgCl_2$, 0.1 mg/ml BSA, 0.45% NP-40, 0.45% Tween 20
Fixative solution	4% Paraformaldehyde in PBS
GST-P1- buffer	50mM NaH_4PO_2, 5mMTris-HCl pH8.0, 150mM NaCl, 1mM EDTA.
His-elution buffer	50 mM NaH_2PO_4, pH 8, 300mM NaCll
His-lysis buffer	50 mM NaH_2PO_4, pH 8, 300mM NaCl, 10 mM Imidazol
His-wash buffer	50 mM NaH_2PO_4, pH 8, 300mM NaCl, 20 mM Imidazol
Leaching buffer	50mM Tris/150mM NaCl
NP-40 buffer	50 mM Tris-HCl pH 7.5, 150 mM NaCl
PMSF	100 mM PMSF dissolved in isopropanol, -20°C
SDS-PAGE running buffer	20 mM Tris-HCl pH 8.0, 190 mM glycine, 0.1 % SDS
Western blotting running buffer	20 mM Tris-HCl pH 8.0, 150 mM glycine, 20% methanol

4.8 Media and supplement for mammalian cells culture

0.5 %Trypsin and 0.53 mM Na-EDTA in Hanks´ B.S.S.	Gibco
10000 units/ml Penicillin G and 10000 µg/ml	Gibco
Dulbecco`s modified Eagle medium (D-MEM) with Sodium pyruvate, L-glutamine and 100mg/l glucose	Gibco
DMEM with 4.5g/l glucose, L-glutamine	Gibco
Dulbecco`s phosphate buffered saline (D-PBS)	Gibco
Fetal calf serum (FCS)	Gibco
Horse Serum (HS)	Gibco
G418	Invitrogen
Ponasterone A (PonA)	Invitrogen
L-glutamine, 200mM (100x)	Gibco
Na-pyruvate, 100mM (100x)	Gibco
Neurobasal medium	Gibco
Streptomycin sulfate in 0.85 % saline	Gibco
Zeocin	Invitrogen

Chapter 5
Methods

5 Methods

5.1 Molecular Biology

5.1.1 DNA constructs

Plasmids were generated using commercially available Gateway® technology (Invitrogen). The entry clones from RZPD (http://www.imagenes-bio.de/search); CRMP1; IOH4496, CRMP2; IOH29086, CRMP3; IOH42101, CRMP4; IOH54070, CRMP5; IOH5686, and GAPDH; RZPDo839G08126D were shuttled into the destination vectors pTLHA1-D-48 and pFLAG-CMV2. His_7-tagged and GST-tagged proteins were constructed by shuttling the entry clones into the destination vectors pDESTco and pGEX-6p-D21, respectively. The GST-Htt1Q51, GST-HttQ23 and TAPHD510Q17 plasmids were previously described (Busch, 2003; Horn, 2006).

5.1.2 Preparation of plasmid DNA

LB medium containing the appropriate antibiotics was inoculated with a single *E. coli* colony carrying the respective plasmid. After overnight incubation at 37°C on a shaker, the cells were harvested by centrifugation at 3000 rpm for 10 min. Plasmid DNA was isolated using the QIAGEN Plasmid Mini or Maxi Kits according to manufacturer's instructions.

5.1.3 Determination of DNA concentration

The concentration of DNA in aqueous solution was determined by measuring the absorbance at 260 nm in a spectrophotometer (Photometer Ultraspec 3000).

5.1.4 DNA electrophoresis

Samples of 500 ng DNA were loaded to a 0.8-1.5% agarose gel containing 0.5 g/ml ethidium bromide. After separation, the DNA was visualized under UV light. TBE 1X was used as a running buffer.

5.2 Biochemistry

5.2.1 Antibodies

Affinity purified polyclonal antibodies against CRMP1 were generated by injecting KLH-MBS-conjugated linear peptides $_{504}$-YEVPATPKYATPAPS-$_{518}$ and $_{513}$-ATPAPSAKSSPSKHQ-$_{527}$ into rabbits (Eurogentec, Belgium). Isoform specificity was verified by dot-blot assays and Western blotting.

5.2.2 Bacterial expression of GST/His$_7$-tagged fusion proteins

All proteins were expressed in *E. coli* BL21 (DE3) pLysS strain (Promega). Each recombinant protein was tested before producing it at large scale. 100 ml of LB broth medium with 100 µg/ml ampicillin (amp) was incubated with a bacterial clone containing the expression vector of interest. The culture was allow to grow overnight at 37°C with constant shaking. The next day, this culture was used to inoculate 1.5 litters of LB medium, containing 100 µg/ml amp, 20 mM MOPS/KOH pH 7.9, 0,2% glucose and 20 µg/ml thiamine. The culture was grown at 37°C until an OD_{600} (optical density) of 0.4-0.6 at 600 nm was reached. The expression of recombinant proteins was induced by adding IPTG for a final concentration of 1 mM. After an additional growth of 4 h at 37°C, the bacterial cells were pelleted by centrifugation at 4000 x g and 4°C for 15 min. After washing, the pellets were snap-frozen in liquid nitrogen and stored at -80 °C. Overexpression of the fusion proteins was confirmed by SDS-PAGE analysis.

5.2.3 Purification of GST fusion proteins

The bacterial cell pellet was resuspended in 25 ml of GST-P1-buffer containing lysozyme and PMSF at 0.5 mg/ml and 1 mM, respectively. After incubation on ice for 45 min, the suspension was lysed twice using French Press and the lysates were centrifuged at 30 000 x g and 4°C for 30 min.

200 mg of glutathione agarose were allowed to swell in 30 ml 1 M NaCl at 4°C overnight. The agarose beads were briefly centrifuged at 1000 rpm and washed three times with H_2O and twice with GST-P1-buffer. After removal of supernatant, beads were incubated with bacterial lysates containing the GST-recombinant protein for 1 h at 4°C on a rotating wheel. The suspension was poured onto a 5 ml

plastic column, washed once with 10 ml of GST-P1-buffer containing 0.1% Triton-X100 and 1 mM PMSF and twice with 10 ml of GST-P1-buffer containing 1 mM PMSF. Elution was achieved by pouring 1 ml of GST-P1-buffer containing 15 mM reduced glutathione onto the column. This elution step was continued until the protein concentration of the eluate was below 0.2 µg/µl. The fractions containing the purified GST fusion protein were pooled and dialyzed overnight against dialysis buffer. The protein solution was aliquoted and, snap-frozen in liquid nitrogen and stored at -80°C until use.

5.2.4 Purification of His fusion proteins

Protein purification was performed using Ni-NTA agarose beads (Qiagen). Briefly, the bacterial cell pellet (1.5 liters culture) was resuspended and incubated with 10 ml His-lysis buffer containing 1 mg/ml lysozyme and 0.5 mM PMSF for 30 min on ice. The suspension was lysed twice using French Press and the lysates were centrifuged at 10 000 x g and 4°C for 30 min.

The Ni-NTA agarose beads were briefly centrifuged at 1000 x and washed three times with His-lysis buffer. 3 ml of Ni-NTA agarose beads were incubated with the bacterial supernatant containing the His-recombinant protein for 1 h at 4°C on a rotating wheel. The suspension was poured onto a 5 ml plastic column, washed once with His-washing buffer containing 1 mM PMSF and twice with 10 ml of His-washing buffer. Elution was achieved by pouring 10 ml of His-elution buffer onto the column. The eluate containing the purified His fusion protein was dialyzed overnight against 10 liters of dialysis buffer. The protein solution was aliquoted and, snap-frozen in liquid nitrogen and stored at -80°C until use.

5.2.5 SDS-polyacrylamide gel electrophoresis (SDS-PAGE)

Samples were diluted in an equal volume of 2X SDS sample buffer, heated for 5 min at 100°C and separated on 8-12% mini SDS-PAGE gel. For protein staining after electrophoresis separation, the gel was incubated in Coomassie blue for 1 hour. The gel was then destained in the destaining solution for 30 min with constant shaking. The protein sizes were determined using Bench marker.

5.2.6 Western blotting

The proteins separated on SDS-gels were blotted onto Protran BA 83 nitrocellulose membrane (Schleicher and Schuell) using SD Semi-dry Transblot Apparatus (Bio-Rad). The blotting was performed at 20 V for 1 hour. The membranes were then incubated in blocking solution for 1 h at room temperature. Subsequently, the immunoblots were incubated with primary antibodies overnight and followed by a secondary antibody conjugated to alkaline phosphatase. For the detection the membranes were immersed for 1-3 min in an AttoPhos buffer containing 200 fold dilution of Attophos reagent (Europa Bioproducts). The signal was visualized by fluorescence under blue light in an Image reader (Fuji) and quantified using the AIDA software.

5.2.7 Ponceau-S staining

After blotting, the nitrocellulose membrane was quickly rinsed with distilled H_2O and incubated in Ponceau-S solution for a few seconds. Subsequently, the membrane was washed with distilled water to remove background staining.

5.2.8 Protein aggregation reaction *in vitro*

2 µM of GST-FALG-Httexon1, 1.3 units Prescission protease and different amount of CRMP1 protein were incubated in Prescission protease buffer at 30 °C for the specified period of time. Aggregates were detected with filter retardation assay.

5.2.9 Detection of recombinant Htt aggregates

The *in vitro* filter trap was performed as described previously (Scherzinger 1997; Wanker 1999). The aggregation reactions were boiled in 4% SDS, 100 mM DTT for 5 min at 100 °C. Aliquots were diluted into 200 µl of 0.2% SDS and filtered through cellulose acetate membranes of 0.2 µM pore size using a BRL dot blot filtration unit. The membranes were washed twice with 200 µl SDS 0.2% per well and the SDS-resistant aggregates retained on the filter were detected using anti-Htt CAG53b antibody, followed by an anti-rabbit secondary antibody conjugated to alkaline phosphatase.

5.2.10 *In vitro* Calpains cleavage of CRMP1

Constitutively active calpain I (purified porcine erythrocytes calpain I), II (rat recombinant calpain) (Calbiochem), and recombinant caspase-3 (Millipore) at the specified concentrations were mixed with 20 µg of normal soluble brain extracts or 2 µg of bacterially expressed full-length His-CRMP1. After incubation at 4°C for 18h in calpain buffer (Kowara, 2005), digestion products were separated on 8-10% SDS-PAGE gel, followed by Western blotting using anti-CRMP1 or His-tag antibodies.

To demonstrate that the endogenous calpain cleaves CRMP1, normal striatum extracts were pretreated either with or without calpain inhibitor calpeptin (10 µM) (Calbiochem), or general caspase-3 Inhibitor Z-VAD-FMK (20 µM) (R&D Systems). After 30 minutes incubation, calcium at 5 mM concentration was added to the brain lysates. The samples were incubated at 4 °C for 18 hours and 20 µg of brain extracts were analyzed by SDS-PAGE and Western blotting.

5.2.11 N-terminal microsequencing

His-tagged CRMP1 protein was digested with active calpain 1 or 2. After digestion, the samples were separated on 8% SDS–PAGE gel and blotted onto a polyvinylidene difluoride (PVDF) membrane (Amersham Biosciences) using CAPS buffer and standard methods. Ponceau S stained-CRMP1 bands were cut out and subjected to N-terminal microsequencing using Edman degradation on a 494 Procise ™ protein sequencer (Applied Biosystems)

5.3 Transgenic mice

All animal experiments were performed following animal protection regulations. The R6/2 transgenic mice were purchase from the Jackson Laboratory and bred locally. Mice were fed food and water *ad libitum* and subject to a 12 h light/dark cycle. The genotyping and phenotype analyses were performed as described previously (Suopanki, 2006).

5.3.1 Genotyping

Mouse tail biopsies were digested in 200ul DNA digestion buffer containing proteinase K (0.6 µg/ml) at 55°C overnight. The genotyping of successive offspring was assessed on tail DNA using the primers J1 and J2 and Expand high fidelity polymerase from Roche (The Jackson laboratory; http://www.jax.org). The amplification reaction conditions were as follows:

Step 1: 94°C for 3 min
Step 2: 94°C for 35 sec
Step 3: 61°C for 45 sec
Step 4: 72°C for 45 sec
Step 5: Go to 2, 15 times
Step 6: 94°C for 35 sec
Step 7: 55°C for 30 sec
Step 8: 72°C for 45 sec
Step 9: Go to 6, 35 times
Step 10: 72°C for 4 min
Step 11: 4°C

5.3.2 Preparation of brain extracts for Western blotting

Whole brains were dissected from mice and rapidly frozen by immersion in liquid nitrogen. One-half brain or striatum was homogenized in NP-40 buffer containing 1% NP-40, protease inhibitors and 25 U/ml Benzonase. Total protein concentrations were determined using Bio-Rad protein assay and the lysates were adjusted to 12 µg/µl of total protein. Equal amount of total extracts were analyzed by SDS-

PAGE and Western blotting.

For striatum extraction, both wild-type and transgenic mice were killed by cervical dislocation, and their brains were quickly removed and placed in artificial cerebrospinal fluid buffer (aCSF) bubbled with 95% O_2 and 5% CO_2. Subsequently, the brains were sliced using a vibratome and 300 µM-thick pieces were collected in aCSF buffer. The striatum was dissected under light microscopy and rapidly frozen in liquid nitrogen. The purity of the striatum samples were evaluated by Western blotting.

5.3.3 Tissue preparation and immunohistochemistry

R6/2 mice at 12 weeks of age were deeply anesthetized and perfused with an ice-cold fixative solution. The brains were removed, post-fixed in 4% PFA for 4 hours and subsequently cryoprotected in 30% sucrose. Serial sections of 30 µm were cut using a vibratome (Leica) and free-floating sections were collected in PBS for staining. The sections were permeabilized with 0.3% Triton X-100 and blocked in PBS containing 2% bovine serum albumin (BSA) and 10% normal donkey serum (NDS).

Immunolabelling was performed by incubating the sections overnight at 4 °C in primary antibodies: EM48 (1:200), rabbit anti-CRMP1 (1:400). Fluorescence was detected using Alexa 549 or Alexa 488 conjugated secondary antibodies (1:500 Invitrogen). Colocalization was determined using a Leica DM 2500 confocal microscope (Zeiss)

5.3.4 Co-immunoprecipitation of the Htt-CRMP1 complex from the mouse brain

For the verification of the endogenous Htt and CRMP1 interactions, the wild type mouse brain was homogenized in the 10 volumes of ice-cold NP-40 buffer containing 1% NP-40, 25 U/ml Benzonase and Protease inhibitors. The brain lysate were centrifuged at 14.000 rpm and 4°C for 15 min, to remove insoluble cell debris. 750 µg of total brain lysate in 300 µl NP-40 buffer was incubated with anti-Htt HD1 antibody for 1h at 4°C. After incubation, 30 µl of protein G Sepharose CL-4B beads (Amersham) were added and incubation at 4°C was continued for 1

hour. As controls, non-immune serum corresponding to anti-HD1 antibody, polyclonal anti-synaptobrevin or no primary antibody (empty beads) were used. Unbound proteins were removed by washing three times with lysis buffer. The protein complexes were heat-denatured with 1X SDS-sample buffer at 90°C for 5 min and analyzed by SDS-PAGE and Western blotting with monoclonal anti-Htt 4C8, and anti-CRMP1 antibodies.

5.4 Fly lines

The flies were kept at 25°C on standard medium. The truncated UAS-Htt transgene has been previously described (Kaltenbach, 2007) and was a kind gift from Juan Botas. The GFP (stock 1522) and EGFP fly line (stock 5430) were obtained from the Bloomington *Drosophila* Stock Center. Entry clones IOH4496 (CRMP1) were used to subclone the respective human cDNA into the pTHW vector using commercially available Gateway® technology (Invitrogene). Transgenic flies were generated in the w^{1118} background from BestGene Inc (Chino Hills, USA). For genotyping genomic DNA of transgenic flies was prepared and used for PCR amplification of the respective human cDNA using the primers TAC AAG TTT GTA CAA AAA AGC AGG C and ACC ACT TTG TAC AAG AAA GCT GGG T. The amplification reaction conditions were as follows:

Step 1: 95°C for 2 min
Step 2: 94°C for 30 sec
Step 3: 55°C for 30 sec
Step 4: 72°C for 45 sec
Step 5: Cycle from step 2 to step 4, 25 times
Step 6: 72°C for 4 min
Step 7: 4°C

5.4.1 Western blots for fly experiments

Eye imaginal discs of third instar wandering larvae were prepared and rapidly frozen by immersion in liquid nitrogen. The eye imaginal discs were homogenized

in NP-40 buffer containing 1% NP-40, 25 U/ml Benzonase and Protease inhibitors. Total protein concentrations were determined using Bio-Rad protein assay and the lysates were adjusted to 10 µg/µl of total protein. Equal amount of total extracts were analyzed by SDS-PAGE and Western blotting.

5.4.2 Immunostaining of eye imaginal discs of third instar larvae

Eye imaginal discs of third instar larvae co-expressing a human Htt fragment (Htt336Q128) with or without a human Myc-tagged CRMP1 protein were immunolabeled with anti-Htt 1-82 antibody and anti-Myc 71D10 antibody. Secondary antibodies were: anti-rabbit Alexa Fluor 488 (Invitrogen) and anti-mouse Alexa Fluor 549 (Invitrogen). All antibodies were applied in a concentration of 1:500. Straining was analyzed using a Leica DM 2500 confocal microscope (Zeiss).

5.4.3 Retina degeneration assay

For retina degeneration assay, flies were anesthetized with CO_2 and the heads were dissected and fixed in Bouin's fixative (Sigma). After fixation, the heads were incubated with leaching buffer overnight. The heads were washed several times with 70% ethanol, dehydrated and immersed in pure paraffin. The paraffin blocks were cut into 10µm floating serial sections. Prior histological examinations, sections were dewaxed with xylol and embedded in Entelan (Merck) without additional staining. Around 11 females were analyzed per genotype. The retinal degeneration was monitored by light microscopy.

5.5 Cell Cultures

The COS1 cells were grown in humidified incubator at 37°C and 5% CO_2 in D-MEM medium supplemented with 5% FCS, 100 ug/ml penicillin/streptomycin.

The inducible PC12 cell line expressing exon 1 of the HD gene with 103Qs fused to EGFP, has been previously described (Apostel, 2002). These cells were maintained in complete media with continued selection: high glucose Dulbecco´s modified Eagle´s medium (DMEM) with 10% HS, 5% FCS, 1%

penicillin/streptomycin, 200 µg/ml G418, 2 mM glutamine and Zeocin at 37°C and 5% CO_2. Htt expression was induced by incubating the cells in media containing 5 µM of Ponasterone A (Invitrogen) for the specified period of time.
Plasmids and siRNA transfections were achieved using Lipofectamine 2000 (Invitrogen) following the manufacturer's instructions.

5.5.1 Primary neuronal cell culture

Cerebral cortices isolated from C57BL/6 mice at embryonic (E) day 16 were dissociated by 0.1% trypsin/EDTA and dissected with a fire-polished Pasteur pipette. Cells were seeded at a concentration of 0.3×10^6 cells/well into pre-coated glass cover slips inserted into 24-well plates. The cover slips were pre-coated with Poly-Lysine and collagen. The cells were grown in Neurobasal medium (Gibco), supplemented with B27 (Gibco), 0.5 mM L-glutamine and 1% penicillin/streptomycin. Every three days 50% of the medium was exchanged.

5.5.2 Immunocytochemistry

Primary cortical neuronal or PC12 cells were fixed with 4% paraformaldehyde (PFA). Subsequently, they were permeabilized with 0.3% Triton X-100 and blocked in PBS containing 2% bovine serum albumin (BSA), 10% normal donkey serum (NDS). The anti-CRMP1-504 was applied for 1 hour at 4°C, followed by incubation with secondary antibodies for 30 minutes at RT (donkey anti-rabbit IgG Alexa488 conjugated antibody. Images were taken with the confocal microscope Leica DM 2500, and pictures were merged with ImageJ software.

5.5.3 Immunoprecipitation of the Htt-CRMP1 complex from cell culture

For the verification of the Htt and CRMP1 interaction, COS1 cells were cotransfected with plasmids encoding the first 510 amino acids of Htt with 17 glutamines and a hemagglutin (HA) tagged-CRMP1. 40 hours post-transfection, cell were washed with cold PBS and lysed on ice for 35 min with NP-40 buffer containing 1% NP-40, 25 U/ml Benzonase and protease inhibitor (Roche). Cell extract were centrifuged at 6000 rpm and 4°C for 5 minutes, and the supernatants (total soluble extract) were used for immunoprecipitations. For each

immunoprecipitation experiment, 150 µg proteins in 300 µl NP-40 lysis buffer were used, to which 5 µl of polyclonal anti-Htt HD1 antibody was added. After incubation for 2 hours at 4°C with rotation, 30 µl of protein G Sepharose CL-4B beads (1:1 slurry, Amersham) were added and incubation at 4°C on a rotating wheel was continued for 1 hour. The beads were spun briefly at 1000 rpm and washed three times with 500 µl NP-40 buffer to remove unbound proteins. After washing, the beads were heat-denatured with 1X-SDS-sample buffer at 90°C for 5 min. Immunocomplexes were analyzed by Western blotting using monoclonal anti-Htt 4C8 or with monoclonal anti-HA antibodies. Control experiments were performed with non-immune serum corresponding to anti-HD1 antibody, and with the empty beads.

For tandem affinity purification assay (Stelzel, 2005; Horn, 2006), COS1 cells were transiently cotransfected with plasmids encoding HA-CRMP1 and a protein A (PA)-tagged Htt protein (TAP-Htt510Q17). 40 hours post-transfection, cell were washed with cold PBS and lysed on ice for 35 min with NP-40 buffer containing 1% NP-40, 25 U/ml Benzonase and protease inhibitor (Roche). Cell extract were centrifuged at 6000 rpm and 4°C for 5 minutes, and the supernatants (total soluble extract) were used for the assay. For each experiment, 150 µg proteins in 300 µl NP-40 lysis buffer containing 30 µl of the IgG-coated beads (1:1 slurry, company) were used. After incubation for 1 hour at 4°C with rotation, the beads were briefly pulled down by centrifugation at 1000 rpm for 5 minutes. Unbound proteins were removed by washing three times with 500 µl NP-40 buffer. The bound proteins were heat-denatured with 1X-SDS-sample buffer at 90°C for 5 minutes and the interaction of HA-CRMP1 with TAP-Htt510Q17 was visualized using an anti-HA, or anti-CRMP1 antibodies.

5.5.4 Detection of Htt aggregates from PC 12 cell culture extracts

For the quantification of Htt-heat-insoluble aggregates in PC12 cells, the samples were lysed in NP-40 lysis buffer containing: 25 U/ml Benzonase, 1% Tween20 and Protease inhibitors (Roche). Htt aggregates were analyzed by the filter-trap assay. The signal was visualized by fluorescence under blue light in an Image reader (Fuji) and quantified using the AIDA program.

5.5.5 RNA interference

For silencing of endogenous CRMP1, the PC12 cells were transfected with 50 µM CRMP1-specific siRNA (On-target Plus smart pool siCRMP1 L-041218-01-0005, Dharmacon, USA) or 50 µM of non-coding control siRNA (siGLO green transfection indicator) for 48 hours, followed by induction of mutant Htt for 40 hours. Target gene down-regulation was confirmed by Western blotting.

5.5.6 Cell toxicity assay

For the Detection of apoptotic cells, the Apo-ONE Homogenous caspase-3/7 Assay (Promega) was used according to manufacturer's procedures. Briefly, the cells were incubated with a bifunctional cell lysis/activity buffer containing the pro-fluorescent substrate Z-DEVE-R110. The substrate can be cleaved by active caspase-3/7 revealing a fluorescent group, what can be quantified in a fluorometer with excitation set at 499 nm and emission at 521 nm. The increased in fluorescent signal correlates with elevated caspase-3/7 activity.

5.6 Atomic force microscopy (AFM)

GST-Htt exon 1 fusion proteins were incubated with Prescission protease to induce polyQ-meditated protein aggregation (Busch, 2003). Aliquots of 20 µl were adsorbed to a surface of freshly cleaved mica (5 x 5 mm) for 2 minutes. Salts and unbound materials were removed through three washes by adding 30 µl of distilled water and immediately absorbing excess liquid into filter paper. AFM images were recorded in intermittent contact mode using a NanoWizard II scanning probe microscope (JPK, Berlin, Germany). Overviews (30 µm x 30 µm) were recorded before detailed pictures of representative areas were recorded for each sample.

5.7 Data analysis

Error bars in all graphs represent SD of at least three independent experiments. Statistical significance was determined by unpaired two-tailed t-test.

6 List of Abbreviations

AD Alzheimer's disease

AFM Atomic Force Microscopy

Akt v-akt murine thymoma viral oncogene homolog 1

ATM ataxia telangiectasia mutated

BDNF brain-derived neutrophic factor

BRCA1 breast cancer 1, early onset

BRCA2 breast cancer 2, early onset

CAG Cytosine, Adenine and Guanine

CBP CREB-binding protein

CHEK2 CHK2 checkpoint homolog

CHIP carboxy terminus of Hsp70p-interacting protein

CREB1 cAMP responsive element binding protein1

CRMP Collapsin Response Mediator Protein

DRPLA dentate-rubral and pallido-luysian atrophy

DTT dithiothreitole

EDTA ethylenediamine tetraacetic acid

DARPP-32 dopamine and cAMP regulated phosphoprotein,

EGFP Enhanced Green Fluorescent Protein

GARP GRB2-related adaptor protein

GIT1 G protein-coupled receptor kinase interacting ArfGAP 1

GRB2 growth factor receptor bound protein 2

GST glutathione-S-transferase

HA haemagglutinin

HAP1Htt-associated protein

HD Huntington's disease

HIP1 Htt interacting protein 1

HIP14 Htt interacting protein 14

His histidine

Hsp heat shock protein

Htt Huntingtin

OD optical density

PACSIN1 protein kinase C and casein kinase substrate in neurons
PC12 rat adrenal phaeochromosytoma
PD Parkinson's disease
PMSF phenylmethylsulfonyl fluoride
PolyQ polyglutamine
PPI protein-protein interaction
MAP3K10 mitogen-activated protein kinase kinase kinase 10
RAS p21 protein activator (GTPase activating protein) 1
RNA ribonucleic acid
rpm rotations per minute
SBMA spinal and bulbar muscular atrophy
SCA spinocerebellar ataxias
SDS sodium dodecyl sulphate
SDS-PAGE sodium dodecyl sulphate polyacrylamide gel electrophoresis
Ser serine
SH3GL3 SH3-domain GRB2-like 3
SP1 Sp1 transcription factor
TBS tris buffered saline
TBP TATA-binding protein
TCERG1 transcription elongation regulator 1
TEMED N,N,N',N'-tetramethylethylenediamine,
1,2-bis(dimethylamino)-ethane
TP53 Tumor protein 53
TRiC TCP1 ring complex
Tris tris(hydroxymethyl)aminomethane
Y2H yeast 2 hydride
UPS ubiquitin proteasome systems
UNC33 UNCoordinated-33

7 Bibliography

1. A novel gene containing a trinucleotide repeat that is expanded and unstable on Huntington's disease chromosomes. The Huntington's Disease Collaborative Research Group. Cell, 1993. 72(6): p. 971-83.
2. Aiken, C.T., A.J. Tobin, and E.S. Schweitzer, A cell-based screen for drugs to treat Huntington's disease. Neurobiol Dis, 2004. 16(3): p. 546-55.
3. Albin, R.L. and D.A. Tagle, Genetics and molecular biology of Huntington's disease. Trends Neurosci, 1995. 18(1): p. 11-4.
4. Albin, R.L., A.B. Young, and J.B. Penney, The functional anatomy of basal ganglia disorders. Trends Neurosci, 1989. 12(10): p. 366-75.
5. Andrade, M.A. and P. Bork, HEAT repeats in the Huntington's disease protein. Nat Genet, 1995. 11(2): p. 115-6.
6. Apostol, B.L., et al., Mutant huntingtin alters MAPK signaling pathways in PC12 and striatal cells: ERK1/2 protects against mutant huntingtin-associated toxicity. Hum Mol Genet, 2006. 15(2): p. 273-85.
7. Arimura, N., et al., Phosphorylation of collapsin response mediator protein-2 by Rho-kinase. Evidence for two separate signaling pathways for growth cone collapse. J Biol Chem, 2000. 275(31): p. 23973-80.
8. Arrasate, M., et al., Inclusion body formation reduces levels of mutant huntingtin and the risk of neuronal death. Nature, 2004. 431(7010): p. 805-10.
9. Auvergnon, N., et al., Altered expression of CRMPs in the brain of bovine spongiform encephalopathy-infected mice during disease progression. Brain Res, 2009.
10. Bae, B.I., et al., Mutant huntingtin: nuclear translocation and cytotoxicity mediated by GAPDH. Proc Natl Acad Sci U S A, 2006. 103(9): p. 3405-9.
11. Banik, N.L., et al., Increased calpain content and progressive degradation of neurofilament protein in spinal cord injury. Brain Res, 1997. 752(1-2): p. 301-6.
12. Bao, J., et al., Expansion of polyglutamine repeat in huntingtin leads to abnormal protein interactions involving calmodulin. Proc Natl Acad Sci U S A, 1996. 93(10): p. 5037-42.
13. Barabasi, A.L. and Z.N. Oltvai, Network biology: understanding the cell's functional organization. Nat Rev Genet, 2004. 5(2): p. 101-13.

14. Bartus, R.T., et al., Calpain as a novel target for treating acute neurodegenerative disorders. Neurol Res, 1995. 17(4): p. 249-58.
15. Bartus, R.T., et al., Calpain inhibitor AK295 protects neurons from focal brain ischemia. Effects of postocclusion intra-arterial administration. Stroke, 1994. 25(11): p. 2265-70.
16. Beighton, P. and M.R. Hayden, Huntington's chorea. S Afr Med J, 1981. 59(8): p. 250.
17. Bhattacharyya, N.P., Huntington's disease: a monogenic disorder with cellular and biochemical complexities. FEBS J, 2008. 275(17): p. 4251.
18. Bretin, S., et al., Differential expression of CRMP1, CRMP2A, CRMP2B, and CRMP5 in axons or dendrites of distinct neurons in the mouse brain. J Comp Neurol, 2005. 486(1): p. 1-17.
19. Bretin, S., et al., Calpain product of WT-CRMP2 reduces the amount of surface NR2B NMDA receptor subunit. J Neurochem, 2006. 98(4): p. 1252-65.
20. Budihardjo, I., et al., Biochemical pathways of caspase activation during apoptosis. Annu Rev Cell Dev Biol, 1999. 15: p. 269-90.
21. Burke, J.R., et al., Huntingtin and DRPLA proteins selectively interact with the enzyme GAPDH. Nat Med, 1996. 2(3): p. 347-50.
22. Burnett, B.G., et al., Expression of expanded polyglutamine targets profilin for degradation and alters actin dynamics. Neurobiol Dis, 2008. 30(3): p. 365-74.
23. Busch, A., et al., Mutant huntingtin promotes the fibrillogenesis of wild-type huntingtin: a potential mechanism for loss of huntingtin function in Huntington's disease. J Biol Chem, 2003. 278(42): p. 41452-61.
24. Byk, T., et al., Identification and molecular characterization of Unc-33-like phosphoprotein (Ulip), a putative mammalian homolog of the axonal guidance-associated unc-33 gene product. J Neurosci, 1996. 16(2): p. 688-701.
25. Calvano, S.E., et al., A network-based analysis of systemic inflammation in humans. Nature, 2005. 437(7061): p. 1032-7.
26. Carter, R.J., et al., Characterization of progressive motor deficits in mice transgenic for the human Huntington's disease mutation. J Neurosci, 1999. 19(8): p. 3248-57.
27. Charrier, E., et al., Collapsin response mediator proteins (CRMPs):

involvement in nervous system development and adult neurodegenerative disorders. Mol Neurobiol, 2003. 28(1): p. 51-64.
28. Cheillan, D., et al., Abnormal expression of truncated CRMP-1 protein in the brain cortex of MPSIIIB mice. Mol Genet Metab, 2008. 94(1): p. 135-8.
29. Chen, N., et al., Subtype-specific enhancement of NMDA receptor currents by mutant huntingtin. J Neurochem, 1999. 72(5): p. 1890-8.
30. Chung, M.A., et al., Alteration of collapsin response mediator protein-2 expression in focal ischemic rat brain. Neuroreport, 2005. 16(15): p. 1647-53.
31. Ciechanover, A. and P. Brundin, The ubiquitin proteasome system in neurodegenerative diseases: sometimes the chicken, sometimes the egg. Neuron, 2003. 40(2): p. 427-46.
32. Cole, A.R., et al., Distinct priming kinases contribute to differential regulation of collapsin response mediator proteins by glycogen synthase kinase-3 in vivo. J Biol Chem, 2006. 281(24): p. 16591-8.
33. Cole, A.R., et al., GSK-3 phosphorylation of the Alzheimer epitope within collapsin response mediator proteins regulates axon elongation in primary neurons. J Biol Chem, 2004. 279(48): p. 50176-80.
34. Cole, A.R., et al., Collapsin response mediator protein-2 hyperphosphorylation is an early event in Alzheimer's disease progression. J Neurochem, 2007. 103(3): p. 1132-44.
35. Conneally, P.M., Huntington disease: genetics and epidemiology. Am J Hum Genet, 1984. 36(3): p. 506-26.
36. Cornett, J., et al., Polyglutamine expansion of huntingtin impairs its nuclear export. Nat Genet, 2005. 37(2): p. 198-204.
37. Cowan, C.M., et al., Polyglutamine-modulated striatal calpain activity in YAC transgenic huntington disease mouse model: impact on NMDA receptor function and toxicity. J Neurosci, 2008. 28(48): p. 12725-35.
38. Cowan, C.M. and L.A. Raymond, Selective neuronal degeneration in Huntington's disease. Curr Top Dev Biol, 2006. 75: p. 25-71.
39. Cummings, C.J., et al., Chaperone suppression of aggregation and altered subcellular proteasome localization imply protein misfolding in SCA1. Nat Genet, 1998. 19(2): p. 148-54.

40. Davies, S.W., et al., Formation of neuronal intranuclear inclusions underlies the neurological dysfunction in mice transgenic for the HD mutation. Cell, 1997. 90(3): p. 537-48.
41. de la Monte, S.M., J.P. Vonsattel, and E.P. Richardson, Jr., Morphometric demonstration of atrophic changes in the cerebral cortex, white matter, and neostriatum in Huntington's disease. J Neuropathol Exp Neurol, 1988. 47(5): p. 516-25.
42. de Lichtenberg, U., et al., Dynamic complex formation during the yeast cell cycle. Science, 2005. 307(5710): p. 724-7.
43. Deo, R.C., et al., Structural bases for CRMP function in plexin-dependent semaphorin3A signaling. EMBO J, 2004. 23(1): p. 9-22.
44. DiFiglia, M., et al., Huntingtin is a cytoplasmic protein associated with vesicles in human and rat brain neurons. Neuron, 1995. 14(5): p. 1075-81.
45. DiFiglia, M., et al., Aggregation of huntingtin in neuronal intranuclear inclusions and dystrophic neurites in brain. Science, 1997. 277(5334): p. 1990-3.
46. DiProspero, N.A., et al., Early changes in Huntington's disease patient brains involve alterations in cytoskeletal and synaptic elements. J Neurocytol, 2004. 33(5): p. 517-33.
47. Djousse, L., et al., Evidence for a modifier of onset age in Huntington disease linked to the HD gene in 4p16. Neurogenetics, 2004. 5(2): p. 109-14.
48. Dohmen, R.J., SUMO protein modification. Biochim Biophys Acta, 2004. 1695(1-3): p. 113-31.
49. Dragatsis, I., M.S. Levine, and S. Zeitlin, Inactivation of Hdh in the brain and testis results in progressive neurodegeneration and sterility in mice. Nat Genet, 2000. 26(3): p. 300-6.
50. Dunah, A.W., et al., Sp1 and TAFII130 transcriptional activity disrupted in early Huntington's disease. Science, 2002. 296(5576): p. 2238-43.
51. Faber, P.W., et al., Huntingtin interacts with a family of WW domain proteins. Hum Mol Genet, 1998. 7(9): p. 1463-74.
52. Fukada, M., et al., Molecular characterization of CRMP5, a novel member of the collapsin response mediator protein family. J Biol Chem, 2000. 275(48): p. 37957-65.

53. Fukata, Y., et al., CRMP-2 binds to tubulin heterodimers to promote microtubule assembly. Nat Cell Biol, 2002. 4(8): p. 583-91.
54. Gafni, J. and L.M. Ellerby, Calpain activation in Huntington's disease. J Neurosci, 2002. 22(12): p. 4842-9.
55. Gafni, J., et al., Inhibition of calpain cleavage of huntingtin reduces toxicity: accumulation of calpain/caspase fragments in the nucleus. J Biol Chem, 2004. 279(19): p. 20211-20.
56. Gan, L. and L. Mucke, Paths of convergence: sirtuins in aging and neurodegeneration. Neuron, 2008. 58(1): p. 10-4.
57. Gervais, F.G., et al., Recruitment and activation of caspase-8 by the Huntingtin-interacting protein Hip-1 and a novel partner Hippi. Nat Cell Biol, 2002. 4(2): p. 95-105.
58. Goehler, H., et al., A protein interaction network links GIT1, an enhancer of huntingtin aggregation, to Huntington's disease. Mol Cell, 2004. 15(6): p. 853-65.
59. Good, P.F., et al., A role for semaphorin 3A signaling in the degeneration of hippocampal neurons during Alzheimer's disease. J Neurochem, 2004. 91(3): p. 716-36.
60. Goshima, Y., et al., Collapsin-induced growth cone collapse mediated by an intracellular protein related to UNC-33. Nature, 1995. 376(6540): p. 509-14.
61. Graham, R.K., et al., Cleavage at the caspase-6 site is required for neuronal dysfunction and degeneration due to mutant huntingtin. Cell, 2006. 125(6): p. 1179-91.
62. Graveland, G.A., R.S. Williams, and M. DiFiglia, Evidence for degenerative and regenerative changes in neostriatal spiny neurons in Huntington's disease. Science, 1985. 227(4688): p. 770-3.
63. Groves, M.R., et al., The structure of the protein phosphatase 2A PR65/A subunit reveals the conformation of its 15 tandemly repeated HEAT motifs. Cell, 1999. 96(1): p. 99-110.
64. Gu, Y., N. Hamajima, and Y. Ihara, Neurofibrillary tangle-associated collapsin response mediator protein-2 (CRMP-2) is highly phosphorylated on Thr-509, Ser-518, and Ser-522. Biochemistry, 2000. 39(15): p. 4267-75.
65. Guidetti, P., et al., Early degenerative changes in transgenic mice

expressing mutant huntingtin involve dendritic abnormalities but no impairment of mitochondrial energy production. Exp Neurol, 2001. 169(2): p. 340-50.
66. Gutekunst, C.A., et al., Nuclear and neuropil aggregates in Huntington's disease: relationship to neuropathology. J Neurosci, 1999. 19(7): p. 2522-34.
67. Hamajima, N., et al., A novel gene family defined by human dihydropyrimidinase and three related proteins with differential tissue distribution. Gene, 1996. 180(1-2): p. 157-63.
68. Harjes, P. and E.E. Wanker, The hunt for huntingtin function: interaction partners tell many different stories. Trends Biochem Sci, 2003. 28(8): p. 425-33.
69. Harper, P.S., The epidemiology of Huntington's disease. Hum Genet, 1992. 89(4): p. 365-76.
70. Hay, D.G., et al., Progressive decrease in chaperone protein levels in a mouse model of Huntington's disease and induction of stress proteins as a therapeutic approach. Hum Mol Genet, 2004. 13(13): p. 1389-405.
71. Hayden, M.R., et al., Huntington's chorea on the island of Mauritius. S Afr Med J, 1981. 60(26): p. 1001-2.
72. Hedgecock, E.M., et al., Axonal guidance mutants of Caenorhabditis elegans identified by filling sensory neurons with fluorescein dyes. Dev Biol, 1985. 111(1): p. 158-70.
73. Hedreen, J.C. and S.E. Folstein, Early loss of neostriatal striosome neurons in Huntington's disease. J Neuropathol Exp Neurol, 1995. 54(1): p. 105-20.
74. Hedreen, J.C., et al., Neuronal loss in layers V and VI of cerebral cortex in Huntington's disease. Neurosci Lett, 1991. 133(2): p. 257-61.
75. Hermel, E., et al., Specific caspase interactions and amplification are involved in selective neuronal vulnerability in Huntington's disease. Cell Death Differ, 2004. 11(4): p. 424-38.
76. Ho, L.W., et al., Wild type Huntingtin reduces the cellular toxicity of mutant Huntingtin in mammalian cell models of Huntington's disease. J Med Genet, 2001. 38(7): p. 450-2.
77. Hodges, A., et al., Regional and cellular gene expression changes in human Huntington's disease brain. Hum Mol Genet, 2006. 15(6): p. 965-77.
78. Hodgson, J.G., et al., A YAC mouse model for Huntington's disease with full-

length mutant huntingtin, cytoplasmic toxicity, and selective striatal neurodegeneration. Neuron, 1999. 23(1): p. 181-92.
79. Holbert, S., et al., The Gln-Ala repeat transcriptional activator CA150 interacts with huntingtin: neuropathologic and genetic evidence for a role in Huntington's disease pathogenesis. Proc Natl Acad Sci U S A, 2001. 98(4): p. 1811-6.
80. Horn, S.C., et al., Huntingtin interacts with the receptor sorting family protein GASP2. J Neural Transm, 2006. 113(8): p. 1081-90.
81. Hou, S.T., et al., Calpain-cleaved collapsin response mediator protein-3 induces neuronal death after glutamate toxicity and cerebral ischemia. J Neurosci, 2006. 26(8): p. 2241-9.
82. Huang, C.C., et al., Amyloid formation by mutant huntingtin: threshold, progressivity and recruitment of normal polyglutamine proteins. Somat Cell Mol Genet, 1998. 24(4): p. 217-33.
83. Huh, W.K., et al., Global analysis of protein localization in budding yeast. Nature, 2003. 425(6959): p. 686-91.
84. Humbert, S., et al., The IGF-1/Akt pathway is neuroprotective in Huntington's disease and involves Huntingtin phosphorylation by Akt. Dev Cell, 2002. 2(6): p. 831-7.
85. Huntington, G., On chorea. George Huntington, M.D. J Neuropsychiatry Clin Neurosci, 2003. 15(1): p. 109-12.
86. Inagaki, N., et al., CRMP-2 induces axons in cultured hippocampal neurons. Nat Neurosci, 2001. 4(8): p. 781-2.
87. Iwata, A., et al., HDAC6 and microtubules are required for autophagic degradation of aggregated huntingtin. J Biol Chem, 2005. 280(48): p. 40282-92.
88. Jana, N.R., et al., Altered proteasomal function due to the expression of polyglutamine-expanded truncated N-terminal huntingtin induces apoptosis by caspase activation through mitochondrial cytochrome c release. Hum Mol Genet, 2001. 10(10): p. 1049-59.
89. Jiang, S.X., et al., Calpain cleavage of collapsin response mediator proteins in ischemic mouse brain. Eur J Neurosci, 2007. 26(4): p. 801-9.
90. Kalchman, M.A., et al., Huntingtin is ubiquitinated and interacts with a

specific ubiquitin-conjugating enzyme. J Biol Chem, 1996. 271(32): p. 19385-94.
91. Kaltenbach, L.S., et al., Huntingtin interacting proteins are genetic modifiers of neurodegeneration. PLoS Genet, 2007. 3(5): p. e82.
92. Kaminosono, S., et al., Suppression of mutant Huntingtin aggregate formation by Cdk5/p35 through the effect on microtubule stability. J Neurosci, 2008. 28(35): p. 8747-55.
93. Kegel, K.B., et al., Huntingtin associates with acidic phospholipids at the plasma membrane. J Biol Chem, 2005. 280(43): p. 36464-73.
94. Kim, Y.J., et al., Caspase 3-cleaved N-terminal fragments of wild-type and mutant huntingtin are present in normal and Huntington's disease brains, associate with membranes, and undergo calpain-dependent proteolysis. Proc Natl Acad Sci U S A, 2001. 98(22): p. 12784-9.
95. Kimura, T., et al., Tubulin and CRMP-2 complex is transported via Kinesin-1. J Neurochem, 2005. 93(6): p. 1371-82.
96. Kowara, R., et al., Calpain-mediated truncation of dihydropyrimidinase-like 3 protein (DPYSL3) in response to NMDA and H2O2 toxicity. J Neurochem, 2005. 95(2): p. 466-74.
97. Kowara, R., K.L. Moraleja, and B. Chakravarthy, Involvement of nitric oxide synthase and ROS-mediated activation of L-type voltage-gated Ca2+ channels in NMDA-induced DPYSL3 degradation. Brain Res, 2006. 1119(1): p. 40-9.
98. Krull, L.H., et al., Synthetic Polypeptides Containing Side-Chain Amide Groups: Water-Insoluble Polymers. Biochemistry, 1965. 4: p. 626-33.
99. Kuemmerle, S., et al., Huntington aggregates may not predict neuronal death in Huntington's disease. Ann Neurol, 1999. 46(6): p. 842-9.
100. Landles, C. and G.P. Bates, Huntingtin and the molecular pathogenesis of Huntington's disease. Fourth in molecular medicine review series. EMBO Rep, 2004. 5(10): p. 958-63.
101. Leavitt, B.R., et al., Wild-type huntingtin reduces the cellular toxicity of mutant huntingtin in vivo. Am J Hum Genet, 2001. 68(2): p. 313-24.
102. Li, S.H. and X.J. Li, Aggregation of N-terminal huntingtin is dependent on the length of its glutamine repeats. Hum Mol Genet, 1998. 7(5): p. 777-82.
103. Li, S.H. and X.J. Li, Huntingtin-protein interactions and the pathogenesis of

Huntington's disease. Trends Genet, 2004. 20(3): p. 146-54.
104. Li, W., R.K. Herman, and J.E. Shaw, Analysis of the Caenorhabditis elegans axonal guidance and outgrowth gene unc-33. Genetics, 1992. 132(3): p. 675-89.
105. Li, W., et al., Expression and characterization of full-length human huntingtin, an elongated HEAT repeat protein. J Biol Chem, 2006. 281(23): p. 15916-22.
106. Li, X.J., The early cellular pathology of Huntington's disease. Mol Neurobiol, 1999. 20(2-3): p. 111-24.
107. Li, X.J., M. Friedman, and S. Li, Interacting proteins as genetic modifiers of Huntington disease. Trends Genet, 2007. 23(11): p. 531-3.
108. Li, X.J., et al., A huntingtin-associated protein enriched in brain with implications for pathology. Nature, 1995. 378(6555): p. 398-402.
109. Lim, J., et al., A protein-protein interaction network for human inherited ataxias and disorders of Purkinje cell degeneration. Cell, 2006. 125(4): p. 801-14.
110. Liu, B., et al., Exploring candidate genes for human brain diseases from a brain-specific gene network. Biochem Biophys Res Commun, 2006. 349(4): p. 1308-14.
111. Liu, Y.F., R.C. Deth, and D. Devys, SH3 domain-dependent association of huntingtin with epidermal growth factor receptor signaling complexes. J Biol Chem, 1997. 272(13): p. 8121-4.
112. Liu, Y.F., D. Dorow, and J. Marshall, Activation of MLK2-mediated signaling cascades by polyglutamine-expanded huntingtin. J Biol Chem, 2000. 275(25): p. 19035-40.
113. Loscalzo, J., I. Kohane, and A.L. Barabasi, Human disease classification in the postgenomic era: a complex systems approach to human pathobiology. Mol Syst Biol, 2007. 3: p. 124.
114. Lumsden, A.L., et al., Huntingtin-deficient zebrafish exhibit defects in iron utilization and development. Hum Mol Genet, 2007. 16(16): p. 1905-20.
115. Lunkes, A., et al., Proteases acting on mutant huntingtin generate cleaved products that differentially build up cytoplasmic and nuclear inclusions. Mol Cell, 2002. 10(2): p. 259-69.
116. Lunkes, A. and J.L. Mandel, A cellular model that recapitulates major

pathogenic steps of Huntington's disease. Hum Mol Genet, 1998. 7(9): p. 1355-61.
117. Luo, S., et al., Cdk5 phosphorylation of huntingtin reduces its cleavage by caspases: implications for mutant huntingtin toxicity. J Cell Biol, 2005. 169(4): p. 647-56.
118. Mangiarini, L., et al., Exon 1 of the HD gene with an expanded CAG repeat is sufficient to cause a progressive neurological phenotype in transgenic mice. Cell, 1996. 87(3): p. 493-506.
119. Marsh, J.L., J. Pallos, and L.M. Thompson, Fly models of Huntington's disease. Hum Mol Genet, 2003. 12 Spec No 2: p. R187-93.
120. Martin, J.B. and J.F. Gusella, Huntington's disease. Pathogenesis and management. N Engl J Med, 1986. 315(20): p. 1267-76.
121. Mastroberardino, P.G., et al., 'Tissue' transglutaminase ablation reduces neuronal death and prolongs survival in a mouse model of Huntington's disease. Cell Death Differ, 2002. 9(9): p. 873-80.
122. McMurray, C.T., Neurodegeneration: diseases of the cytoskeleton? Cell Death Differ, 2000. 7(10): p. 861-5.
123. Miller, V.M., et al., CHIP suppresses polyglutamine aggregation and toxicity in vitro and in vivo. J Neurosci, 2005. 25(40): p. 9152-61.
124. Minturn, J.E., et al., TOAD-64, a gene expressed early in neuronal differentiation in the rat, is related to unc-33, a C. elegans gene involved in axon outgrowth. J Neurosci, 1995. 15(10): p. 6757-66.
125. Modregger, J., et al., PACSIN 1 interacts with huntingtin and is absent from synaptic varicosities in presymptomatic Huntington's disease brains. Hum Mol Genet, 2002. 11(21): p. 2547-58.
126. Morton, A.J., et al., Progressive formation of inclusions in the striatum and hippocampus of mice transgenic for the human Huntington's disease mutation. J Neurocytol, 2000. 29(9): p. 679-702.
127. Mouatt-Prigent, A., et al., Increased M-calpain expression in the mesencephalon of patients with Parkinson's disease but not in other neurodegenerative disorders involving the mesencephalon: a role in nerve cell death? Neuroscience, 1996. 73(4): p. 979-87.
128. Muchowski, P.J., et al., Hsp70 and hsp40 chaperones can inhibit self-

assembly of polyglutamine proteins into amyloid-like fibrils. Proc Natl Acad Sci U S A, 2000. 97(14): p. 7841-6.
129. Muchowski, P.J. and J.L. Wacker, Modulation of neurodegeneration by molecular chaperones. Nat Rev Neurosci, 2005. 6(1): p. 11-22.
130. Myers, R.H., Huntington's disease genetics. NeuroRx, 2004. 1(2): p. 255-62.
131. Myers, R.H., et al., Decreased neuronal and increased oligodendroglial densities in Huntington's disease caudate nucleus. J Neuropathol Exp Neurol, 1991. 50(6): p. 729-42.
132. Nasir, J., et al., Targeted disruption of the Huntington's disease gene results in embryonic lethality and behavioral and morphological changes in heterozygotes. Cell, 1995. 81(5): p. 811-23.
133. Neuwald, A.F. and T. Hirano, HEAT repeats associated with condensins, cohesins, and other complexes involved in chromosome-related functions. Genome Res, 2000. 10(10): p. 1445-52.
134. Okun, M.S. and N. Thommi, Americo Negrette (1924 to 2003): diagnosing Huntington disease in Venezuela. Neurology, 2004. 63(2): p. 340-3.
135. Orr, H.T. and H.Y. Zoghbi, Trinucleotide repeat disorders. Annu Rev Neurosci, 2007. 30: p. 575-621.
136. Ouimet, C.C. and P. Greengard, Distribution of DARPP-32 in the basal ganglia: an electron microscopic study. J Neurocytol, 1990. 19(1): p. 39-52.
137. Ouimet, C.C., K.C. Langley-Gullion, and P. Greengard, Quantitative immunocytochemistry of DARPP-32-expressing neurons in the rat caudatoputamen. Brain Res, 1998. 808(1): p. 8-12.
138. Paulsen, J.S., et al., Clinical markers of early disease in persons near onset of Huntington's disease. Neurology, 2001. 57(4): p. 658-62.
139. Perry, J. and N. Kleckner, The ATRs, ATMs, and TORs are giant HEAT repeat proteins. Cell, 2003. 112(2): p. 151-5.
140. Perutz, M., Polar zippers: their role in human disease. Protein Sci, 1994. 3(10): p. 1629-37.
141. Pujana, M.A., et al., Network modeling links breast cancer susceptibility and centrosome dysfunction. Nat Genet, 2007. 39(11): p. 1338-49.

142. Qin, Q., et al., A novel GTPase, CRAG, mediates promyelocytic leukemia protein-associated nuclear body formation and degradation of expanded polyglutamine protein. J Cell Biol, 2006. 172(4): p. 497-504.
143. Quach, T.T., et al., Involvement of collapsin response mediator proteins in the neurite extension induced by neurotrophins in dorsal root ganglion neurons. Mol Cell Neurosci, 2004. 25(3): p. 433-43.
144. Quinn, C.C., et al., TUC-4b, a novel TUC family variant, regulates neurite outgrowth and associates with vesicles in the growth cone. J Neurosci, 2003. 23(7): p. 2815-23.
145. Rigamonti, D., et al., Huntingtin's neuroprotective activity occurs via inhibition of procaspase-9 processing. J Biol Chem, 2001. 276(18): p. 14545-8.
146. Rigaut, G., et al., A generic protein purification method for protein complex characterization and proteome exploration. Nat Biotechnol, 1999. 17(10): p. 1030-2.
147. Rockabrand, E., et al., The first 17 amino acids of Huntingtin modulate its sub-cellular localization, aggregation and effects on calcium homeostasis. Hum Mol Genet, 2007. 16(1): p. 61-77.
148. Rosenberg, N.K., S.A. Sorensen, and A.L. Christensen, Neuropsychological characteristics of Huntington's disease carriers: a double blind study. J Med Genet, 1995. 32(8): p. 600-4.
149. Ross, C.A., When more is less: pathogenesis of glutamine repeat neurodegenerative diseases. Neuron, 1995. 15(3): p. 493-6.
150. Ross, C.A. and M.A. Poirier, Opinion: What is the role of protein aggregation in neurodegeneration? Nat Rev Mol Cell Biol, 2005. 6(11): p. 891-8.
151. Rosslenbroich, V., et al., Collapsin response mediator protein-4 regulates F-actin bundling. Exp Cell Res, 2005. 310(2): p. 434-44.
152. Saito, K., et al., Widespread activation of calcium-activated neutral proteinase (calpain) in the brain in Alzheimer disease: a potential molecular basis for neuronal degeneration. Proc Natl Acad Sci U S A, 1993. 90(7): p. 2628-32.
153. Sanchez, I., C. Mahlke, and J. Yuan, Pivotal role of oligomerization in expanded polyglutamine neurodegenerative disorders. Nature, 2003. 421(6921): p. 373-9.

154. Scherzinger, E., et al., Huntingtin-encoded polyglutamine expansions form amyloid-like protein aggregates in vitro and in vivo. Cell, 1997. 90(3): p. 549-58.
155. Schilling, B., et al., Huntingtin phosphorylation sites mapped by mass spectrometry. Modulation of cleavage and toxicity. J Biol Chem, 2006. 281(33): p. 23686-97.
156. Schilling, G., et al., Intranuclear inclusions and neuritic aggregates in transgenic mice expressing a mutant N-terminal fragment of huntingtin. Hum Mol Genet, 1999. 8(3): p. 397-407.
157. Shao, J. and M.I. Diamond, Polyglutamine diseases: emerging concepts in pathogenesis and therapy. Hum Mol Genet, 2007. 16 Spec No. 2: p. R115-23.
158. Shao, J., et al., Phosphorylation of profilin by ROCK1 regulates polyglutamine aggregation. Mol Cell Biol, 2008. 28(17): p. 5196-208.
159. Sharp, A.H., et al., Widespread expression of Huntington's disease gene (IT15) protein product. Neuron, 1995. 14(5): p. 1065-74.
160. Shirvan, A., et al., Semaphorins as mediators of neuronal apoptosis. J Neurochem, 1999. 73(3): p. 961-71.
161. Siman, R., et al., The calcium-activated protease calpain I and ischemia-induced neurodegeneration. Adv Neurol, 1996. 71: p. 167-74; discussion 174-5.
162. Sittler, A., et al., SH3GL3 associates with the Huntingtin exon 1 protein and promotes the formation of polygln-containing protein aggregates. Mol Cell, 1998. 2(4): p. 427-36.
163. Smith, P.D., et al., Calpain-regulated p35/cdk5 plays a central role in dopaminergic neuron death through modulation of the transcription factor myocyte enhancer factor 2. J Neurosci, 2006. 26(2): p. 440-7.
164. Soto, C., Unfolding the role of protein misfolding in neurodegenerative diseases. Nat Rev Neurosci, 2003. 4(1): p. 49-60.
165. Sotrel, A., et al., Morphometric analysis of the prefrontal cortex in Huntington's disease. Neurology, 1991. 41(7): p. 1117-23.
166. Stauber, J., et al., MALDI imaging of formalin-fixed paraffin-embedded tissues: application to model animals of Parkinson disease for biomarker hunting. J Proteome Res, 2008. 7(3): p. 969-78.
167. Steffan, J.S., et al., SUMO modification of Huntingtin and Huntington's

disease pathology. Science, 2004. 304(5667): p. 100-4.
168. Steffan, J.S., et al., The Huntington's disease protein interacts with p53 and CREB-binding protein and represses transcription. Proc Natl Acad Sci U S A, 2000. 97(12): p. 6763-8.
169. Stelzl, U., et al., A human protein-protein interaction network: a resource for annotating the proteome. Cell, 2005. 122(6): p. 957-68.
170. Stenmark, P., et al., The structure of human collapsin response mediator protein 2, a regulator of axonal growth. J Neurochem, 2007. 101(4): p. 906-17.
171. Strehlow, A.N., J.Z. Li, and R.M. Myers, Wild-type huntingtin participates in protein trafficking between the Golgi and the extracellular space. Hum Mol Genet, 2007. 16(4): p. 391-409.
172. Su, K.Y., et al., Mice deficient in collapsin response mediator protein-1 exhibit impaired long-term potentiation and impaired spatial learning and memory. J Neurosci, 2007. 27(10): p. 2513-24.
173. Sun, Y., et al., Polyglutamine-expanded huntingtin promotes sensitization of N-methyl-D-aspartate receptors via post-synaptic density 95. J Biol Chem, 2001. 276(27): p. 24713-8.
174. Suzuki, Y., et al., Collapsin response mediator protein-2 accelerates axon regeneration of nerve-injured motor neurons of rat. J Neurochem, 2003. 86(4): p. 1042-50.
175. Tahimic, C.G., et al., Evidence for a role of Collapsin response mediator protein-2 in signaling pathways that regulate the proliferation of non-neuronal cells. Biochem Biophys Res Commun, 2006. 340(4): p. 1244-50.
176. Takano, H. and J.F. Gusella, The predominantly HEAT-like motif structure of huntingtin and its association and coincident nuclear entry with dorsal, an NF-kB/Rel/dorsal family transcription factor. BMC Neurosci, 2002. 3: p. 15.
177. Tam, S., et al., The chaperonin TRiC controls polyglutamine aggregation and toxicity through subunit-specific interactions. Nat Cell Biol, 2006. 8(10): p. 1155-62.
178. Tang, T.S., et al., Huntingtin and huntingtin-associated protein 1 influence neuronal calcium signaling mediated by inositol-(1,4,5) triphosphate receptor type 1. Neuron, 2003. 39(2): p. 227-39.

179. Torashima, T., et al., Lentivector-mediated rescue from cerebellar ataxia in a mouse model of spinocerebellar ataxia. EMBO Rep, 2008. 9(4): p. 393-9.
180. Touma, E., et al., Calpain-mediated cleavage of collapsin response mediator protein(CRMP)-2 during neurite degeneration in mice. Eur J Neurosci, 2007. 26(12): p. 3368-81.
181. Trottier, Y., et al., Cellular localization of the Huntington's disease protein and discrimination of the normal and mutated form. Nat Genet, 1995. 10(1): p. 104-10.
182. Trushina, E., et al., Microtubule destabilization and nuclear entry are sequential steps leading to toxicity in Huntington's disease. Proc Natl Acad Sci U S A, 2003. 100(21): p. 12171-6.
183. Tsuji, T., et al., m-Calpain (calcium-activated neutral proteinase) in Alzheimer's disease brains. Neurosci Lett, 1998. 248(2): p. 109-12.
184. Uchida, Y., et al., Semaphorin3A signalling is mediated via sequential Cdk5 and GSK3beta phosphorylation of CRMP2: implication of common phosphorylating mechanism underlying axon guidance and Alzheimer's disease. Genes Cells, 2005. 10(2): p. 165-79.
185. Ueyama, H., et al., Expression of three calpain isoform genes in human skeletal muscles. J Neurol Sci, 1998. 155(2): p. 163-9.
186. Veyrac, A., et al., Expression of collapsin response mediator proteins 1, 2 and 5 is differentially regulated in newly generated and mature neurons of the adult olfactory system. Eur J Neurosci, 2005. 21(10): p. 2635-48.
187. Vonsattel, J.P. and M. DiFiglia, Huntington disease. J Neuropathol Exp Neurol, 1998. 57(5): p. 369-84.
188. Vonsattel, J.P., et al., Neuropathological classification of Huntington's disease. J Neuropathol Exp Neurol, 1985. 44(6): p. 559-77.
189. Walaas, S.I., D.W. Aswad, and P. Greengard, A dopamine- and cyclic AMP-regulated phosphoprotein enriched in dopamine-innervated brain regions. Nature, 1983. 301(5895): p. 69-71.
190. Wang, K.K., Calpain and caspase: can you tell the difference? Trends Neurosci, 2000. 23(1): p. 20-6.
191. Wang, L.H. and S.M. Strittmatter, A family of rat CRMP genes is

differentially expressed in the nervous system. J Neurosci, 1996. 16(19): p. 6197-207.
192. Wang, L.H. and S.M. Strittmatter, Brain CRMP forms heterotetramers similar to liver dihydropyrimidinase. J Neurochem, 1997. 69(6): p. 2261-9.
193. Wanker, E.E., et al., HIP-I: a huntingtin interacting protein isolated by the yeast two-hybrid system. Hum Mol Genet, 1997. 6(3): p. 487-95.
194. Wexler, N.S., et al., Venezuelan kindreds reveal that genetic and environmental factors modulate Huntington's disease age of onset. Proc Natl Acad Sci U S A, 2004. 101(10): p. 3498-503.
195. Wu, J., F. Lin, and Z. Qin, Sequestration of glyceraldehyde-3-phosphate dehydrogenase to aggregates formed by mutant huntingtin. Acta Biochim Biophys Sin (Shanghai), 2007. 39(11): p. 885-90.
196. Xia, J., et al., Huntingtin contains a highly conserved nuclear export signal. Hum Mol Genet, 2003. 12(12): p. 1393-403.
197. Yamashita, N., et al., Regulation of spine development by semaphorin3A through cyclin-dependent kinase 5 phosphorylation of collapsin response mediator protein 1. J Neurosci, 2007. 27(46): p. 12546-54.
198. Yanai, A., et al., Palmitoylation of huntingtin by HIP14 is essential for its trafficking and function. Nat Neurosci, 2006. 9(6): p. 824-31.
199. Yeger-Lotem, E., et al., Bridging high-throughput genetic and transcriptional data reveals cellular responses to alpha-synuclein toxicity. Nat Genet, 2009. 41(3): p. 316-23.
200. Yoshida, H., A. Watanabe, and Y. Ihara, Collapsin response mediator protein-2 is associated with neurofibrillary tangles in Alzheimer's disease. J Biol Chem, 1998. 273(16): p. 9761-8.
201. Yoshimura, T., et al., GSK-3beta regulates phosphorylation of CRMP-2 and neuronal polarity. Cell, 2005. 120(1): p. 137-49.
202. Zabel, C., et al., A large number of protein expression changes occur early in life and precede phenotype onset in a mouse model for huntington disease. Mol Cell Proteomics, 2009. 8(4): p. 720-34.
203. Zeitlin, S., et al., Increased apoptosis and early embryonic lethality in mice nullizygous for the Huntington's disease gene homologue. Nat Genet, 1995. 11(2):

p. 155-63.
204. Zeron, M.M., et al., Mutant huntingtin enhances excitotoxic cell death. Mol Cell Neurosci, 2001. 17(1): p. 41-53.
205. Zhai, W., et al., In vitro analysis of huntingtin-mediated transcriptional repression reveals multiple transcription factor targets. Cell, 2005. 123(7): p. 1241-53.
206. Zhang, Y., et al., Huntingtin inhibits caspase-3 activation. EMBO J, 2006. 25(24): p. 5896-906.
207. Zhang, Z., et al., Calpain-mediated collapsin response mediator protein-1, -2, and -4 proteolysis after neurotoxic and traumatic brain injury. J Neurotrauma, 2007. 24(3): p. 460-72.
208. Zoghbi, H.Y. and H.T. Orr, Glutamine repeats and neurodegeneration. Annu Rev Neurosci, 2000. 23: p. 217-47.
209. Zuccato, C., et al., Loss of huntingtin-mediated BDNF gene transcription in Huntington's disease. Science, 2001. 293(5529): p. 493-8.

Selbständigkeitserklärung

Hiermit erkläre ich, die vorliegende Arbeit selbständig ohne fremde Hilfe verfasst und nur die angegebene Literatur und Hilfsmittel verwendet zu haben. Die Promotionsordnung der Mathematisch-Naturwissenschaftlichen Fakultät I Humboldt-Universität zu Berlin vom 01. September 2005 habe ich gelesen und akzeptiert.

Yacine Bounab